

DEVELOPMENT OF NOVEL TARGETS FOR  
CANCER-INDUCED BONE PAIN

DEVELOPMENT OF NOVEL TARGETS FOR CANCER-INDUCED BONE PAIN

By JENNIFER FAZZARI, B.Sc.

A Thesis Submitted to the School of Graduate Studies in Partial Fulfilment of the  
Requirements for the Degree Doctor of Philosophy

McMaster University © Copyright by Jennifer Fazzari, April 2018

McMaster University DOCTOR OF PHILOSOPHY (2018) Hamilton, Ontario (Science)

TITLE: Development of Novel Targets for Cancer-induced Bone Pain AUTHOR:  
Jennifer Fazzari B.Sc. (McMaster University) SUPERVISOR: Professor G. Singh  
NUMBER OF PAGES: xiv, 179

## **LAY ABSTRACT**

Late-stage cancers can spread from the primary site to other body sites including the bone. Breast cancer is one subtype that has a propensity to spread to the bone where it can induce severe pain that is resistant to common treatments. Due to changes in how cancer cells obtain and use nutrients, the cell increases its secretion of the molecule glutamate which can induce pain making this an important target in developing new therapeutics to treat cancer pain. Treatment strategies include blocking the release of glutamate from the cancer cell or by preventing its production. Novel molecules were identified for their ability to block glutamate release from an aggressive breast cancer cell line with one such compound, capsazepine, reducing the development of pain behaviour in an animal model of cancer pain. However, the drug, CB-839, targeting glutamate production in cancer did not alter pain behaviours in the same model.

## ABSTRACT

A high proportion of advanced-stage breast cancer patients will experience bone metastases resulting in skeletal-related comorbidities including cancer-induced bone pain (CIBP). CIBP affects the quality of life of these patients and current treatments are associated with dose-limiting side-effects that negatively impact patient care. Novel mechanisms must therefore be explored to identify targeted therapies to address this unmet clinical problem. Targeting cancer-specific mechanisms is one strategy to treat this unique pain state peripherally. Glutamate is a key neurotransmitter and signaling molecule in the central nervous system and peripheral tissues including the bone. Particularly aggressive cancers that metastasize to the bone secrete high levels of glutamate via the glutamate/cystine antiporter (system  $x_c^-$ ) which can disrupt normal bone turnover and induce CIBP. Therefore, identification of small molecule inhibitors of glutamate release from metastatic breast cancer cells is a novel approach to targeting CIBP. Using high-throughput screening, library compounds were tested for their ability to reduce glutamate release from MDA-MB-231 cells known to secrete high levels of glutamate through system  $x_c^-$  and induce CIBP *in vivo*. One compound, capsazepine (CPZ), was confirmed to inhibit the functional unit of system  $x_c^-$  (xCT) and successfully delay the onset of, and reverse nociceptive behaviours in a validated animal model. Another lead compound was found to show potent antagonism against glutaminase (GLS), the enzyme catalyzing the intracellular conversion of glutamine to glutamate. This offered another strategy to target glutamate-induced nociception upstream of xCT activity. The effects of GLS inhibition on CIBP behaviours was tested with the specific GLS antagonist, CB-839 but did not significantly modulate nociception, highlighting a redundancy in glutamine metabolism that confers metabolic flexibility in different cancer

cell lines. These studies identify novel molecules to target CIBP and reveal that their antinociceptive effects are dependent on the glutamatergic target and metabolic status of the cancer subtype.

## ACKNOWLEDGEMENTS:

Over the course of working towards this degree, I have had the opportunity to work with many individuals who have made the work comprising this dissertation possible. Without the help, guidance, expertise and kindness of these individuals, reaching this accomplishment would not have been possible. At some point over the years, each person has generously sacrificed their valuable time to help me learn and guide me to succeed.

I would first like to thank my supervisor Dr. Gurmit Singh for giving me the opportunity to pursue my graduate studies and apply my love of research to a field I find meaningful. Thank you for having the patience to help guide me to “stay focused”. To each member of my supervisory committee, thank you for your professional and personal guidance. Having your support gave me the reassurance that I could draw on your years of experience for guidance and direction.

I would like to show my appreciation of Dr. Katja Linher-Melville. Her guidance, expertise and support throughout my graduate studies was invaluable and I cannot express the great respect I have for her as a scientist and friend. She is someone I look up to for both her intelligence and kindness. Similarly Natalie Zacal made the lab such a happy place to be with her sense of humour and positive attitude that never seemed to waiver. She was always there to help organize, plan and help me carry out my experiments without hesitation. Together they would devote endless hours from their busy days to make sure all the needs of the students were met and that everyone was able to achieve their goals. Having them both as colleagues and friends made the lab

feel like family. Thank you to Dr. Hanxin Lin for helping me get my project started in the Singh lab. Working with him endowed me with a work ethic and attention to detail that I carried throughout my PhD studies and will keep with me throughout my career. I would also like to thank the technical staff whose contributions and expertise were invaluable to my work. Thank you to Cecelia Murphy, Flavia Alves and Amber Faraday for making so many of my experiments possible. To every member of the Singh lab that I have had the opportunity to learn from over the course of my graduate studies, thank you.

Most importantly thank you to my family for encouraging my imagination and curious nature and giving me the supportive environment throughout my life to explore, learn and grow. I dedicate this dissertation to my mother whose fight, resilience, strength and love gave me the passion to pursue this research to the highest level. I can only hope that my simple contributions will have an impact, no matter how small, on bettering the life of even one individual fighting cancer like she was.

Thank you again to everyone for your patience, kindness and genuine desire to see me succeed.

## TABLE OF CONTENTS:

<b>LAY ABSTRACT</b> .....	<b>iii</b>
<b>ABSTRACT</b> .....	<b>iv</b>
<b>ACKNOWLEDGEMENTS:</b> .....	<b>vi</b>
<b>TABLE OF CONTENTS:</b> .....	<b>viii</b>
<b>LIST OF FIGURES AND TABLES:</b> .....	<b>xi</b>
<b>LIST OF ABBREVIATIONS</b> .....	<b>xiii</b>
<b>DECLARATION OF ACADEMIC ACHIEVEMENT</b> .....	<b>xv</b>
<b>CHAPTER 1: INTRODUCTION</b> .....	<b>1</b>
<i>OVERVIEW:</i> .....	2
<i>SUMMARY OF PAIN PROCESSING:</i> .....	3
<i>PHYSIOLOGY OF BONE AFFERENT NEURONS:</i> .....	4
<i>MECHANISMS OF CANCER PAIN:</i> .....	5
<i>THE CYSTINE/GLUTAMATE ANTIPORTER; SYSTEM X<sub>C</sub><sup>-</sup>:</i> .....	6
<i>TRANSIENT RECEPTOR POTENTIAL CATION CHANNEL, SUBFAMILY V, MEMBER 1 (TRPV1):</i> 9	
<i>TRPV1 in Cancer</i> .....	10
<i>TRPV1 Regulation:</i> .....	11
<i>Role of TRPV1 in Cancer-induced Pain</i> .....	11
<i>Inhibition of TRPV1:</i> .....	13
<i>GLUTAMINASE:</i> .....	14
<i>Role of Glutaminase in the CNS</i> .....	15
<i>Glutaminase Regulation:</i> .....	16
<i>Glutaminase in Cancer:</i> .....	17
<i>Role of Glutaminase in Cancer-Induced Pain:</i> .....	18
<i>Inhibition of Glutaminase:</i> .....	20
<i>CONCLUSION:</i> .....	23
<i>REFERENCES FOR INTRODUCTION:</i> .....	27
<b>CHAPTER 2: INHIBITORS OF GLUTAMATE RELEASE FROM BREAST CANCER CELLS; NEW TARGETS FOR CANCER-INDUCED BONE-PAIN</b> .....	<b>46</b>
<b>PREFACE:</b> .....	<b>47</b>
<b>RATIONALE:</b> .....	<b>48</b>
<b>ABSTRACT:</b> .....	<b>50</b>
<b>INTRODUCTION:</b> .....	<b>51</b>
<b>RESULTS:</b> .....	<b>55</b>
<b>DISCUSSION:</b> .....	<b>58</b>
<b>CONCLUSION:</b> .....	<b>61</b>
<b>METHODS:</b> .....	<b>61</b>
<b>FIGURES:</b> .....	<b>67</b>

<b>REFERENCES CHAPTER 2:</b> .....	<b>72</b>
<b>CHAPTER 3: IDENTIFICATION OF CAPSAZEPINE AS A NOVEL INHIBITOR OF SYSTEM X<sub>c</sub><sup>-</sup> AND CANCER-INDUCED BONE PAIN</b> .....	<b>79</b>
<i>PREFACE:</i> .....	80
<i>ABSTRACT:</i> .....	82
<i>INTRODUCTION:</i> .....	83
<i>METHODS:</i> .....	85
<i>Uptake of [<sup>14</sup>C]-cystine in MDA-MB-231 cells</i> .....	86
<i>Measurement of intracellular reactive oxygen species</i> .....	86
<i>Quantification of xCT mRNA by quantitative real-time polymerase chain reaction</i> .....	87
<i>Animals</i> .....	87
<i>Tumor cell xenografts</i> .....	88
<i>Experimental groups</i> .....	88
<i>Behavioral testing</i> .....	89
<i>Dynamic Plantar Aesthesiometer</i> .....	89
<i>Dynamic Weight Bearing system</i> .....	90
<i>Immunohistochemistry</i> .....	91
<i>Statistical analysis</i> .....	91
<i>RESULTS:</i> .....	92
<i>Radiolabeled cystine uptake identifies capsazepine as an inhibitor of xCT activity</i> .....	92
<i>Intracellular ROS levels are modulated by capsazepine in MDA-MB-231 cells</i> .....	92
<i>xCT transcription increases in response to CPZ treatment</i> .....	93
<i>Behavioral analysis</i> .....	93
<i>Dynamic Plantar Aesthesiometer</i> .....	93
<i>Dynamic Weight Bearing Analysis</i> .....	94
<i>DISCUSSION:</i> .....	95
<b>FIGURES:</b> .....	<b>101</b>
<i>REFERENCES CHAPTER 3:</i> .....	110
<b>CHAPTER 4: EFFECT OF GLUTAMINASE INHIBITION ON CANCER-INDUCED BONE PAIN</b> .....	<b>113</b>
<i>PREFACE:</i> .....	114
<i>RATIONALE:</i> .....	114
<i>ABSTRACT:</i> .....	117
<i>INTRODUCTION:</i> .....	117
<i>MATERIALS AND METHODS:</i> .....	119
<i>Cell culture:</i> .....	119
<i>Quantification of extracellular glutamate:</i> .....	119
<i>Quantification of intracellular ROS production:</i> .....	120
<i>Assessing xCT activity: monitoring uptake of radiolabelled cystine:</i> .....	120
<i>Development of subcutaneous MDA-MB-231 xenograft:</i> .....	121
<i>Development of intrafemoral MDA-MB-231 xenograft:</i> .....	121
<i>Behavioural testing and radiographic lesion assessment:</i> .....	122
<i>Serum glutamate quantification by HPLC/MS:</i> .....	122
<i>Statistics:</i> .....	123
<i>RESULTS:</i> .....	124
<i>CB-839 does not prevent growth of MDA-MB-231 xenografts:</i> .....	124
<i>CB-839 does not prevent development of CIBP behaviours:</i> .....	124
<i>CB-839 reduces glutamate release from MDA-MB-231 cells:</i> .....	125
<i>ROS production and uptake of radiolabelled cystine:</i> .....	125

<i>DISCUSSION:</i> .....	125
<i>CONCLUSION:</i> .....	130
<i>FIGURES:</i> .....	132
<i>REFERENCES CHAPTER 4:</i> .....	139
<b>CHAPTER 5: CONCLUSION AND FUTURE DIRECTIONS .....</b>	<b>143</b>
<i>SUMMARY:</i> .....	144
<i>Objective 1:</i> Establish a high-throughput screening protocol to identify novel inhibitors of glutamate release from MDA-MB-231 cells and identify lead molecules. ....	146
<i>Objective 2:</i> Characterize antinociceptive effects of one lead molecule, Capsazepine, in a CIBP model.....	146
<i>Objective 3:</i> Characterize antinociceptive effects of a glutaminase inhibitor on CIBP model.....	147
<b>Future Directions: .....</b>	<b>148</b>
<i>CONCLUSION:</i> .....	150
<i>REFERENCES CHAPTER 5:</i> .....	152
<b>APPENDIX I: ASSAY DEVELOPMENT AND OPTIMIZATION .....</b>	<b>155</b>
<b>Adaptation of the Amplex Red assay .....</b>	<b>156</b>
<i>Compound Interference:</i> .....	156
<i>Optimizing Cell Number in Follow-up Testing:</i> .....	158
<i>Impact of H<sub>2</sub>O<sub>2</sub> release on Amplex Red Fluorescence:</i> .....	159
<b>Radiolabeled cystine uptake assay: .....</b>	<b>161</b>
<b>Development of HPLC-MS Protocol for Glutamate Quantification:.....</b>	<b>163</b>
<b>APPENDIX II: ADDITIONAL EXPERIMENTS .....</b>	<b>168</b>
<b>Further characterization of SKF-38393: .....</b>	<b>169</b>
<i>Intracellular GSH</i> .....	170
<i>Characterize transporter activity of HEK239T retroviral transduced xCT line:</i> .....	171
<i>Testing CB-839 in Mouse Mammary Carcinoma Cell Line:</i> .....	173
<i>Dose Response</i> .....	173
<i>Subcutaneous tumour growth</i> .....	174
<i>Knockdown of GLS through transient siRNA transfection:</i> .....	175
<i>REFERENCES FOR APPENDICES:</i> .....	178

## LIST OF FIGURES AND TABLES:

### CHAPTER 1

Figure 1: Overview of peripheral nociception induced by tumour- derived glutamate. .... 25

### CHAPTER 2

Figure 1: High-throughput screening of 29,586 compounds for inhibitors of glutamate release by MDA-MB-231 cells..... 67

Figure 2: Chemical structure of 8 compounds showing potent inhibition of glutamate release after secondary screening. .... 69

Figure 3: IC<sub>50</sub> curves for capsazepine, NNDP, SKF38393 and sulfasalazine. .... 70

Figure 4: Cytotoxicity of SKF38393, NNDP and capsazepine in MDA-MB-231, MCF-7 and Mat-Ly-Lu cells. .... 71

### CHAPTER 3

Figure 1: Quantification of cystine acquisition in MDA-MB-231 cells in the presence of capsazepine (CPZ)..... 101

Figure 2: Capsazepine treatment induces the production of reactive oxygen species..... 102

Figure 3: Treatment with 25 µM capsazepine significantly induces xCT expression by 24 and 48 hours relative to dimethyl sulfoxide (DMSO) treatment. .... 104

Figure 4: Histological analysis of tumor xenografts in bone represented by hematoxylin and eosin staining..... 105

Figure 5: DPA force-withdrawl scores of tumour-bearing paws..... 106

Figure 6: Dynamic Weight Bearing (DWB) behavioural assessments..... 108

### CHAPTER 4

Figure 1: Growth of subcutaneous MDA-MB-231 tumours in Balb/c nude mice treated with CB-839 or vehicle. .... 133

Figure 2: Concentration of glutamate in serum from animals with subcutaneous MDA-MB-231 tumours treated with CB-839 or vehicle. .... 134

Figure 3 : Assessment of pain behaviours- dynamic weight bearing (A), dynamic plantar aesthesiometer (B). .... 135

Figure 4: Radiographic lesion scoring of MDA-MB-231 tumours at endpoint..... 136

Figure 5: Concentration of extracellular glutamate (A) and cell proliferation (B) over a dose range of CB-839 +/- sodium pyruvate in culture media. .... 137

Figure 6: Production of reactive oxygen species over the course of 24 and 72 hrs and cystine uptake after 72 hr treatment with 1 µM CB-839..... 138

Figure 7: Glutathione synthesis for ROS detoxification drives metabolic adaptations to maintain glutamate production and cystine acquisition in the absence of GLS activity..... 138

### APPENDIX I

TABLE 1: Slopes from the glutamate standard curves (0-50 µM) generated using the Amplex Red Glutamic Acid/Glutamate oxidase assay spiked with varying concentrations of the test molecules. .... 157

Figure 1: Functional groups from molecules affecting the Amplex Red glutamic acid/glutamate oxidase assay ..... 157

Figure 2: Amplex Red reaction scheme.....	158
Figure 3: H <sub>2</sub> O <sub>2</sub> production following treatment with compound hits from high-throughput screening for inhibitors of glutamate release from MDA-MB-231 cells.....	160
<b>APPENDIX II</b>	
Figure 4: SKF-38393 induces a decrease in xCT promoter activity. ....	170
Figure 5: SKF-38393 decreases intracellular glutathione levels in a dose-dependent manner. ....	171
Figure 6: Treatment of 4T1 Mammary Carcinoma Cells with CB-839 .....	173
Figure 7: Tumour volume measurements of subcutaneous 4T1 tumours in Balb/c mice treated with CB-839 or vehicle.....	174
Figure 8: Transient siRNA-mediated knockdown of GLS in HCC1806 and MDA-MB-231 triple-negative breast cancer cell lines after 72 hrs. ....	176
Figure 9: Extracellular glutamate levels following transient GLS siRNA transfection. ....	177

## LIST OF ABBREVIATIONS

**4F2hc**- 4F2 heavy chain  
**Acetyl-CoA**- Acetyl coenzyme A  
**ANOVA**- Analysis of Variance  
**ASC transporter**- Alanine-serine-cysteine transporter  
**ATF4**- Activating Transcription Factor 4  
**ATP**- Adenosine triphosphate  
**BPTES**- Bis-2-(5-phenylacetamido-1,3,4-thiadiazol-2-yl)ethyl sulfide  
**cDNA**- complimentary DNA  
**CGRP**- Calcitonin Gene-related Peptide  
**CIBP**- Cancer-induced bone pain  
**CNS**- Central Nervous System  
**CPZ**- Capsazepine  
**Cys-Cys**- Cystine  
**DCFDA- 2',7'** –dichlorofluorescein diacetate  
**dFBS**- dialyzed FBS  
**DMEM**- Dulbecco's Modified Eagle Medium  
**DMSO**- Dimethyl sulfoxide  
**DON**- 6-Diazo-5-oxo-L-norleucine  
**DPA**- Dynamic Plantar Aesthesiometer  
**DRG**- Dorsal Root Ganglion  
**DWB**- Dynamic Weight Bearing  
**EDTA**- Ethylenediaminetetraacetic acid  
**EGF**- Epidermal Growth Factor  
**ER**- Estrogen Receptor  
**ERK**- Extracellular Signal-regulated Kinase-1  
**FBS**- Fetal Bovine Serum  
**GA**- Glutaminase  
**GAB**- Glutaminase B  
**GAC**- Glutaminase C  
**GDH**- Glutamate dehydrogenase  
**GLS**- Glutaminase  
**GSH**- Glutathione  
**HBSS**- Hanks Balanced Salt Solution  
**HPLC**- High-Performance Liquid Chromatography  
**HPLC/MS**- High-Performance Liquid Chromatography coupled to Mass Spectrometry  
**HRP**- Horse Radish Peroxidase  
**HTS**- High-Throughput Screening  
**IC50**- Half Maximal Inhibitory Concentration

**IFN  $\alpha$**  - Interferon Alpha  
**IGF-1**- Insulin-like Growth Factor 1  
**JNK**- c-Jun N-terminal Kinase  
**KEAP-1**- Kelch-like ECH-Associated Protein 1  
**KGA**- Kidney-type Glutaminase  
**LGA**- Liver-type Glutaminase  
**LOPAC**- Library of Pharmacologically Active Compounds  
**MAPK**- Mitogen Activated Protein Kinase  
**MEK**- MAPK/ERK Kinase  
**mGluR**- Metabotropic Glutamate Receptor  
**mRNA**- Messenger RNA  
**mTOR**- Mammalian Target of Rapamycin  
**N,N-DP**- N,N-dipropyl-dopamine hydrobromide  
**NAC**- N-acetyl cysteine  
**NCATS**- National Centre for Advancing Translational Sciences  
**NGF**- Nerve Growth Factors  
**NIH**- National Institute of Health  
**NMDA**- N-methyl-D-aspartate  
**NRF2**- Nuclear Factor Erythroid 2-Related Factor 2  
**OAA**- Oxaloacetate  
**PBS**- Phosphate Buffered Saline  
**PNS**- Peripheral Nervous System  
**PC**- Pyruvate Carboxylase  
**ROS**- Reactive Oxygen Species  
**RPMI**- Roswell Park Memorial Institute  
**RT-PCR**- Real-Time Polymerase Chain Reaction  
**SEM**- Standard Error of the Mean  
**siRNA**- Small Interfering Ribonucleic Acid  
**SSZ**- Sulfasalazine  
**STAT**- Signal Transducer and Activator of Transcription  
**TCA**- Tricarboxylic Acid Cycle  
**TNBC**- Triple Negative Breast Cancer  
**TRPV1**- Transient Receptor Potential Vanilloid 1; Transient Receptor Potential cation channel 1  
**VGLUT-1**- Vesicular Glutamate Transporter-1  
**xCT**- light chain of system x<sub>c</sub><sup>-</sup>  
 **$\alpha$ -KG**-  $\alpha$ -ketoglutarate

## DECLARATION OF ACADEMIC ACHIEVEMENT

This dissertation is presented as a combination of 3 manuscripts-

1. Fazzari, J., Lin, H., Murphy, C., Ungard, R. & Singh, G. Inhibitors of glutamate release from breast cancer cells; new targets for cancer-induced bone-pain. *Sci. Rep.* **5**, (2015).
2. Fazzari, J., Balenko, M. D., Zacal, N. & Singh, G. Identification of capsazepine as a novel inhibitor of system xc- and cancer-induced bone pain. *J Pain Res* **10**, 915–925 (2017).
3. Fazzari, J., Singh, G. Effect of glutaminase inhibition on development of cancer-induced bone pain. In submission to *Journal of Pharmacology and Experimental Therapeutics*

I have also published a book chapter entitled:

Cancer-induced Edema/Lymphedema in *Oncodynamics: Effects of Cancer Cells on the Body*. (Springer International Publishing, 2016).

And published the following review article:

Fazzari, J., Linher-Melville, K. & Singh, G. Tumour-Derived Glutamate: Linking Aberrant Cancer Cell Metabolism to Peripheral Sensory Pain Pathways. *Curr Neuropharmacol* **15**, 620–636 (2017)

# **CHAPTER 1: INTRODUCTION**

## OVERVIEW:

Breast cancer is still the most common cancer diagnosis for Canadian woman (Canadian Breast Cancer Foundation) and the focus of a vast amount of research on developing therapeutics that target tumour growth and improve prognosis. As a result of these efforts, deaths have decreased by 42% since their peak in 1988, however many patients are currently living with cancer-induced morbidities which often remain under addressed or demand treatments plagued by dose-limiting side effects<sup>1</sup>. As the Canadian population ages, with 1 in 4 Canadians expected to be over the age of 65 by 2030, the number of cancer cases is expected to increase dramatically (Canadian Cancer Statistics, 2017). With mortality rates declining over the past 30 years, and over 60% of patients surviving at least five years after diagnosis, the rate of cancer-related morbidities will therefore increase dramatically in this population (Canadian Cancer Society; May 2015). A high proportion of breast cancer patients will experience metastases increasing their risk of such comorbidities which include bone fracture, hypercalcemia and decreased mobility. The development of cancer-induced bone pain (CIBP), however, is the most debilitating and significantly compromises patient productivity and quality of life as a whole. CIBP often increases with disease progression and becomes more difficult to manage. Often, patients begin to experience another type of pain despite being on an analgesic regimen. This is known as breakthrough pain and is distinct and often more severe than the dull, chronic, ongoing nature of CIBP alone<sup>2,3</sup>. Breakthrough pain is often evoked by movement of the tumour bearing limb<sup>4-6</sup> which significantly impacts patient functionality. Furthermore, the continuous, chronic nature of CIBP demands sustained analgesia and prolonged opioid

use with many patients requiring dose escalation for sustained relief<sup>7</sup> to the point where adequate analgesia can only be achieved at the expense of diminished quality of life<sup>8–10</sup>. Without the discovery of a new class of analgesics, opioids will remain the standard intervention for CIBP<sup>7,11</sup>.

## SUMMARY OF PAIN PROCESSING:

The central nervous system (CNS) receives diverse endogenous and environmental stimuli, transmitting sensory signals from the peripheral tissues to the brain for the processing of an emotional and behavioural response. Within the peripheral nervous system (PNS), the dorsal root ganglia (DRG) are comprised of somatic sensory neurons that act as mechano-receptors, pruriceptors, thermoreceptors and nociceptors<sup>12,13</sup>. Peripheral signals arising from noxious stimuli (those that can induce tissue damage) result in the activation of nociceptors and the transmission of nociceptive signals to the CNS. Under most circumstances this is coupled to the perception of pain. The distinction between nociception and pain, however, is important as they can be decoupled from one another in pathological states where the transmission of a nociceptive stimulus may not result in the perception of pain and likewise the perception of pain may not necessarily be associated with a detectable noxious stimulus<sup>14</sup>. Particularly intense stimuli have the potential to elicit acute pain, and recurring injury or tissue damage enhance both peripheral and central components that contribute to the transmission of pain signals, leading to hypersensitivity. The majority of sensory neurons transmit information on to postsynaptic neurons in the dorsal horn of the spinal cord via the most abundant excitatory neurotransmitter, glutamate<sup>15–17</sup>. In

response, the brain actively interprets this sensory input and elicits a descending coordinated response (reviewed by Heinricher et al. 2009<sup>18</sup>).

## PHYSIOLOGY OF BONE AFFERENT NEURONS:

The bone is a dynamic tissue that is highly innervated. There are nerve fibres that innervate mineralized bone, bone marrow and the outer periosteal layer<sup>19–22</sup>. The characteristics of these neurons are consistent with those that have a role in nociception. Nociceptive neurons (or nociceptors) respond to noxious stimuli and are identified physically by being small in diameter and thinly myelinated or unmyelinated. They are further identified immunohistochemically as having a peptidergic (Calcitonin Gene Related Peptide [CGRP]- expressing) or non-peptidergic (CGRP negative, Isolectin B4 binding) molecular phenotype<sup>23,24</sup>.

The degree of innervation in the bone, the type of nerve fibres present and their associated mechanical, chemical and thermal thresholds are significant when trying to delineate the pathophysiology of cancer-induced bone pain. Tumours that often metastasize to the bone do not illicit pain at their primary site but become exceptionally painful upon colonization of the bone suggesting that the environment in which these nerves exist differs from that of other innervated tissues. Several reviews give in depth review of the physiology of bone afferents<sup>19,25–27</sup>. The sensory nerves of the periosteum are easily compressed as they line hard cortical bone and are therefore sensitive to low threshold mechanical stimuli<sup>25</sup>. The nerves innervating the marrow are sensitive to changes in intraosseous pressure<sup>28,29</sup> which can be associated with pathological

conditions including malignancies<sup>30</sup>. Furthermore, nerves at these sites are also activated by chemical and thermal stimuli<sup>31,32,28</sup>.

## MECHANISMS OF CANCER PAIN:

The tumour microenvironment is very heterogeneous and is composed of diverse cell types, growth factors, and both inflammatory and neurochemical mediators. Considering the variety of stimuli that the afferent fibers innervating the bone can respond to it is clear that the complex tumour microenvironment contributes to the etiology of CIBP. Please see Lozano-Ondua 2013 for an in depth overview of these mechanisms<sup>33</sup>. One prominent mechanism is oxidative stress. Oxidative stress is a hallmark of malignancy and is associated with a variety of chronic pain states<sup>34–38</sup>. The unregulated growth of cancer cells is associated with high metabolic activity and a concomitant rise in reactive oxygen species (ROS) that must be neutralized to sustain cell survival. In order to maintain redox equilibrium, the cancer cell upregulates antioxidant mechanisms to reduce their ROS burden (reviewed by Balendiran et al. 2004<sup>39</sup>). The predominant antioxidant in the cell is glutathione (GSH) where it exists in micromolar concentrations. A tripeptide of glutamate, cysteine and glycine, GSH synthesis relies on the availability of these amino acids.

Cysteine is a non-essential amino acid but some cells lack the ability to synthesize it *de novo* and the intracellular demand for cysteine in most cells exceeds rates of production. Therefore, cells rely on its extracellular availability either in circulating plasma *in vivo* or tissue culture media when grown *in vitro*<sup>40</sup>. Cysteine exists predominantly in its oxidized form, cystine (Cys-Cys)<sup>41,42</sup> in the extracellular space.

Glutamate is readily available in the cell due to robust glutamine uptake by the alanine-serine-cysteine (ASC) transporter. Therefore, cystine acquisition is the rate-limiting step in GSH synthesis<sup>43,44</sup>. This oxidative stress response is linked to nociception through glutamate as the import of cystine is coupled to the export of glutamate.

Glutamate is an important signaling molecule in a variety of tissues and aberrant glutamatergic signaling can result in disruption of normal tissue homeostasis. In addition to the spleen, pancreas, lung, heart, liver and other organs of the digestive and reproductive system (reviewed by Gill 2001<sup>45</sup>), the bone is also sensitive to glutamate signaling<sup>46,47</sup>. Glutamate has a paracrine function in the restricted bone environment and coordinates communication between cell types with even small changes greatly influencing the skeleton<sup>48</sup>. Prominent cells of the bone include osteoblasts and osteoclasts which are responsible for bone deposition and resorption, respectively. Both these cell types have been shown to release glutamate<sup>49,50</sup> and respond to extracellular glutamate<sup>51</sup>. Aberrant glutamatergic signalling has been associated with various peripheral diseases, including cancer. Plasma amino acid analysis of cancer patients has revealed elevated levels of plasma glutamate relative to healthy controls. This is associated with cancer cell metabolism itself, inflammation and other metabolic perturbations associated with the malignant state<sup>52–56</sup>.

## THE CYSTINE/GLUTAMATE ANTIporter; SYSTEM X<sub>C</sub><sup>-</sup>:

Glutamate release from cancer cells has been associated with over-expression of the cystine/glutamate antiporter, system x<sub>C</sub><sup>-</sup><sup>57,58</sup>, which is up-regulated as an antioxidant defense in response to high levels of ROS associated with altered glutamine

metabolism. System  $x_c^-$  is a heterodimeric amino acid transporter (HAT) that facilitates the  $\text{Na}^+$ -independent transport of L-cystine into the cell in exchange for L-glutamate. This exchange occurs in an obligatory 1:1 manner<sup>43</sup> and is the main exporter of glutamate. System  $x_c^-$  is composed of two subunits; a heavy chain and a light chain. The heavy chain is a ubiquitous glycoprotein called 4F2hc, which facilitates the transport of the light chain to the membrane and is used as a subunit in a variety of other amino acid transporters<sup>59</sup>. The light chain, xCT, is a twelve transmembrane integral membrane protein and is the subunit that confers substrate specificity to this transport system. The molecular activity of the transporter was determined by Sato and colleagues by cloning the murine form of the protein and analyzing its activity in *Xenopus oocytes*<sup>60</sup>. It was found that transport activity is sensitive to pH as extracellular pH dictates the concentrations of cystine relative to cysteine. Between the ranges of 5.8-8.0 the disulfide form predominates and transport activity therefore, increases within this pH range<sup>61</sup>. The high levels of intracellular glutamate and the low intracellular levels of cystine, generates a concentration gradient that also partly drives the activity of xCT<sup>62,63</sup>.

The primary role of system  $x_c^-$  in the tumour is to acquire cystine for the intracellular synthesis of GSH<sup>64</sup>. In addition to intracellular GSH synthesis, cystine reduction to cysteine across the plasma membrane also confers antioxidant potential by mitigating extracellular levels of ROS<sup>65</sup>. As an obligatory antiporter, import of cystine through system  $x_c^-$  must be coupled to the release of glutamate. Increased levels of 2glutamate are therefore, ultimately a by-product of the metabolic changes that promote the rapid growth and continuous survival of cancer cells. This phenomenon has been

well documented<sup>42,66</sup> and is prevalent in many cancers including those of the breast. Breast cancer cells secrete high concentrations of glutamate via system x<sub>c</sub><sup>-</sup><sup>57,67</sup> and often metastasize to the bone<sup>68</sup> where aberrant glutamate signaling can disrupt normal bone homeostasis and result in pathology<sup>69</sup>.

Expression of xCT at the mRNA level is affected by ROS *via* the KEAP-1/NRF2 pathway<sup>70</sup>. Promoter activity is also controlled by nutrient sensing mechanisms mediated by Activating Transcription Factor 4 (ATF4)<sup>71</sup> and further gene expression is mediated by STAT3 and/or STAT5 as well as the RNA-binding protein huR<sup>72</sup>. It has also recently been discovered that xCT activity is modulated post-transcriptionally via phosphorylation by mTOR<sup>73</sup>. Upregulation of this transporter, therefore, allows the cell to mitigate diverse changes in its environment allowing for continuous and rapid cell growth.

Glutamate export through system x<sub>c</sub><sup>-</sup> represents an intermediate mechanism linking the dysregulated production of glutamate at the tumour site with its detrimental extracellular effects (reviewed by Reissner 2014<sup>74</sup>), including the glutamate-promoted migration and invasion potential of aggressive cancer cells<sup>75</sup> and most importantly in this context, increased cancer-induced pain. Having implicated this particular transporter in *in vivo* pain models, further investigation into the mechanisms by which excess glutamate initiates nociceptive responses in cancer can lead to improved therapeutic interventions.

In the periphery, glutamate is a mediator of inflammation and tissue injury and plays a role in physiological nociceptive transmission<sup>76</sup> through both ionotropic<sup>77-79</sup> and

metabotropic<sup>80,81</sup> glutamate receptor activation. Several studies have shown that in both humans<sup>82,83</sup> and animal models<sup>84–86</sup>, glutamate is released from peripheral terminals of C-fiber neurons, increasing its local concentration. This excitatory amino acid is then able to stimulate neighboring glutamate receptors in an autocrine fashion, promoting not only the development, but also the maintenance and propagation, of nociception. Many of these nociceptive responses can be blocked by local, peripheral administration of ionotropic glutamate receptor antagonists<sup>77,79,87</sup>.

Considering the diverse mechanisms that exist to respond to glutamate, research can be focused on developing new strategies to better manage cancer-induced pain in the periphery by targeting tumour-derived glutamate as a major algogenic substance contributing to CIBP. In addition to system  $x_c^-$ , other peripheral targets exist that also have the potential to mitigate CIBP through glutamate.

## TRANSIENT RECEPTOR POTENTIAL CATION CHANNEL, SUBFAMILY V, MEMBER 1 (TRPV1):

TRPV1 was first identified based on its response to heat and vanilloids such as capsaicin<sup>88</sup>. It is a gated, non-selective cation channel of the transient receptor potential family composed of identical tetramers comprised of six transmembrane domains<sup>89</sup>. TRPV1 is permeable to  $Ca^{2+}$  and localizes to both spinal nociceptive afferent fibres<sup>90–92</sup> and supraspinal structures where they can also play a role in central sensitization<sup>93,94</sup>, enabling it to modulate membrane potential and to transduce sensory signals along excitable cells. Cation permeability of TRPV1 is not static and can vary its ionic selectivity based on both the type and concentration of agonist<sup>95</sup>. Therefore, this channel plays a major role in integrating a variety of noxious stimuli<sup>92</sup> with pain

perception by initiating and propagating nociceptive signalling cascades along small, unmyelinated primary afferent fibres<sup>88</sup>.

### *TRPV1 in Cancer*

TRPV1 expression has been documented in colon<sup>96</sup>, pancreatic<sup>97</sup>, and prostate<sup>98</sup> cancers. Interestingly, the effects of capsaicin vary between cancer cell types, possibly due to off-target effects or the level of channel expression. Also, the role of TRPV1 in cell proliferation varies, which could be due to the degree of Ca<sup>2+</sup> signaling induced by channel activation. For example, it has been shown that capsaicin does not affect the proliferation of TRPV1-expressing MCF-7 breast cancer cells, but does induce apoptosis<sup>99</sup>. The latter effect has recently been associated with a rise in intracellular free Ca<sup>2+</sup> concentrations upon TRPV1 activation<sup>100</sup>. The same anti-tumour activity has been observed in gliomas, in which TRPV1 gene expression is inversely correlated to tumour grade<sup>101</sup>. However, due to the heterogeneity of responses elicited by TRPV1 activation in cancer cells, therapeutically targeting this channel may present a risky strategy as its inhibition has been reported to promote proliferation in some cancers<sup>102</sup>. Expression levels of TRP family proteins, including TRPV1, can be used as a marker of cancer progression<sup>103</sup>. In addition, TRPV1 expression levels in peripheral cancers have been correlated to pain scores<sup>97</sup>, suggesting that channels not directly localizing to afferent nerve terminals may initiate a pain response, possibly by inducing the release of mediators such as glutamate from these terminals<sup>104,105</sup>. In an osteosarcoma model of bone cancer- induced pain, TRPV1 expression increased in the DRG<sup>105</sup>, and TRPV1 antagonists inhibit both central<sup>93</sup> and peripheral<sup>106</sup> nociceptive transmission.

### *TRPV1 Regulation:*

In response to tissue injury and inflammation, endogenous factors are modulated in order to increase the response to pain, whereby pain-transducing factors are up-regulated in sensory nerve endings, heightening their ability to perceive noxious stimuli associated with pathological changes. Translocation of TRPV1 to the cell membrane is essential for its activity and is mediated by a variety of factors, including bradykinin, insulin-like growth factor (IGF-1)<sup>107</sup>, and nerve growth factor (NGF)<sup>108</sup>. Ultimately, TRPV1 activation is voltage dependent, relying on membrane depolarization. The specific factors that initiate channel activation also, in part, shift the membrane potential to a voltage that sensitizes the channel to temperature<sup>109</sup>. Therefore, persistent depolarization of neurons would be expected to reduce the threshold for temperature-mediated activation of TRPV1, allowing it to promote allodynia and hyperalgesia in response to physiological changes in temperature<sup>109</sup>.

### *Role of TRPV1 in Cancer-induced Pain*

Numerous studies have documented the role of TRPV1 in nociception in diverse tissues, including those composed of non-excitabile cells where this channel can function in conjunction with glutamatergic signaling to evoke a nociceptive response from peripheral mediators including tumour-secreted factors. Therefore there is a potential role of TRPV1 in the propagation of cancer-induced pain.

The transmission of sensory information by glutamate and glutamate receptor activation is potentiated by TRPV1 phosphorylation. TRPV1 contains phosphorylation sites on its cytoplasmic N- and C-termini, and its phosphorylation status underlies its ability to respond to noxious stimuli<sup>110</sup>. Extracellular glutamate in the periphery promotes

phosphorylation of TRPV1 on the terminals of primary afferents, resulting in channel sensitization. Group I metabotropic glutamate receptors (mGluRs; R1 and R5) are also expressed on the peripheral termini of unmyelinated nociceptive afferents, propagating glutamate-induced hyper- and thermal sensitivity<sup>111</sup>. In this manner, increases in local extracellular glutamate levels can initiate a nociceptive response. This nociceptive processing can be amplified by increasing the number of TRPV1 receptors that are available on peripheral afferents. Similar to mGluR expression, N-methyl-D-aspartate (NMDA) receptors localize along the length of DRG neurons, including their peripheral processes<sup>112</sup>, where they would be proximal to TRPV1 channels. NMDA receptors are ionotropic glutamate receptors that are responsible for increased synaptic strength and long-term potentiation of C-fiber synapses<sup>113,114</sup>. The functional localization of these glutamate receptors on peripheral afferent terminals has been further confirmed by the induction of allodynia and hyperalgesia following peripheral administration of agonists against this class of ionotropic receptor<sup>115</sup>.

When applying these interconnected processes to the bone microenvironment, it becomes evident how these mechanisms are able to play a role in propagating cancer-induced bone pain signals. TRPV1 is expressed on sensory fibres that innervate mineralized bone<sup>116</sup>. Extracellular agonists of TRPV1 increase during inflammation and in response to cancer<sup>117,118</sup>. This channel can therefore respond to local changes in the bone microenvironment that arise in response to dysregulated glutamate signalling, which is known to occur in the presence of malignancy<sup>47,119–121</sup>. Given the multiple chemical mediators, including those involved in inflammation and bone degradation (acid), as well as tumour-secreted factors (glutamate), TRPV1 may become sensitized

and activated under physiological conditions by its endogenous agonists. Indeed, subcutaneous injection of capsaicin has been shown to induce peripheral glutamate release, which could be inhibited by pre-administration of capsazepine, a TRPV1 antagonist<sup>122,123</sup>.

### *Inhibition of TRPV1:*

TRPV1 has emerged as an attractive target for pharmacological intervention in pathological conditions associated with pain, including cancer-induced bone pain<sup>116,124</sup>. Desensitization of TRPV1 on peripheral afferent terminals renders these termini insensitive to a wide range of agonists that induce nociception through channel activation, including glutamate. TRPV1 antagonism has been an active area of medicinal chemistry, resulting in the synthesis of novel antagonists (reviewed by Jara-Osegura et al. 2008<sup>125</sup>). Some of these compounds display only modest efficacy in reducing nociceptive behaviours associated with chronic pain, potentially due to the multi-modal nature of TRPV1 sensitization<sup>126</sup>. However, A-425619, AMG 9810, AMG 517, and AMG 8163 display antagonism against heat-, proton- and capsaicin- induced TRPV1 activation, demonstrating enhanced abilities to reduce pain<sup>125</sup>. JNJ-17203212 has been shown to relieve pain symptoms in an osteolytic sarcoma model, specifically implicating TRPV1 antagonism with reduced cancer-induced bone pain<sup>116</sup>.

The effectiveness of a potential TRPV1-targeted therapeutic agent for treating pain may vary given the array of stimuli that modulate TRPV1 activity. Targeting TRPV1 also poses the risk of impairing the perception of noxious stimuli to such an extent as to evoke pathological changes in core body temperature and increasing the risk of burn-related injuries<sup>127,128</sup>.

## GLUTAMINASE:

Glutaminase (GA), also referred to as phosphate-activated GLS, L- glutaminase, and glutamine aminohydrolase, is a mitochondrial enzyme that catalyzes the hydrolytic conversion of glutamine into glutamate, with the formation of ammonia ( $\text{NH}_3$ )<sup>129</sup>. It is thought that  $\text{NH}_3$  diffuses from the mitochondria out of the cell, or is utilized to produce carbamoyl phosphate<sup>130</sup>. Glutamate dehydrogenase subsequently converts glutamate into  $\alpha$ -ketoglutarate, which is further metabolized in the tricarboxylic acid (TCA) cycle to produce adenosine triphosphate (ATP) and essential cellular building blocks. Glutamate also serves as one of the precursors for glutathione (GSH) synthesis. The enzymatic activity of GA serves to maintain normal tissue homeostasis, also contributing to the Warburg effect<sup>131</sup> by facilitating the “addiction” of cancer cells to glutamine as an alternative energy source<sup>132</sup>.

There are currently four structurally unique human isoforms of GA. The glutaminase 1 gene (*GLS1*) encodes two differentially spliced variants of “kidney-type”, with *GLS2* encoding two variants of “liver-type”<sup>132,133</sup> that arise due to alternative transcription initiation and the use of an alternate promoter<sup>134</sup>. The “kidney-type” GAs differ primarily in their C-terminal regions, with the longer isoform referred to as KGA and the shorter as glutaminase C (GAC)<sup>135</sup>, collectively called GLS<sup>136</sup>. The two isoforms of “liver-type” GA include a long form, glutaminase B (GAB)<sup>137</sup>, and short form, LGA, with the latter containing a domain in its C-terminus that mediates its association with proteins containing a PDZ domain<sup>138</sup>. The GA isoforms have unique kinetic properties and are expressed in distinct tissues<sup>139</sup>.

A tissue distribution profile of human GA expression revealed that *GLS2* is primarily present in the liver, also being detected in the brain, pancreas, and breast cancer cells<sup>140</sup>. Both *GLS1* transcripts (KGA and GAC) are expressed in the kidney, brain, heart, lung, pancreas, placenta, and breast cancer cells<sup>135,141</sup>. GLS has also been shown to localize to surface granules in human polymorphonuclear neutrophils<sup>142</sup>, and both LGA and KGA proteins are expressed in human myeloid leukemia cells and medullar blood isolated from patients with acute lymphoblastic leukemia<sup>143</sup>. KGA is up-regulated in brain, breast, B cell, cervical, and lung cancers, with its inhibition slowing the proliferation of representative cancer cell lines *in vitro*<sup>144–148</sup>, and GAC is also expressed in numerous cancer cell lines<sup>144,149</sup>. Two or more GA isoforms may be coexpressed in one cell type (reviewed by Szeliga 2009<sup>132</sup>), suggesting that the mechanisms underlying this enzyme's actions are likely complex. Given that the most significant differences between the GA isoforms map to domains important in protein-protein interactions and cellular localization, it is likely that each mediates distinct functions and undergoes differential regulation in a cell type-dependent manner<sup>150</sup>.

### *Role of Glutaminase in the CNS*

In the CNS, the metabolism of glutamine, glutamate, and NH<sub>3</sub> is closely regulated by the interaction between neurons, surrounding protective glial cells (astrocytes), and cerebral blood flow. This controlled metabolism, referred to as the glutamate-glutamine cycle, is essential for maintaining proper glutamate levels in the brain, with GLS driving its synthesis<sup>138</sup>. The localization of GLS to spinal and sensory neurons indicates that it also serves as a marker for glutamate neurotransmission in the CNS<sup>151</sup>. GLS is active in the presynaptic terminals of CNS neurons, where it functions to convert astrocyte-

derived glutamine into glutamate, which is then loaded into synaptic vesicles and released into the synapse. Glutamate subsequently undergoes rapid re-uptake by local astrocytes, which recycle it into glutamine and the cycle restarts. As a major neurotoxin,  $\text{NH}_3$  also factors into this process. Disorders resulting from elevated levels of circulating  $\text{NH}_3$ , such as urea cycle disorders and liver dysfunction, can adversely affect the CNS and, in severe instances, cause death. The primary negative effects of hyperammonemia within the CNS are disruptions in astrocyte metabolism and neurotoxicity. Circulating  $\text{NH}_3$  that enters the brain reacts with glutamate through the activity of glutamine synthetase to form glutamine, and changes in this process can significantly alter glutamate levels in synaptic neurons, leading to pain and disease<sup>152</sup>.

#### *Glutaminase Regulation:*

Relative to healthy tissue, the levels of GLS protein are increased in breast tumours<sup>144</sup>. In particular, increased GAC levels have been associated with a higher grade of invasive ductal breast carcinoma<sup>136</sup>. The oncogene c-Myc positively affects glutamine metabolism, as its up-regulation is sufficient to drive mitochondrial glutaminolysis<sup>153,154</sup>. Of the two GLS isoforms, mitochondrial GAC is stimulated by c-Myc in transformed fibroblasts and breast cancer cells<sup>144</sup>. c-Myc also indirectly influences GLS expression through its action on microRNA (miR) 23a and 23b<sup>155</sup>. Under normal conditions, miR23a and b bind to the 3' untranslated region of GLS transcripts, thereby preventing translation. c-Myc transcriptionally suppresses miR-23a/b expression, de-repressing the block on GLS translation and thereby facilitating glutamine metabolism<sup>155</sup>. Interestingly, acting through its p65 subunit, NF- $\kappa$ B also positively regulates GLS expression by inhibiting miR-23a<sup>156</sup>. NF- $\kappa$ B is the common intermediary that modulates GLS activation

downstream of Rho GTPase signalling<sup>13</sup>. Another protein regulating glutamine metabolism is signal transducer and activator of transcription (STAT) 1, the phosphorylated/ activated form of which binds within the GLS1 promoter region, with interferon alpha (IFN $\alpha$ ) -stimulated STAT1 activation up-regulating GLS1 expression<sup>157</sup>. Mitogen- activated protein kinase (MAPK) signaling and changes in GA expression are also linked based on a report demonstrating that KGA binds directly to MEK-ERK<sup>158</sup>. Activation of the MEK-ERK pathway in response to epidermal growth factor (EGF) treatment, or pathway inactivation by the selective MEK1/2 inhibitor U0126, activates or represses KGA activity, respectively, suggesting a phosphorylation-dependent mode of regulation<sup>158</sup>. This latter point is in line with alkaline phosphatase exposure completely blocking basal GAC activity<sup>144</sup>.

### *Glutaminase in Cancer:*

The main functions of glutamine are storing nitrogen in the muscle and trafficking it through the circulation to different tissues<sup>159,160</sup>. While mammals are able to synthesize glutamine, its supply may be surpassed by cellular demand during the onset and progression of disease, or in rapidly proliferating cells. Glutamine is utilized in metabolic reactions that require either its  $\gamma$ -nitrogen (for nucleotide and hexosamine synthesis) or its  $\alpha$ -nitrogen/ carbon skeleton, with glutamate acting as its intermediary metabolite. Although cancer cells generally have considerable intracellular glutamate reserves, adequate maintenance of these pools requires continuous metabolism of glutamine into glutamate. The GLS-mediated conversion of glutamine into glutamate has been correlated with tumour growth rates *in vivo*<sup>161,162</sup>. By limiting GLS activity, the proliferation of cancer cells decreases, and growth rates of xenografts have been shown

to be reduced<sup>155,163</sup>. Human melanomas exhibit significantly higher GLS activity compared to surrounding non-cancerous patient-matched skin<sup>164</sup>. In addition, the expression and activity of GLS are up-regulated in various tumour types and cancer cell lines. While glutamine may contribute to cellular metabolism through other mechanisms, the activity of GLS is essential for altered metabolic processes that support the rapid proliferation characteristic of cancer cells. Several cellular pathways related to amino acid synthesis, the TCA cycle, and redox balance are supported by glutamine-based metabolism through its intermediary, glutamate. Metabolites derived from glutamate are directly relevant to tumour growth. These include nucleotide and hexosamine biosynthesis, glycosylation reactions, synthesis of nonessential amino acids, antioxidant synthesis (*via* GSH), production of respiratory substrates and reducing equivalents, and ammoniogenesis (reviewed by DeBerardinis 2010<sup>165</sup>).

#### *Role of Glutaminase in Cancer-Induced Pain:*

Upon injection into human skin or muscle, glutamate causes acute pain, and painful conditions such as arthritis, myalgia, and tendonitis (reviewed by Miller et al. 2011<sup>166</sup>), as well as Multiple Sclerosis (MS), are associated with increased glutamate levels in affected tissues. Human chronic pain has been studied using animal models and through the injection of inflammatory agents such as complete Freund's adjuvant<sup>167</sup>. During inflammation, various neurotransmitters, including glutamate, as well as stimuli such as ATP, cations such as hydrogen ions (H<sup>+</sup>), and prostaglandins, sensitize primary afferent neurons by lowering their activation threshold, increasing spontaneous neural activity, and increasing and/or prolonging neural firing<sup>166</sup>. One mechanism by which sensory neurons alter their responses to inflammation, noxious

stimulation, or tissue damage is to increase the expression and availability of neurotransmitters. Indeed, the levels of glutamate are higher in inflamed tissues, and during inflammation, glutamate sensitizes the axons of primary afferent neurons by decreasing their firing threshold and inducing a hyper-excitability state<sup>168</sup>. The primary afferent neuron may act as a significant possible source of glutamate, and in both humans and animal models, antagonism of glutamate receptors that are expressed on axons of primary afferent neurons during inflammation lessens pain<sup>166</sup>. It has been shown that the peripheral inhibition of GA using 6-diazo-5-oxo-L-norleucine (DON) relieves inflammatory pain, which is supported by work in rats demonstrating that GA itself may act as a peripheral inflammatory mediator<sup>169</sup>. Inflammation also up-regulates the expression of substance P and CGRP in the DRG<sup>170,171</sup> and the spinal dorsal horn<sup>172</sup>, as well as in the joints and skin<sup>173,174</sup>, with these changes providing a marker of pain-sensing neurons. Neurons that release substance P and CGRP are also glutamatergic<sup>175,176</sup> and produce glutamate through enhanced GA activity<sup>166,177</sup>. However, how chronic glutamate production is regulated in pain models remains understudied. It is known that in response to noxious stimuli, acute glutamate release from primary afferent terminals<sup>178–181</sup>, occurring concomitant with the release of substance P and CGRP, drives spinal neuron sensitization, which has been associated with chronic changes<sup>182</sup>. Induced inflammation in the simian knee joint increases fibers in the spinal cord that are immunoreactive for glutamate by approximately 30% at 4 hours and 40% at 8 hours, consistent with a sustained effect<sup>179</sup>. Indeed, in rat spinal cords, extracellular glutamate levels are 150% higher than controls at 24 hours<sup>180</sup>, further supporting that glutamate release from central primary afferent neurons is

prolonged and activity-dependent during inflammation. These findings indicate that the production and release of glutamate are altered in response to pain, most likely due to modified flux control and local changes in the GA-mediated glutamate-glutamine cycle<sup>183</sup>. In support of this latter notion, persistent inflammation, which was experimentally induced by complete Freund's adjuvant in a rat model of arthritis, was shown to increase GA expression and enzymatic activity in DRG neurons<sup>184</sup>. It was hypothesized that elevated GA in primary sensory neurons could increase the production of glutamate in spinal primary afferent terminals, thereby either directly contributing to central or peripheral sensitization<sup>184</sup>. In an animal model of MS, GA was found to be highly expressed and correlated with axonal damage in macrophages and microglial cells associated with active lesions<sup>185</sup>. A comparison of white matter from various inflammatory neurologic diseases, including MS, with non-inflammatory conditions revealed high GA reactivity only during inflammation<sup>185</sup>. It is likely that dysregulated glutamate homeostasis contributes to axonal dystrophy in MS, and that manipulating the imbalanced glutamate-glutamine cycle may be of therapeutic relevance. GA, as an important regulator of glutamate production, could therefore be targeted for the development of novel therapeutics aimed at treating pain, including cancer-induced pain.

### *Inhibition of Glutaminase:*

DON, a non-selective irreversible glutamine-competitive inhibitor with several other targets<sup>186</sup>, has been used to effectively block KGA activity<sup>187</sup>. Other glutamine analogs with diazo groups, including azaserine and acivicin, irreversibly bind to the active site of

GA, but also affect various other enzymes that utilize glutamine as a substrate, as well as glutamine transporters<sup>186</sup>. DON and azotomycin showed promising antitumour activity against human cell lines implanted into nude mice, although clinical trials with these small-molecule inhibitors were less efficacious and associated with toxicities<sup>188</sup>. New small molecules have been discovered that inhibit both KGA and its GAC splice variant. Molecule 968, allosterically regulates GAC without competing with glutamine<sup>144,189</sup>. Its inhibitory potential has been described in various cancer cell lines *in vitro* and in a mouse xenograft model<sup>144</sup>, although its hydrophobic nature has made it difficult to apply *in vivo*. The effects of 968 on metabolically sensitive epigenetic markers and their effects on cancer-related genes were also examined. In this context, GLS inhibition enhanced histone acetylation at H4 while down-regulating the expression of *AKT* and *ERBB2*, suggesting that 968 could potentially be applied as an effective epigenetic therapeutic agent<sup>190,191</sup>. In addition, 968 has been used to test whether GLS-driven glutamine metabolism has evolved in cancer cells more as a means to control intracellular pH through the release of  $\text{NH}_3$  than to provide metabolites to fuel the TCA cycle<sup>141</sup>. Although not in line with established doctrine, this study presents evidence that modulating cellular acidity is an important component of glutamine metabolism. Glutamine withdrawal elicits less drastic effects on the viability of HeLa or MCF-7 cells when their growth media is maintained at a neutral pH 7.3 rather than under acidic conditions (corresponding to pH 6.3), with 968 treatment inhibiting cell proliferation only at the lower pH. However, cell lines resistant to glutamine withdrawal have been shown to regain sensitivity to this amino acid when exposed to glutamine synthetase inhibitors, and glutamine synthetase, through its production of glutamine, consumes  $\text{NH}_3$ , thereby

potentially acidifying the cellular microenvironment, which were not considered in the study<sup>192</sup>. Nevertheless, these findings present an intriguing secondary consequence of glutamine metabolism in cancer cells, meriting further investigation into acid/base balance.

Bis-2-(5-phenylacetamido-1,2,4-thiadiazol-2-yl)ethyl sulfide (BPTES) has emerged as an important allosteric GLS inhibitor that specifically targets KGA over LGA. BPTES binds at the interface where two KGA dimers join to form a tetramer, stabilizing a region near its active site and controlling access to its catalytic pocket, thereby inactivating the enzyme<sup>136,193,194</sup>. Similar to 968, BPTES inhibits KGA activity in various tumour types<sup>147,148</sup>, but, unlike 968, BPTES remains effective even in the presence of inorganic phosphate. BPTES analogs have been designed to improve upon its poor metabolic stability and low aqueous solubility<sup>194</sup>. Other small molecules have been described that inhibit KGA and/or GAC<sup>195</sup>, including thiourea molecules designed to function as farnesyl diphosphate mimetics that haven been proven to be efficacious against GA activity<sup>196</sup>. However, even the most potent novel compound was less efficacious than 968, BPTES, or DON.

Recently, CB-839, a novel, orally bioavailable inhibitor selective for KGA and GAC, has been developed and characterized, which potently blocks the proliferation of HCC-1806 triple-negative breast cancer cells *in vitro* while also decreasing glutamine catabolism and the levels of glutamate, GSH, and intermediates of the TCA cycle<sup>197</sup>. Interestingly, in the T47D estrogen receptor-positive breast cancer cell line, no anti-proliferative effect was observed in response to CB-839, although its administration did modestly down-regulate glutamine metabolism and the levels of its metabolites. A screen of 23 breast

cancer cell lines revealed that while expression of LGA, KGA, and GAC could be detected at some level in most cells, GAC protein levels were high, primarily in triple-negative cell lines compared to estrogen-receptor positive cells. In addition, the triple-negative subtype was associated with increased GLS activity and was also most sensitive to CB-839 treatment. In two xenograft models, CB-839 mediated significant anti-tumour activity. CB-839 may therefore be a promising novel therapeutic molecule for targeting glutamine-dependent tumours in patients, as well for treating cancer-induced pain or inflammatory pain linked to increased glutamate levels in the CNS, meriting further investigation and clinical testing.

## CONCLUSION:

The benefit of blocking glutamate release from cancer cells, irrespective of the underlying mechanism(s), is to alleviate cancer-induced bone pain peripherally, potentially expanding the clinical application of “anti-cancer” small molecule inhibitors as analgesics. Furthermore, investigating these targets may reveal how tumour-derived glutamate propagates stimuli that elicit pain. An overview of peripheral nociception induced by tumour-derived glutamate is depicted in Figure 1.

These investigations reveal the multifaceted nature of glutamate in the cell and the importance this molecule plays in many different facets of cellular metabolism and signaling. Its implications in different pathways and systems increases the number of potential mechanisms for targeting its production and transport. Despite this, however, redundancy in glutamate-dependant pathways that are crucial for cell survival highlights

the importance/reliance on this amino acid in cancer cells potentially making a difficult target for single agent therapies.

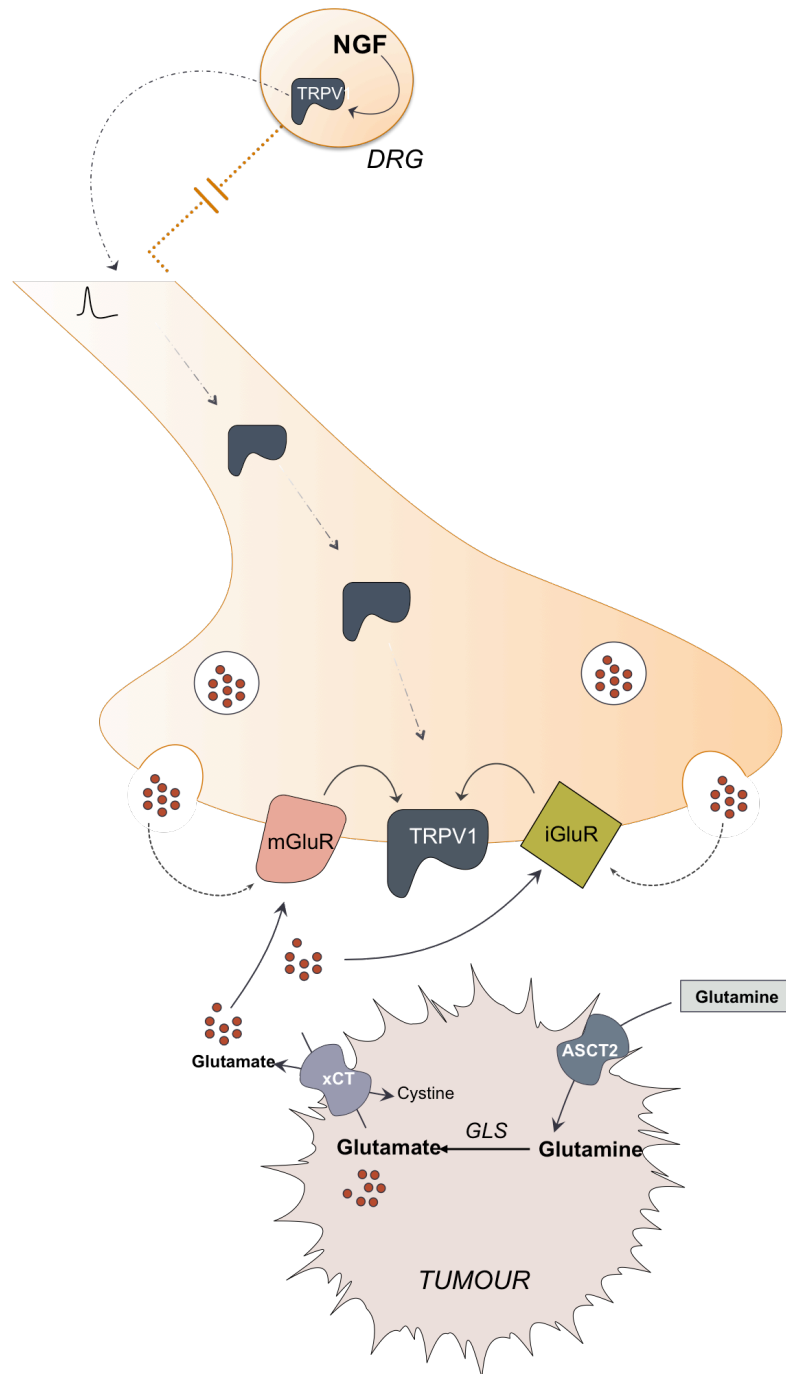


**Figure 1: Overview of peripheral nociception induced by tumour- derived glutamate.**

Dysregulated cancer cell metabolism promotes glutamine uptake by ASCT2 transporter and production of large intracellular glutamate pools that drive the activity of the cystine/glutamate transporter, xCT to accommodate the intracellular demand for cysteine, the limiting reagent in glutathione synthesis. Upregulation of glutaminase

(GLS) and system  $x_c^-$  increases the extracellular concentration of glutamate that can be perceived by proximal nociceptive terminals that can translate glutamate into a nociceptive signal by integrating the activities of glutamate receptors with TRPV1. These terminals also release glutamate that can act in an autocrine fashion also activating these same glutamate receptors. TRPV1 translocation to these terminals increases in response to peripheral noxious stimuli through the action of NGF in the dorsal root ganglion.

## REFERENCES FOR INTRODUCTION:

1. Mercadante, S. Pain treatment and outcomes for patients with advanced cancer who receive follow-up care at home. *Cancer* **85**, 1849–1858 (1999).
2. Hwang, S. S., Chang, V. T. & Kasimis, B. Cancer breakthrough pain characteristics and responses to treatment at a VA medical center. *Pain* **101**, 55–64 (2003).
3. Portenoy, R. K. & Hagen, N. A. Breakthrough pain: definition, prevalence and characteristics. *Pain* **41**, 273–281 (1990).
4. Mercadante, S. Malignant bone pain: pathophysiology and treatment. *Pain* **69**, 1–18 (1997).
5. Mercadante, S. & Arcuri, E. Breakthrough pain in cancer patients: Pathophysiology and treatment. *Cancer Treat. Rev.* **24**, 425–432 (1998).
6. Portenoy, R. K. & Lesage, P. Management of cancer pain. *Lancet Lond. Engl.* **353**, 1695–1700 (1999).
7. Blum, R. H., Novetsky, D., Shasha, D. & Fleishman, S. The multidisciplinary approach to bone metastases. *Oncol. Williston Park N* **17**, 845–857; discussion 862-863, 867 (2003).
8. Nersesyan, H. & Slavin, K. V. Current approach to cancer pain management: Availability and implications of different treatment options. *Ther. Clin. Risk Manag.* **3**, 381–400 (2007).
9. McNicol, E. Opioid Side Effects and Their Treatment in Patients with Chronic Cancer and Noncancer Pain. *J. Pain Palliat. Care Pharmacother.* **22**, 270–281 (2008).
10. Paice, J. A. & Ferrell, B. The management of cancer pain. *CA. Cancer J. Clin.* **61**, 157–182 (2011).
11. Mercadante, S., Arcuri, E., Ferrera, P., Villari, P. & Mangione, S. Alternative treatments of breakthrough pain in patients receiving spinal analgesics for cancer pain. *J. Pain Symptom Manage.* **30**, 485–491 (2005).
12. Basbaum, A. I., Bautista, D. M., Scherrer, G. & Julius, D. Cellular and molecular mechanisms of pain. *Cell* **139**, 267–284 (2009).

13. Delmas, P., Hao, J. & Rodat-Despoix, L. Molecular mechanisms of mechanotransduction in mammalian sensory neurons. *Nat. Rev. Neurosci.* **12**, 139–153 (2011).
14. Garland, E. L. Pain Processing in the Human Nervous System: A Selective Review of Nociceptive and Biobehavioral Pathways. *Prim. Care* **39**, 561–571 (2012).
15. Broman, J., Anderson, S. & Ottersen, O. P. Enrichment of glutamate-like immunoreactivity in primary afferent terminals throughout the spinal cord dorsal horn. *Eur. J. Neurosci.* **5**, 1050–1061 (1993).
16. De Biasi, S. & Rustioni, A. Glutamate and substance P coexist in primary afferent terminals in the superficial laminae of spinal cord. *Proc. Natl. Acad. Sci. U. S. A.* **85**, 7820–7824 (1988).
17. Schneider, S. P. & Perl, E. R. Comparison of primary afferent and glutamate excitation of neurons in the mammalian spinal dorsal horn. *J. Neurosci. Off. J. Soc. Neurosci.* **8**, 2062–2073 (1988).
18. Heinricher, M. M., Tavares, I., Leith, J. L. & Lumb, B. M. Descending control of nociception: Specificity, recruitment and plasticity. *Brain Res. Rev.* **60**, 214–225 (2009).
19. Mach, D. B. *et al.* Origins of skeletal pain: sensory and sympathetic innervation of the mouse femur. *Neuroscience* **113**, 155–166 (2002).
20. Grönblad, M., Liesi, P., Korkala, O., Karaharju, E. & Polak, J. Innervation of human bone periosteum by peptidergic nerves. *Anat. Rec.* **209**, 297–299 (1984).
21. Hohmann, E. L., Elde, R. P., Rysavy, J. A., Einzig, S. & Gebhard, R. L. Innervation of periosteum and bone by sympathetic vasoactive intestinal peptide-containing nerve fibers. *Science* **232**, 868–871 (1986).
22. Bjurholm, A., Krecibergs, A., Brodin, E. & Schultzberg, M. Substance P- and CGRP-immunoreactive nerves in bone. *Peptides* **9**, 165–171 (1988).
23. Ivanusic, J. J. Size, neurochemistry, and segmental distribution of sensory neurons innervating the rat tibia. *J. Comp. Neurol.* **517**, 276–283 (2009).

24. Aso, K. *et al.* Nociceptive phenotype of dorsal root ganglia neurons innervating the subchondral bone in rat knee joints. *Eur. J. Pain Lond. Engl.* **18**, 174–181 (2014).
25. Nencini, S. & Ivanusic, J. J. The Physiology of Bone Pain. How Much Do We Really Know? *Front. Physiol.* **7**, (2016).
26. Jimenez-Andrade, J. M. *et al.* Pathological Sprouting of Adult Nociceptors in Chronic Prostate Cancer-Induced Bone Pain. *J. Neurosci.* **30**, 14649–14656 (2010).
27. Mantyh, P. W. Bone cancer pain: from mechanism to therapy. *Curr. Opin. Support. Palliat. Care* **8**, 83–90 (2014).
28. Seike, W. Electrophysiological and histological studies on the sensibility of the bone marrow nerve terminal. *Yonago Acta Med.* **20**, 192–211 (1976).
29. Furusawa, S. A neurophysiological study on the sensibility of the bone marrow. *Nihon Seikeigeka Gakkai Zasshi* **44**, 365–370 (1970).
30. Sottnik, J. L., Dai, J., Zhang, H., Campbell, B. & Keller, E. T. Tumor-induced pressure in the bone microenvironment causes osteocytes to promote the growth of prostate cancer bone metastases. *Cancer Res.* **75**, 2151–2158 (2015).
31. Zhao, J. & Levy, D. The sensory innervation of the calvarial periosteum is nociceptive and contributes to headache-like behavior. *Pain* **155**, 1392–1400 (2014).
32. Sakada, S. & Nemoto, T. Response to thermal stimulation of fast- and slow-adapting free-fiber ending units in the cat mandibular periosteum. *Bull. Tokyo Dent. Coll.* **13**, 227–250 (1972).
33. Lozano-Ondoua, A. N., Symons-Liguori, A. M. & Vanderah, T. W. Cancer-induced bone pain: Mechanisms and models. *Neurosci. Lett.* **557 Pt A**, 52–59 (2013).
34. Wang, Z.-Q. *et al.* A newly identified role for superoxide in inflammatory pain. *J. Pharmacol. Exp. Ther.* **309**, 869–878 (2004).
35. Scheid, T. *et al.* Sciatic nerve transection modulates oxidative parameters in spinal and supraspinal regions. *Neurochem. Res.* **38**, 935–942 (2013).

36. Little, J. W. *et al.* Supraspinal Peroxynitrite Modulates Pain Signaling by Suppressing the Endogenous Opioid Pathway. *J. Neurosci.* **32**, 10797–10808 (2012).
37. Kallenborn-Gerhardt, W., Schröder, K., Geisslinger, G. & Schmidtko, A. NOXious signaling in pain processing. *Pharmacol. Ther.* **137**, 309–317 (2013).
38. Hacimuftuoglu, A. *et al.* Antioxidants attenuate multiple phases of formalin-induced nociceptive response in mice. *Behav. Brain Res.* **173**, 211–216 (2006).
39. Balendiran, G. K., Dabur, R. & Fraser, D. The role of glutathione in cancer. *Cell Biochem. Funct.* **22**, 343–352 (2004).
40. Gout, P. W., Kang, Y. J., Buckley, D. J., Bruchofsky, N. & Buckley, A. R. Increased cystine uptake capability associated with malignant progression of Nb2 lymphoma cells. *Leuk. Off. J. Leuk. Soc. Am. Leuk. Res. Fund UK* **11**, 1329–1337 (1997).
41. Toohey, J. I. Sulfhydryl dependence in primary explant hematopoietic cells. Inhibition of growth in vitro with vitamin B12 compounds. *Proc. Natl. Acad. Sci. U. S. A.* **72**, 73–77 (1975).
42. Conrad, M. & Sato, H. The oxidative stress-inducible cystine/glutamate antiporter, system x (c) (-) : cystine supplier and beyond. *Amino Acids* **42**, 231–246 (2012).
43. Bannai, S. Exchange of cystine and glutamate across plasma membrane of human fibroblasts. *J. Biol. Chem.* **261**, 2256–2263 (1986).
44. Ishii, T., Sugita, Y. & Bannai, S. Regulation of glutathione levels in mouse spleen lymphocytes by transport of cysteine. *J. Cell. Physiol.* **133**, 330–336 (1987).
45. Gill, S. S. & Pulido, O. M. Glutamate receptors in peripheral tissues: current knowledge, future research, and implications for toxicology. *Toxicol. Pathol.* **29**, 208–223 (2001).
46. Takarada, T. & Yoneda, Y. Pharmacological Topics of Bone Metabolism: <br>Glutamate as a Signal Mediator in Bone. *J. Pharmacol. Sci.* **106**, 536–541 (2008).
47. Brakspear, K. S. & Mason, D. J. Glutamate signaling in bone. *Front. Endocrinol.* **3**, 97 (2012).

48. Skerry, T. M. The role of glutamate in the regulation of bone mass and architecture. *J. Musculoskelet. Neuronal Interact.* **8**, 166–173 (2008).
49. Bhangu, P. S., Genever, P. G., Spencer, G. J., Grewal, T. S. & Skerry, T. M. Evidence for targeted vesicular glutamate exocytosis in osteoblasts. *Bone* **29**, 16–23 (2001).
50. Morimoto, R. *et al.* Secretion of L-glutamate from osteoclasts through transcytosis. *EMBO J.* **25**, 4175–4186 (2006).
51. Seidlitz, E. P., Sharma, M. K. & Singh, G. Extracellular glutamate alters mature osteoclast and osteoblast functions. *Can. J. Physiol. Pharmacol.* **88**, 929–936 (2010).
52. Beaton, J. R., McGanity, W. J. & McHenry, E. W. Plasma Glutamic Acid in Malignancy. *Can. Med. Assoc. J.* **65**, 219–221 (1951).
53. Dröge, W. *et al.* Plasma glutamate concentration and lymphocyte activity. *J. Cancer Res. Clin. Oncol.* **114**, 124–128 (1988).
54. Okamoto, N. *et al.* Diagnostic modeling with differences in plasma amino acid profiles between non-cachectic colorectal/breast cancer patients and healthy individuals. *Int. J. Med. Med. Sci.* **1**, 001–008 (2009).
55. Poschke, I., Mao, Y., Kiessling, R. & de Boniface, J. Tumor-dependent increase of serum amino acid levels in breast cancer patients has diagnostic potential and correlates with molecular tumor subtypes. *J. Transl. Med.* **11**, 290 (2013).
56. Barnes, T. *et al.* Plasma amino acid profiles of breast cancer patients early in the trajectory of the disease differ from healthy comparison groups. *Appl. Physiol. Nutr. Metab.* **39**, 740–744 (2014).
57. Sharma, M. K., Seidlitz, E. P. & Singh, G. Cancer cells release glutamate via the cystine/glutamate antiporter. *Biochem. Biophys. Res. Commun.* **391**, 91–95 (2010).
58. Ye, Z. C. & Sontheimer, H. Glioma cells release excitotoxic concentrations of glutamate. *Cancer Res.* **59**, 4383–4391 (1999).

59. Verrey, F., Meier, C., Rossier, G. & Kühn, L. C. Glycoprotein-associated amino acid exchangers: broadening the range of transport specificity. *Pflüg. Arch. Eur. J. Physiol.* **440**, 503–512 (2000).
60. Sato, H., Tamba, M., Ishii, T. & Bannai, S. Cloning and Expression of a Plasma Membrane Cystine/Glutamate Exchange Transporter Composed of Two Distinct Proteins. *J. Biol. Chem.* **274**, 11455–11458 (1999).
61. Bannai, S. & Kitamura, E. Role of proton dissociation in the transport of cystine and glutamate in human diploid fibroblasts in culture. *J. Biol. Chem.* **256**, 5770–5772 (1981).
62. Bannai, S. & Ishii, T. A novel function of glutamine in cell culture: utilization of glutamine for the uptake of cystine in human fibroblasts. *J. Cell. Physiol.* **137**, 360–366 (1988).
63. Christensen, H. N. Role of amino acid transport and countertransport in nutrition and metabolism. *Physiol. Rev.* **70**, 43–77 (1990).
64. Bannai, S. & Ishii, T. Transport of cystine and cysteine and cell growth in cultured human diploid fibroblasts: effect of glutamate and homocysteate. *J. Cell. Physiol.* **112**, 265–272 (1982).
65. Banjac, A. *et al.* The cystine/cysteine cycle: a redox cycle regulating susceptibility versus resistance to cell death. *Oncogene* **27**, 1618–1628 (2008).
66. Lewerenz, J. *et al.* The Cystine/Glutamate Antiporter System  $x_c^-$  in Health and Disease: From Molecular Mechanisms to Novel Therapeutic Opportunities. *Antioxid. Redox Signal.* **18**, 522–555 (2013).
67. Seidlitz, E. P., Sharma, M. K., Saikali, Z., Ghert, M. & Singh, G. Cancer cell lines release glutamate into the extracellular environment. *Clin. Exp. Metastasis* **26**, 781–787 (2009).
68. Rose, A. A. N. & Siegel, P. M. Breast cancer-derived factors facilitate osteolytic bone metastasis. *Bull. Cancer (Paris)* **93**, 931–943 (2006).
69. Kalariti, N., Lembessis, P., Papageorgiou, E., Pissimissis, N. & Koutsilieris, M. Regulation of the mGluR5, EAAT1 and GS expression by glucocorticoids in MG-63 osteoblast-like osteosarcoma cells. *J. Musculoskelet. Neuronal Interact.* **7**, 113–118 (2007).

70. Habib, E., Linher-Melville, K., Lin, H.-X. & Singh, G. Expression of xCT and activity of system xc(-) are regulated by NRF2 in human breast cancer cells in response to oxidative stress. *Redox Biol.* **5**, 33–42 (2015).
71. Ye, P. *et al.* Nrf2- and ATF4-dependent upregulation of xCT modulates the sensitivity of T24 bladder carcinoma cells to proteasome inhibition. *Mol. Cell. Biol.* **34**, 3421–3434 (2014).
72. Shi, J., He, Y., Hewett, S. J. & Hewett, J. A. Interleukin 1 $\beta$  regulation of the system xc-substrate-specific subunit, xCT, in primary mouse astrocytes involves the RNA-binding protein HuR. *J. Biol. Chem.* (2015). doi:10.1074/jbc.M115.697821
73. Gu, Y. *et al.* mTORC2 Regulates Amino Acid Metabolism in Cancer by Phosphorylation of the Cystine-Glutamate Antiporter xCT. *Mol. Cell* **67**, 128-138.e7 (2017).
74. Reissner, K. J. The cystine/glutamate antiporter: when too much of a good thing goes bad. *J. Clin. Invest.* **124**, 3279–3281 (2014).
75. Herner, A. *et al.* Glutamate increases pancreatic cancer cell invasion and migration via AMPA receptor activation and Kras-MAPK signaling. *Int. J. Cancer* **129**, 2349–2359 (2011).
76. Jin, Y. H., Nishioka, H., Wakabayashi, K., Fujita, T. & Yonehara, N. Effect of morphine on the release of excitatory amino acids in the rat hind instep: Pain is modulated by the interaction between the peripheral opioid and glutamate systems. *Neuroscience* **138**, 1329–1339 (2006).
77. Jackson, D. L., Graff, C. B., Richardson, J. D. & Hargreaves, K. M. Glutamate participates in the peripheral modulation of thermal hyperalgesia in rats. *Eur. J. Pharmacol.* **284**, 321–325 (1995).
78. Lawand, N. B., McNearney, T. & Westlund, K. N. Amino acid release into the knee joint: key role in nociception and inflammation. *Pain* **86**, 69–74 (2000).
79. Carlton, S. M., Zhou, S. & Coggeshall, R. E. Evidence for the interaction of glutamate and NK1 receptors in the periphery. *Brain Res.* **790**, 160–169 (1998).

80. Jin, Y.-H. *et al.* Capsaicin-induced glutamate release is implicated in nociceptive processing through activation of ionotropic glutamate receptors and group I metabotropic glutamate receptor in primary afferent fibers. *J. Pharmacol. Sci.* **109**, 233–241 (2009).
81. Masuoka, T., Ishibashi, Takaharu & Nishio, Matomo. Biphasic modulation of noxious heat sensitivity in sensory neurons by peripheral metabotropic glutamate receptors. *Inflamm. Cell Signal.* (2015). doi:10.14800/ics.602
82. Nordlind, K., Johansson, O., Lidén, S. & Hökfelt, T. Glutamate- and aspartate-like immunoreactivities in human normal and inflamed skin. *Virchows Arch. B Cell Pathol. Incl. Mol. Pathol.* **64**, 75–82 (1993).
83. Warncke, T., Stubhaug, A. & Jørum, E. Preinjury treatment with morphine or ketamine inhibits the development of experimentally induced secondary hyperalgesia in man. *Pain* **86**, 293–303 (2000).
84. Davidson, E. M., Coggeshall, R. E. & Carlton, S. M. Peripheral NMDA and non-NMDA glutamate receptors contribute to nociceptive behaviors in the rat formalin test. *Neuroreport* **8**, 941–946 (1997).
85. Cairns, B. E., Sessle, B. J. & Hu, J. W. Evidence that excitatory amino acid receptors within the temporomandibular joint region are involved in the reflex activation of the jaw muscles. *J. Neurosci. Off. J. Soc. Neurosci.* **18**, 8056–8064 (1998).
86. Davidson, E. M. & Carlton, S. M. Intraplantar injection of dextrorphan, ketamine or memantine attenuates formalin-induced behaviors. *Brain Res.* **785**, 136–142 (1998).
87. Lawand, N. B., Willis, W. D. & Westlund, K. N. Excitatory amino acid receptor involvement in peripheral nociceptive transmission in rats. *Eur. J. Pharmacol.* **324**, 169–177 (1997).
88. Caterina, M. J. *et al.* The capsaicin receptor: a heat-activated ion channel in the pain pathway. *Nature* **389**, 816–824 (1997).

89. Laing, R. J. & Dhaka, A. ThermoTRPs and Pain. *Neurosci. Rev. J. Bringing Neurobiol. Neurol. Psychiatry* **22**, 171–187 (2016).
90. Guo, A., Vulchanova, L., Wang, J., Li, X. & Elde, R. Immunocytochemical localization of the vanilloid receptor 1 (VR1): relationship to neuropeptides, the P2X3 purinoceptor and IB4 binding sites. *Eur. J. Neurosci.* **11**, 946–958 (1999).
91. Maione, S. *et al.* Functional Interaction Between TRPV1 and  $\mu$ -Opioid Receptors in the Descending Antinociceptive Pathway Activates Glutamate Transmission and Induces Analgesia. *J. Neurophysiol.* **101**, 2411–2422 (2009).
92. Tominaga, M. *et al.* The Cloned Capsaicin Receptor Integrates Multiple Pain-Producing Stimuli. *Neuron* **21**, 531–543 (1998).
93. Cui, M. *et al.* TRPV1 receptors in the CNS play a key role in broad-spectrum analgesia of TRPV1 antagonists. *J. Neurosci. Off. J. Soc. Neurosci.* **26**, 9385–9393 (2006).
94. Starowicz, K., Cristino, L. & Di Marzo, V. TRPV1 receptors in the central nervous system: potential for previously unforeseen therapeutic applications. *Curr. Pharm. Des.* **14**, 42–54 (2008).
95. Chung, M.-K., Güler, A. D. & Caterina, M. J. TRPV1 shows dynamic ionic selectivity during agonist stimulation. *Nat. Neurosci.* **11**, 555–564 (2008).
96. Dömötör, A. *et al.* Immunohistochemical distribution of vanilloid receptor, calcitonin-gene related peptide and substance P in gastrointestinal mucosa of patients with different gastrointestinal disorders. *InflammoPharmacology* **13**, 161–177 (2005).
97. Hartel, M. *et al.* Vanilloids in pancreatic cancer: potential for chemotherapy and pain management. *Gut* **55**, 519–528 (2006).
98. Czifra, G. *et al.* Increased expressions of cannabinoid receptor-1 and transient receptor potential vanilloid-1 in human prostate carcinoma. *J. Cancer Res. Clin. Oncol.* **135**, 507–514 (2008).

99. Wu, T. T. L., Peters, A. A., Tan, P. T., Roberts-Thomson, S. J. & Monteith, G. R. Consequences of activating the calcium-permeable ion channel TRPV1 in breast cancer cells with regulated TRPV1 expression. *Cell Calcium* **56**, 59–67 (2014).
100. Koşar, P. A., Nazıroğlu, M., Övey, İ. S. & Çiğ, B. Synergic Effects of Doxorubicin and Melatonin on Apoptosis and Mitochondrial Oxidative Stress in MCF-7 Breast Cancer Cells: Involvement of TRPV1 Channels. *J. Membr. Biol.* (2015). doi:10.1007/s00232-015-9855-0
101. Amantini, C. *et al.* Capsaicin-induced apoptosis of glioma cells is mediated by TRPV1 vanilloid receptor and requires p38 MAPK activation. *J. Neurochem.* **102**, 977–990 (2007).
102. Capiod, T. Cell proliferation, calcium influx and calcium channels. *Biochimie* **93**, 2075–2079 (2011).
103. Bödding, M. TRP proteins and cancer. *Cell. Signal.* **19**, 617–624 (2007).
104. Szallasi, A. & Blumberg, P. M. Vanilloid (Capsaicin) Receptors and Mechanisms. *Pharmacol. Rev.* **51**, 159–212 (1999).
105. Niiyama, Y., Kawamata, T., Yamamoto, J., Omote, K. & Namiki, A. Bone cancer increases transient receptor potential vanilloid subfamily 1 expression within distinct subpopulations of dorsal root ganglion neurons. *Neuroscience* **148**, 560–572 (2007).
106. Seabrook, G. R. *et al.* Functional properties of the high-affinity TRPV1 (VR1) vanilloid receptor antagonist (4-hydroxy-5-iodo-3-methoxyphenylacetate ester) iodo-resiniferatoxin. *J. Pharmacol. Exp. Ther.* **303**, 1052–1060 (2002).
107. Van Buren, J. J., Bhat, S., Rotello, R., Pauza, M. E. & Premkumar, L. S. Sensitization and translocation of TRPV1 by insulin and IGF-I. *Mol. Pain* **1**, 17 (2005).
108. Ji, R.-R., Samad, T. A., Jin, S.-X., Schmoll, R. & Woolf, C. J. p38 MAPK Activation by NGF in Primary Sensory Neurons after Inflammation Increases TRPV1 Levels and Maintains Heat Hyperalgesia. *Neuron* **36**, 57–68 (2002).
109. Voets, T. *et al.* The principle of temperature-dependent gating in cold- and heat-sensitive TRP channels. *Nature* **430**, 748–754 (2004).

110. Planells-Cases, R., Garcia-Sanz, N., Morenilla-Palao, C. & Ferrer-Montiel, A. Functional aspects and mechanisms of TRPV1 involvement in neurogenic inflammation that leads to thermal hyperalgesia. *Pflüg. Arch. Eur. J. Physiol.* **451**, 151–159 (2005).
111. Bhave, G., Karim, F., Carlton, S. M. & Gereau Iv, R. W. Peripheral group I metabotropic glutamate receptors modulate nociception in mice. *Nat. Neurosci.* **4**, 417–423 (2001).
112. Carlton, S. M., Hargett, G. L. & Coggeshall, R. E. Localization and activation of glutamate receptors in unmyelinated axons of rat glabrous skin. *Neurosci. Lett.* **197**, 25–28 (1995).
113. Hrabetova, S. *et al.* Distinct NMDA receptor subpopulations contribute to long-term potentiation and long-term depression induction. *J. Neurosci. Off. J. Soc. Neurosci.* **20**, RC81 (2000).
114. Liu, X. G. & Sandkühler, J. Long-term potentiation of C-fiber-evoked potentials in the rat spinal dorsal horn is prevented by spinal N-methyl-D-aspartic acid receptor blockage. *Neurosci. Lett.* **191**, 43–46 (1995).
115. Zhou, S., Bonasera, L. & Carlton, S. M. Peripheral administration of NMDA, AMPA or KA results in pain behaviors in rats. *Neuroreport* **7**, 895–900 (1996).
116. Ghilardi, J. R. *et al.* Selective blockade of the capsaicin receptor TRPV1 attenuates bone cancer pain. *J. Neurosci. Off. J. Soc. Neurosci.* **25**, 3126–3131 (2005).
117. Ahern, G. P., Wang, X. & Miyares, R. L. Polyamines are potent ligands for the capsaicin receptor TRPV1. *J. Biol. Chem.* **281**, 8991–8995 (2006).
118. Babbar, N. & Gerner, E. W. Targeting Polyamines and Inflammation for Cancer Prevention. *Recent Results Cancer Res. Fortschritte Krebsforsch. Progres Dans Rech. Sur Cancer* **188**, 49–64 (2011).
119. Bloom, A. P. *et al.* Breast cancer-induced bone remodeling, skeletal pain, and sprouting of sensory nerve fibers. *J. Pain Off. J. Am. Pain Soc.* **12**, 698–711 (2011).

120. Chenu, C., Serre, C. M., Raynal, C., Burt-Pichat, B. & Delmas, P. D. Glutamate receptors are expressed by bone cells and are involved in bone resorption. *Bone* **22**, 295–299 (1998).
121. Genever, P. G. & Skerry, T. M. Regulation of spontaneous glutamate release activity in osteoblastic cells and its role in differentiation and survival: evidence for intrinsic glutamatergic signaling in bone. *FASEB J. Off. Publ. Fed. Am. Soc. Exp. Biol.* **15**, 1586–1588 (2001).
122. Hu, H.-J. & Gereau, R. W. ERK Integrates PKA and PKC Signaling in Superficial Dorsal Horn Neurons. II. Modulation of Neuronal Excitability. *J. Neurophysiol.* **90**, 1680–1688 (2003).
123. Jin, Y.-H., Takemura, M., Furuyama, A. & Yonehar, N. Interactions Between Glutamate Receptors and TRPV1 Involved in Nociceptive Processing at Peripheral Endings of Primary Afferent Fibers. in *Pharmacology* (ed. Gallelli, L.) (InTech, 2012).
124. Asai, H. *et al.* Heat and mechanical hyperalgesia in mice model of cancer pain. *Pain* **117**, 19–29 (2005).
125. Jara-Oseguera, A., Simon, S. A. & Rosenbaum, T. TRPV1: ON THE ROAD TO PAIN RELIEF. *Curr. Mol. Pharmacol.* **1**, 255–269 (2008).
126. Menéndez, L. *et al.* Analgesic effects of capsazepine and resiniferatoxin on bone cancer pain in mice. *Neurosci. Lett.* **393**, 70–73 (2006).
127. Kort, M. E. & Kym, P. R. TRPV1 antagonists: clinical setbacks and prospects for future development. *Prog. Med. Chem.* **51**, 57–70 (2012).
128. Szolcsányi, J. & Sándor, Z. Multimeric TRPV1 nocisensor: a target for analgesics. *Trends Pharmacol. Sci.* **33**, 646–655 (2012).
129. Matés, J. M. *et al.* Glutamine homeostasis and mitochondrial dynamics. *Int. J. Biochem. Cell Biol.* **41**, 2051–2061 (2009).
130. Suzuki, S. *et al.* Phosphate-activated glutaminase (GLS2), a p53-inducible regulator of glutamine metabolism and reactive oxygen species. *Proc. Natl. Acad. Sci. U. S. A.* **107**, 7461–7466 (2010).

131. Warburg, O. On the origin of cancer cells. *Science* **123**, 309–314 (1956).
132. Szeliga, M. & Obara-Michlewska, M. Glutamine in neoplastic cells: focus on the expression and roles of glutaminases. *Neurochem. Int.* **55**, 71–75 (2009).
133. Botman, D., Tigchelaar, W. & Van Noorden, C. J. F. Determination of phosphate-activated glutaminase activity and its kinetics in mouse tissues using metabolic mapping (quantitative enzyme histochemistry). *J. Histochem. Cytochem. Off. J. Histochem. Soc.* **62**, 813–826 (2014).
134. Martín-Rufián, M. *et al.* Mammalian glutaminase Gls2 gene encodes two functional alternative transcripts by a surrogate promoter usage mechanism. *PLoS One* **7**, e38380 (2012).
135. Elgadi, K. M., Meguid, R. A., Qian, M., Souba, W. W. & Abcouwer, S. F. Cloning and analysis of unique human glutaminase isoforms generated by tissue-specific alternative splicing. *Physiol. Genomics* **1**, 51–62 (1999).
136. Cassago, A. *et al.* Mitochondrial localization and structure-based phosphate activation mechanism of Glutaminase C with implications for cancer metabolism. *Proc. Natl. Acad. Sci.* **109**, 1092–1097 (2012).
137. de la Rosa, V. *et al.* A novel glutaminase isoform in mammalian tissues. *Neurochem. Int.* **55**, 76–84 (2009).
138. Olalla, L., Aledo, J. C., Bannenberg, G. & Márquez, J. The C-terminus of human glutaminase L mediates association with PDZ domain-containing proteins. *FEBS Lett.* **488**, 116–122 (2001).
139. Curthoys, N. P. & Watford, M. Regulation of glutaminase activity and glutamine metabolism. *Annu. Rev. Nutr.* **15**, 133–159 (1995).
140. Gómez-Fabre, P. M. *et al.* Molecular cloning, sequencing and expression studies of the human breast cancer cell glutaminase. *Biochem. J.* **345 Pt 2**, 365–375 (2000).

141. Aledo, J. C., Gómez-Fabre, P. M., Olalla, L. & Márquez, J. Identification of two human glutaminase loci and tissue-specific expression of the two related genes. *Mamm. Genome Off. J. Int. Mamm. Genome Soc.* **11**, 1107–1110 (2000).
142. Castell, L., Vance, C., Abbott, R., Marquez, J. & Eggleton, P. Granule localization of glutaminase in human neutrophils and the consequence of glutamine utilization for neutrophil activity. *J. Biol. Chem.* **279**, 13305–13310 (2004).
143. Pérez-Gómez, C. *et al.* Co-expression of glutaminase K and L isoenzymes in human tumour cells. *Biochem. J.* **386**, 535–542 (2005).
144. Wang, J.-B. *et al.* Targeting Mitochondrial Glutaminase Activity Inhibits Oncogenic Transformation. *Cancer Cell* **18**, 207–219 (2010).
145. van den Heuvel, A. P. J., Jing, J., Wooster, R. F. & Bachman, K. E. Analysis of glutamine dependency in non-small cell lung cancer: GLS1 splice variant GAC is essential for cancer cell growth. *Cancer Biol. Ther.* **13**, 1185–1194 (2012).
146. Huang, W. *et al.* A proposed role for glutamine in cancer cell growth through acid resistance. *Cell Res.* **23**, 724–727 (2013).
147. Le, A. *et al.* Glucose-independent glutamine metabolism via TCA cycling for proliferation and survival in B cells. *Cell Metab.* **15**, 110–121 (2012).
148. Seltzer, M. J. *et al.* Inhibition of glutaminase preferentially slows growth of glioma cells with mutant IDH1. *Cancer Res.* **70**, 8981–8987 (2010).
149. Szeliga, M. *et al.* Relative expression of mRNAs coding for glutaminase isoforms in CNS tissues and CNS tumors. *Neurochem. Res.* **33**, 808–813 (2008).
150. Márquez, J. *et al.* New insights into brain glutaminases: beyond their role on glutamatergic transmission. *Neurochem. Int.* **55**, 64–70 (2009).
151. Cangro, C. B., Sweetnam, P. M., Neale, J. H., Haser, W. G. & Curthoys, N. P. Selective localization of glutaminase in spinal and sensory nerve cells. A potential marker for glutamate neurotransmission. *JAMA* **251**, 797 (1984).

152. Bosoi, C. R. & Rose, C. F. Identifying the direct effects of ammonia on the brain. *Metab. Brain Dis.* **24**, 95–102 (2009).
153. Wise, D. R. *et al.* Myc regulates a transcriptional program that stimulates mitochondrial glutaminolysis and leads to glutamine addiction. *Proc. Natl. Acad. Sci. U. S. A.* **105**, 18782–18787 (2008).
154. Yuneva, M., Zamboni, N., Oefner, P., Sachidanandam, R. & Lazebnik, Y. Deficiency in glutamine but not glucose induces MYC-dependent apoptosis in human cells. *J. Cell Biol.* **178**, 93–105 (2007).
155. Gao, P. *et al.* c-Myc suppression of miR-23a/b enhances mitochondrial glutaminase expression and glutamine metabolism. *Nature* **458**, 762–765 (2009).
156. Rathore, M. G. *et al.* The NF- $\kappa$ B member p65 controls glutamine metabolism through miR-23a. *Int. J. Biochem. Cell Biol.* **44**, 1448–1456 (2012).
157. Zhao, L. *et al.* Interferon- $\alpha$  regulates glutaminase 1 promoter through STAT1 phosphorylation: relevance to HIV-1 associated neurocognitive disorders. *PLoS One* **7**, e32995 (2012).
158. Thangavelu, K. *et al.* Structural basis for the allosteric inhibitory mechanism of human kidney-type glutaminase (KGA) and its regulation by Raf-Mek-Erk signaling in cancer cell metabolism. *Proc. Natl. Acad. Sci. U. S. A.* **109**, 7705–7710 (2012).
159. Bergström, J., Fürst, P., Norée, L. O. & Vinnars, E. Intracellular free amino acid concentration in human muscle tissue. *J. Appl. Physiol.* **36**, 693–697 (1974).
160. Kuhn, K. S., Schuhmann, K., Stehle, P., Darmaun, D. & Fürst, P. Determination of glutamine in muscle protein facilitates accurate assessment of proteolysis and de novo synthesis-derived endogenous glutamine production. *Am. J. Clin. Nutr.* **70**, 484–489 (1999).
161. Knox, W. E., Horowitz, M. L. & Friedell, G. H. The proportionality of glutaminase content to growth rate and morphology of rat neoplasms. *Cancer Res.* **29**, 669–680 (1969).

162. Linder-Horowitz, M., Knox, W. E. & Morris, H. P. Glutaminase activities and growth rates of rat hepatomas. *Cancer Res.* **29**, 1195–1199 (1969).
163. Lobo, C. *et al.* Inhibition of glutaminase expression by antisense mRNA decreases growth and tumorigenicity of tumour cells. *Biochem. J.* **348 Pt 2**, 257–261 (2000).
164. Zacharias, D. P. M. *et al.* Human cutaneous melanoma expresses a significant phosphate-dependent glutaminase activity: a comparison with the surrounding skin of the same patient. *Cell Biochem. Funct.* **21**, 81–84 (2003).
165. DeBerardinis, R. J. & Cheng, T. Q's next: the diverse functions of glutamine in metabolism, cell biology and cancer. *Oncogene* **29**, 313–324 (2010).
166. Miller, K. E., Hoffman, E. M., Sutharshan, M. & Schechter, R. Glutamate pharmacology and metabolism in peripheral primary afferents: Physiological and pathophysiological mechanisms. *Pharmacol. Ther.* **130**, 283–309 (2011).
167. Besson, J. M. The neurobiology of pain. *Lancet Lond. Engl.* **353**, 1610–1615 (1999).
168. Kidd, B. L. & Urban, L. A. Mechanisms of inflammatory pain. *Br. J. Anaesth.* **87**, 3–11 (2001).
169. Hoffman, E. M. & Miller, K. E. Peripheral inhibition of glutaminase reduces carrageenan-induced Fos expression in the superficial dorsal horn of the rat. *Neurosci. Lett.* **472**, 157–160 (2010).
170. Hanesch, U., Pfrommer, U., Grubb, B. D., Heppelmann, B. & Schaible, H. G. The proportion of CGRP-immunoreactive and SP-mRNA containing dorsal root ganglion cells is increased by a unilateral inflammation of the ankle joint of the rat. *Regul. Pept.* **46**, 202–203 (1993).
171. Bulling, D. G., Kelly, D., Bond, S., McQueen, D. S. & Seckl, J. R. Adjuvant-induced joint inflammation causes very rapid transcription of beta-preprotachykinin and alpha-CGRP genes in innervating sensory ganglia. *J. Neurochem.* **77**, 372–382 (2001).

172. Marlier, L., Poulat, P., Rajaofetra, N. & Privat, A. Modifications of serotonin-, substance P- and calcitonin gene-related peptide-like immunoreactivities in the dorsal horn of the spinal cord of arthritic rats: a quantitative immunocytochemical study. *Exp. Brain Res.* **85**, 482–490 (1991).
173. Nahin, R. L. & Byers, M. R. Adjuvant-induced inflammation of rat paw is associated with altered calcitonin gene-related peptide immunoreactivity within cell bodies and peripheral endings of primary afferent neurons. *J. Comp. Neurol.* **349**, 475–485 (1994).
174. Lee, M. *et al.* Complete Freund's adjuvant-induced intervertebral discitis as an animal model for discogenic low back pain. *Anesth. Analg.* **109**, 1287–1296 (2009).
175. Battaglia, G. & Rustioni, A. Coexistence of glutamate and substance P in dorsal root ganglion neurons of the rat and monkey. *J. Comp. Neurol.* **277**, 302–312 (1988).
176. Miller, K. E., Douglas, V. D. & Kaneko, T. Glutaminase immunoreactive neurons in the rat dorsal root ganglion contain calcitonin gene-related peptide (CGRP). *Neurosci. Lett.* **160**, 113–116 (1993).
177. Miller, K. E., Richards, B. A. & Kriebel, R. M. Glutamine-, glutamine synthetase-, glutamate dehydrogenase- and pyruvate carboxylase-immunoreactivities in the rat dorsal root ganglion and peripheral nerve. *Brain Res.* **945**, 202–211 (2002).
178. Skilling, S. R., Smullin, D. H., Beitz, A. J. & Larson, A. A. Extracellular amino acid concentrations in the dorsal spinal cord of freely moving rats following veratridine and nociceptive stimulation. *J. Neurochem.* **51**, 127–132 (1988).
179. Sluka, K. A., Dougherty, P. M., Sorkin, L. S., Willis, W. D. & Westlund, K. N. Neural changes in acute arthritis in monkeys. III. Changes in substance P, calcitonin gene-related peptide and glutamate in the dorsal horn of the spinal cord. *Brain Res. Brain Res. Rev.* **17**, 29–38 (1992).

180. Yang, L. C., Marsala, M. & Yaksh, T. L. Characterization of time course of spinal amino acids, citrulline and PGE<sub>2</sub> release after carrageenan/kaolin-induced knee joint inflammation: a chronic microdialysis study. *Pain* **67**, 345–354 (1996).
181. Dmitrieva, N., Rodríguez-Malaver, A. J., Pérez, J. & Hernández, L. Differential release of neurotransmitters from superficial and deep layers of the dorsal horn in response to acute noxious stimulation and inflammation of the rat paw. *Eur. J. Pain Lond. Engl.* **8**, 245–252 (2004).
182. Woolf, C. J. & Ma, Q. Nociceptors--noxious stimulus detectors. *Neuron* **55**, 353–364 (2007).
183. Kvamme, E., Torgner, I. A. & Roberg, B. Kinetics and localization of brain phosphate activated glutaminase. *J. Neurosci. Res.* **66**, 951–958 (2001).
184. Miller, K. E. *et al.* Glutaminase Immunoreactivity and Enzyme Activity Is Increased in the Rat Dorsal Root Ganglion Following Peripheral Inflammation. *Pain Res. Treat.* **2012**, (2012).
185. Werner, P., Pitt, D. & Raine, C. S. Multiple sclerosis: altered glutamate homeostasis in lesions correlates with oligodendrocyte and axonal damage. *Ann. Neurol.* **50**, 169–180 (2001).
186. Kisner, D. L., Catane, R. & Muggia, F. M. The rediscovery of DON (6-diazo-5-oxo-L-norleucine). *Recent Results Cancer Res. Fortschritte Krebsforsch. Prog. Dans Rech. Sur Cancer* **74**, 258–263 (1980).
187. Pinkus, L. M. Glutamine binding sites. *Methods Enzymol.* **46**, 414–427 (1977).
188. Catane, R., Von Hoff, D. D., Glaubiger, D. L. & Muggia, F. M. Azaserine, DON, and azotomycin: three diazo analogs of L-glutamine with clinical antitumor activity. *Cancer Treat. Rep.* **63**, 1033–1038 (1979).
189. Katt, W. P., Ramachandran, S., Erickson, J. W. & Cerione, R. A. Dibenzophenanthridines as inhibitors of glutaminase C and cancer cell proliferation. *Mol. Cancer Ther.* **11**, 1269–1278 (2012).

190. Simpson, N. E., Tryndyak, V. P., Beland, F. A. & Pogribny, I. P. An in vitro investigation of metabolically sensitive biomarkers in breast cancer progression. *Breast Cancer Res. Treat.* **133**, 959–968 (2012).
191. Simpson, N. E., Tryndyak, V. P., Pogribna, M., Beland, F. A. & Pogribny, I. P. Modifying metabolically sensitive histone marks by inhibiting glutamine metabolism affects gene expression and alters cancer cell phenotype. *Epigenetics* **7**, 1413–1420 (2012).
192. Tardito, S. *et al.* L-Asparaginase and inhibitors of glutamine synthetase disclose glutamine addiction of  $\beta$ -catenin-mutated human hepatocellular carcinoma cells. *Curr. Cancer Drug Targets* **11**, 929–943 (2011).
193. Robinson, M. M. *et al.* Novel mechanism of inhibition of rat kidney-type glutaminase by bis-2-(5-phenylacetamido-1,2,4-thiadiazol-2-yl)ethyl sulfide (BPTES). *Biochem. J.* **406**, 407–414 (2007).
194. Hartwick, E. W. & Curthoys, N. P. BPTES inhibition of hGA(124-551), a truncated form of human kidney-type glutaminase. *J. Enzyme Inhib. Med. Chem.* **27**, 861–867 (2012).
195. Erdmann, N. *et al.* Glutamate production by HIV-1 infected human macrophage is blocked by the inhibition of glutaminase. *J. Neurochem.* **102**, 539–549 (2007).
196. Vega-Pérez, J. M. *et al.* Isoprenyl-thiourea and urea derivatives as new farnesyl diphosphate analogues: synthesis and in vitro antimicrobial and cytotoxic activities. *Eur. J. Med. Chem.* **58**, 591–612 (2012).
197. Gross, M. I. *et al.* Antitumor activity of the glutaminase inhibitor CB-839 in triple-negative breast cancer. *Mol. Cancer Ther.* **13**, 890–901 (2014).

**CHAPTER 2: INHIBITORS OF GLUTAMATE  
RELEASE FROM BREAST CANCER CELLS; NEW  
TARGETS FOR CANCER-INDUCED BONE-PAIN**

## PREFACE:

In this chapter, an author-generated version of the manuscript entitled:

“Inhibitors of glutamate release from breast cancer cells; new targets for cancer-induced bone-pain” published in *Scientific Reports* February 2015 is included. The paper is reproduced with permission from **Nature Publishing Group** as stated in the licence and copyright agreement:

*“Scientific Reports does not require authors to assign copyright of their published original research papers to the journal. Articles are published under a [CC BY license](#) (Creative Commons Attribution 4.0 International License). The CC BY license allows for maximum dissemination and re-use of open access materials and is preferred by many research funding bodies. Under this license users are free to share (copy, distribute and transmit) and remix (adapt) the contribution including for commercial purposes, providing they attribute the contribution in the manner specified by the author or licensor.”*

In the following manuscript, I conducted a high-throughput screen alongside Dr. Hanxin Lin. I performed all follow up experiments, cell culturing and treatments including optimization of the Amplex Red protocol (Appendix 1). I am responsible for writing and revising the manuscript as well as preparing all figures. The objective of this first chapter was to screen for small molecules including synthetic derivatives and bioactives from

the Canadian Compound Library at McMaster University with the goal of identifying potential novel inhibitors of glutamate release from the MDA-MB-231 breast cancer cell line that models an aggressive, triple negative cancer with high metastatic potential. This line is used in our lab to generate a cancer-induced bone pain model and was therefore deemed appropriate to use this cell line for screening. Glutamate concentrations were measured in cell culture media after an incubation period of 48 hours with the test compound using the Amplex Red assay. This assay was adapted to screening conditions by Dr. Hanxin Lin to ensure stability of the fluorescent probe, cell plating density and optimal incubation times. The automated high-throughput liquid handling protocols were designed by Cecilia Murphy of the Centre for Microbial Chemical Biology at McMaster University who also prepared compound libraries, performed Z' factor calculation, and initial data analysis composing Figure 1 in the following publication as well as compound hit identification.

## RATIONALE:

Targeting system  $x_c^-$  has proven to be a viable way to modulate CIBP behaviours in an animal model of this condition. Based on the hypothesis that CIBP is at least in part mediated by glutamate released from invading cancer cells and glutamate's role in dysregulated bone remodeling and nociception this antiporter remains an attractive therapeutic target for developing novel treatments for CIBP. Previously, the anti-rheumatic drug, Sulfasalazine (SSZ) was found to have off-target effects as an inhibitor of system  $x_c^-$  and was able to delay the onset of CIBP behaviours. Due to the poor bioavailability of the drug, required dose and unwanted side-effects, SSZ does not represent a viable therapeutic to be repurposed outside of preclinical models for

treatment of CIBP. Therefore, identifying other molecules targeting this antiporter was the goal of this first study and represents the preliminary stages in development of novel CIBP treatment strategies.

Please note the following publication uses American spelling as per the request of the journal.

## ABSTRACT:

Glutamate is an important signaling molecule in a wide variety of tissues. Aberrant glutamatergic signaling disrupts normal tissue homeostasis and induces several disruptive pathological conditions including pain. Breast cancer cells secrete high levels of glutamate and often metastasize to bone. Exogenous glutamate can disrupt normal bone turnover and may be responsible for cancer-induced bone pain (CIBP). CIBP is a significant co-morbidity that affects quality of life for many advanced-stage breast cancer patients. Current treatment options are commonly accompanied by serious side-effects that negatively impact patient care. Identifying small molecule inhibitors of glutamate release from aggressive breast cancer cells advances a novel, mechanistic approach to targeting CIBP that could advance treatment for several pathological conditions. Using high-throughput screening, we investigated the ability of approximately 30,000 compounds from the Canadian Compound Collection to reduce glutamate release from MDA-MB-231 breast cancer cells. This line is known to secrete high levels of glutamate and has been demonstrated to induce CIBP by this mechanism. Positive chemical hits were based on the potency of each molecule relative to a known pharmacological inhibitor of glutamate release, sulfasalazine. Efficacy was confirmed and drug-like molecules were identified as potent inhibitors of glutamate secretion from MDA-MB-231, MCF-7 and Mat-Ly-Lu cells.

## INTRODUCTION:

Bone metastasis is a common characteristic of advanced, highly aggressive breast cancer<sup>1</sup>. A high proportion of breast cancer patients presenting with bone metastases experience significant co-morbidities such as bone fracture and hypercalcemia<sup>2 3</sup>. The most prominent, however, is the manifestation of severe, intractable cancer-induced bone pain (CIBP)<sup>4</sup>. This unique chronic pain state can significantly compromise patient quality of life and functional status. Furthermore, therapeutic strategies for severe cancer pain are often constrained by dose-limiting side effects and acquired treatment resistance. The satisfactory management of chronic pain is essential to successful palliative care in cancer patients. In patients with tumours, 15-75% present with significant chronic pain. While pain management is increasingly a priority in cancer care, the cancer-induced pain state is poorly characterized and treatment outcomes can frequently exacerbate the poor quality of life experienced by most patients<sup>5</sup>. As CIBP has been demonstrated to be a unique pain state distinct from other chronic pain conditions<sup>6</sup>, there is the potential and the need to develop unique treatments for CIBP. Investigating and targeting the factors that initiate CIBP may allow for the development of effective therapeutics with minimal side effects. Investigating the effects of tumour-secreted factors on the host microenvironment, such as the bone, will provide insights into the physiological mechanisms underlying CIBP. In turn, this will aid in the development of novel pharmacological strategies for targeted pain interventions.

Glutamate is both an ubiquitous cell-signaling molecule in many tissues and a well-characterized excitatory neurotransmitter in the central nervous system (CNS), where it is involved in nociception and pain sensitization<sup>7, 8</sup>. Both metabotropic and

ionotropic glutamate receptors are involved in pain hypersensitivity<sup>9</sup>, and glutamate secretion is associated with peripheral tissue injury and inflammation<sup>10, 11</sup>. Glutamate is also implicated peripherally in a variety of non-malignant painful states including polymyalgia<sup>12</sup>, arthritis<sup>13, 14</sup> and other inflammatory disorders<sup>10, 15</sup>. Therefore, glutamate plays a key role in both central and peripheral propagation of pain including the development of features of chronic pain and hypersensitivity. In addition to its role in the CNS, glutamate is also an important metabolic component and signaling molecule in the periphery<sup>16, 17</sup>. Among the spleen, pancreas, lung, heart, liver and other organs of the digestive and reproductive system, bone is also sensitive to glutamatergic signaling<sup>18, 19</sup>. In the restricted environment of the bone, glutamate acts in an autocrine and paracrine manner, coordinating intra- and intercellular communication between prominent cells of the bone such as osteoblasts and osteoclasts. Signaling between these cells coordinates bone deposition and resorption in a glutamate-dependent manner<sup>19, 20, 21</sup>.

Intracellular glutamate is primarily a product of glutamine metabolism in cancer cells with a proportion of this glutamate pool destined for secretion<sup>22, 23, 24</sup>. In cancer cells, amplified secretion of glutamate, as well as other aspects of dysregulated glutamatergic signaling, have been shown to correlate with a malignant phenotype<sup>25, 26, 27</sup>. For example, exogenous glutamate secretion from glioma cells in the CNS allows tumour expansion and metastasis through excitotoxic cell death of proximal neurons and glial cells<sup>28</sup>. In the periphery, cancer cell lines including breast and prostate cancers associated with bone metastases also exhibit increased secretion of glutamate that contributes to the disruption of normal bone homeostasis and CIBP<sup>21</sup>.

Increased glutamine consumption is a hallmark of many neoplasms and cancer cells. Many aggressive breast cancer cell lines have been observed to be glutamine auxotrophs<sup>29</sup>. Glutamine is the major energy source for many tumours, as it is able to meet the bioenergetic demands of cancer cells while providing macromolecular intermediates that are required for rapid growth and proliferation<sup>30</sup>. Glutamine metabolism is initiated by the glutaminase-mediated conversion of L-glutamine to L-glutamate. With further processing by glutamate dehydrogenase, the resulting product,  $\alpha$ -ketoglutarate, can directly enter the TCA cycle. Furthermore, glutamine metabolism provides molecular precursors for glutathione synthesis which maintain redox equilibrium in rapidly proliferating cancer cells<sup>31, 32</sup>. In malignancies, the demand for glutamine rapidly surmounts its endogenous supply, exceeding that needed for biosynthetic processing alone<sup>33</sup>. Generally classified as a non-essential amino acid, an exogenous glutamine supply becomes essential for cancer cell metabolism and survival.

Glutamate signaling involves several classes of receptors. In transformed cells, metabotropic glutamate receptors have been shown to confer oncogenic potential<sup>34, 35</sup>. Such G-protein coupled receptors with oncogenic activity are associated with increased local levels of their ligand. The production of a ligand such as glutamate, by either the tumour itself or surrounding tissue promotes ectopic expression and continued activation of its receptors<sup>36, 37</sup>. The growth of several types of tumours such as glioma<sup>26, 38</sup>, breast cancer<sup>27</sup> and melanoma<sup>25, 39</sup> has been attenuated by inhibiting glutamatergic signaling in xenografts and cultured cell lines.

A variety of mechanisms may affect the secretion of glutamate from cancer cells. In addition to pathways that produce an intracellular source of glutamate, mechanisms that transport this amino acid across the plasma membrane should be considered as targets for pharmacological inhibition. Notably, breast and prostate cancer cells secrete high concentrations of glutamate through the activity of the cystine/glutamate antiporter, system  $x_c^{-24, 38}$ . Survival of these tumours, amongst others, is dependent on this system, where its inhibition effects cell growth and viability<sup>40, 29</sup>. System  $x_c^{-}$  is a  $Na^{+}$ -independent, anionic amino acid transporter<sup>41</sup>. It is composed of heavy and light chain subunits, 4F2hc and xCT, respectively<sup>42</sup>. A ubiquitous glycoprotein, 4F2hc facilitates the transport of the light chain to the plasma membrane<sup>43</sup>. The light chain, xCT is an integral membrane protein with twelve transmembrane domains. It is this subunit that confers specificity to this transport system, facilitating the 1:1 exchange of the anionic form of cystine for L-glutamate<sup>44</sup>. MDA-MB-231 triple-negative breast cancer cells express several glutamate receptors and transporters driving both glutamate secretion and uptake<sup>38</sup>. It has been shown that glutamate secretion from these cells is limited by an inhibitor of system  $x_c^{-}$ , sulfasalazine (SSZ)<sup>45</sup>. However, inhibition of the vesicular glutamate transporter (VGLUT-1) does not affect glutamate release<sup>38</sup>. This suggests that a large proportion of glutamate is secreted through system  $x_c^{-}$ . In addition, we have previously shown that in a mouse model of CIBP, treatment with SSZ attenuated pain behaviours in mice harbouring intrafemoral MDA-MB-231 xenografts<sup>46</sup>. Furthermore, the excitotoxic levels of glutamate release from glioma is also attributed to the activity of system  $x_c^{-}$ <sup>47</sup>. System  $x_c^{-}$  inhibition has also demonstrated advantageous results in several other cancer-associated pathologies. These include inducing a reduction in

epileptic seizures associated with glioma<sup>48</sup>, decreasing cellular resistance to chemotherapy<sup>49</sup>, and increasing cell susceptibility to oxidative stress, leading to greater cancer cell death<sup>50</sup>. Although a widely utilized drug for ulcerative colitis and rheumatoid arthritis, SSZ is not an immediately viable therapeutic option for system  $x_C^-$  inhibition due to its limited bioavailability when administered orally. The inhibitory action of SSZ on system  $x_C^-$  is dependent on the whole molecule not its colonic metabolites, sulfapyridine and 5-aminosalicylic acid<sup>40, 45</sup>. It is therefore of considerable interest to identify other compounds that act on a target such as system  $x_C^-$  in order to treat CIBP. Inhibiting the release of glutamate from the cancer cells themselves is a novel, mechanistic strategy to eliminate the causative agent of several pathological conditions caused by metastatic cancer, including severe CIBP.

## RESULTS:

### *High-throughput screening for the inhibition of glutamate release from MDA-MB-231 cells:*

A live cell-based screen was used for primary screening to achieve physiologically relevant results and thus foster the selection of higher-quality candidate compounds. In the Amplex Red assay, L-glutamate present in cell culture media is measured indirectly based on the level of  $H_2O_2$  produced from the oxidation of L-glutamate by L-glutamate oxidase (producing  $\alpha$ -ketoglutarate,  $NH_3$ , and  $H_2O_2$ ). Peroxide production is then quantified through the generation of a fluorescent product, resorufin by a horseradish peroxidase (HRP)-catalyzed reaction with the Amplex Red reagent. Initially, the Z' factor was calculated to identify the statistical window to assess the effectiveness of the Amplex Red assay for extracellular glutamate in high-throughput screening (HTS). This

window exists at least 3 standard deviations below the extracellular glutamate levels of the high control, DMSO, and 3 standard deviations above the low control, SSZ after a 48 hour incubation. The Z' factor calculated for production of the fluorescent product of the assay, resorufin, was consistently higher than 0.6. With the maximum Z' factor being 1, this assay was determined to be suitable for HTS.

Fluorescence was measured 10 times at 90 second intervals for each plate. The rate change of relative fluorescent units versus time was calculated and used as indicator of inhibitory potency. The results were expressed as a ratio of the rate change between a testing compound and the positive control, SSZ (Fig. 1). A ratio of 1.0 means that the test compound, at a 10  $\mu$ M screening concentration, has the same potency of inhibition as 200 $\mu$ M SSZ. Approximately 500 positive hits were identified from the primary screening. Among these compounds, 110 were 0.2-fold (i.e. 5 times) more potent than SSZ, 127 were less than 0.4-fold, 292 were less than 1-fold, and 320 were less than 1.1-fold. These 320 compounds were selected for secondary screening. During secondary screening, cell viability was assessed visually following treatment with the compounds selected from the primary screen. A potent cytotoxic compound would not qualify as a viable therapeutic candidate, as it most likely would have targets outside the tumour in healthy tissue when administered in vivo. Eliminating these compounds with potent cytotoxicity narrowed the range of positive hits before progressing to secondary screening. Ultimately, 7 compounds were identified as viable potent inhibitors of glutamate release with low to moderate cytotoxicity. These compounds were (R,R)-cis-Diethyltetrahydro-2,8-chrysendiol, (+/-)-SKF38393 hydrochloride, N,N-dipropyl dopamine hydrobromide (NNDP), capsazepine, SKF83565 hydrobromide,

KM02894 and BTB01303 (Fig. 2). Among them, SKF38393, SKF83565 and NNDP are well-characterized dopamine receptor agonists, while capsazepine is a vanilloid receptor antagonist. Interestingly, these four compounds share a substituted benzazepine functional group. Substituted benzazepine derivatives (1-phenyl-1H-3-benzazepines) have been shown to have specificity for the dopamine D1 receptor<sup>51</sup>. Due to supplier availability, SKF83565 and KM02894 were not available for subsequent testing. (R,R)-cis-Diethyltetrahydro-2,8-chrysendiol and BTB01303 were eliminated due to structurally predicted auto-fluorescence that may interfere with the glutamate release assay. As a result, SKF38393, NNDP and capsazepine were selected for follow-up testing to assess their cytotoxicity and inhibitory effect on glutamate release in a 96-well plate format. Ultimately, capsazepine, SKF 38393 and NNDP showed low to moderate cytotoxicity (Fig. 3) and dose-dependent inhibition of glutamate release (Fig. 4).

#### *IC<sub>50</sub> Values for SKF 38393, N,N-dipropyldopamine and Capsazepine:*

In the Amplex Red reaction, glutamate is initially converted to  $\alpha$ -ketoglutarate by glutamate oxidase, which produces  $H_2O_2$ . This initiates the HRP-catalyzed reaction with the Amplex Red reagent to generate the fluorescent product, resorufin, which is quantified to indirectly measure glutamate. Therefore, the final fluorescent readout is potentially affected by  $H_2O_2$  released by the cells when testing a range of concentrations. Our data showed that  $H_2O_2$  production was not a confounding factor except at high doses of SKF38393 and capsazepine ( $\geq 100 \mu M$ ; data not shown). These concentrations were eliminated from further testing. SKF38393, NNDP and capsazepine had  $IC_{50}$  values lower than that of SSZ, suggesting greater potency than the positive

control. After normalizing to viable cell number quantified 48 hours post inoculation, the  $IC_{50}$  of capsazepine, SKF38393, NNDP and SSZ was calculated as 17.72, 20.12, 25.45 and 79.59  $\mu$ M, respectively (Fig. 4). Therefore, capsazepine, SKF38393 and NNDP are more potent inhibitors of glutamate release from cancer cells than SSZ.

## DISCUSSION:

The objective of this study was to identify small molecule inhibitors of glutamate secretion from human breast cancer cells. HTS of small molecules is an important stage of drug discovery. HTS allows for the identification of new agents that target glutamate release from an aggressive, metastatic breast cancer cell line that we have previously used to induce a cancer-induced pain state<sup>46</sup>. This investigation represents a novel approach to treating cancer pain and is a stepping-stone in developing new, targeted therapeutic strategies for this unique chronic pain state.

As a means of identifying potential mechanisms that contribute to excess glutamate release from cancer cells, the small molecules selected from our HTS implicate several novel molecular targets. Due to the high metabolic activity of cancer cells, the production of antioxidants must be upregulated to effectively maintain redox equilibrium. Glutamate release from cancer cells is thought to be a byproduct of a protective mechanism against oxidative stress. Synthesis of glutathione (GSH), the predominant cellular antioxidant, relies on the acquisition of cysteine as the rate-limiting step. Cysteine is acquired extracellularly in its oxidized form, cystine, through the action of the cystine/glutamate antiporter system  $x_C^-$ . This transport activity, which is

upregulated in cancer cells, necessitates the release of glutamate and is responsible for the majority of glutamate release in several cancer cell lines<sup>38</sup>.

The inhibition of intracellular glutaminase is another potential mechanism that would affect the concentration of intracellular glutamate available for secretion. Collins et al.<sup>23</sup> have shown that approximately 30% of secreted glutamate is derived from imported glutamine by way of glutaminase activity. Should any of our molecules disrupt glutaminase activity, the proportion of glutamate available for export would decrease. Glutamate secretion in cancer cells is affected by the extracellular concentration of cystine, and intracellular glutaminase activity does not correlate with glutamine consumption in breast cancer cells<sup>23</sup>. This suggests that glutaminase activity alone cannot account for changes in glutamate secretion. The majority of exported glutamate is however, coupled to the import of cystine<sup>23</sup>, again supporting a role for system  $x_C^-$  in the secretion of a large proportion of released glutamate. This is consistent with the observations of Bannai and Ishii in fibroblasts<sup>52</sup>. Furthermore, we have shown that system  $x_C^-$  activity is also associated with CIBP, where a known inhibitor of this antiporter, SSZ, reduces pain behaviours linked to the growth of MDA-MB-231 tumours in the distal femur<sup>46</sup>. While the compounds identified in our screen may inhibit glutamate release by a variety of mechanisms, system  $x_C^-$  is likely a major target.

The known functions of SKF38393 and N,N-dipropyl dopamine as dopamine receptor agonists, offers additional mechanisms that warrant further investigation into the role of the dopamine signaling pathway in malignant cells. The D1 dopamine receptor is linked to downstream activation of adenylyl cyclase and cAMP production<sup>53</sup>. Agonist versus antagonist activity of 1-phenyl-1H-3-benzazepines is dependent on the

substituent occupying position 7 of the benzazepine molecule<sup>54</sup>. All molecules identified in our screening that contain the benzazepine group show agonistic properties by this method. The D1 receptor is expressed by breast cancer cells<sup>55</sup>, and dopamine itself is an effective adjuvant to increase the efficacy of anticancer agents<sup>56</sup>. Furthermore, there is evidence linking dopamine agonists to the functional reversal of the GLT-1 transporter<sup>57</sup>. The GLT-1 transporter has been shown by our laboratory to be present at the mRNA level in MDA-MB-231 cells and may therefore contribute to glutamate secretion in these cells<sup>38</sup>.

In addition to dopamine signaling, the Transient Receptor Potential cation channel 1 (TRPV1) may play a role in glutamate secretion. Also known as the type 1 vanilloid receptor, this ion channel is well characterized in pain pathways, with the excitotoxin capsaicin being a common agonist. One of the compounds identified in our screen, capsazepine, is a synthetic analog of capsaicin, that acts as a TRPV1 antagonist<sup>58</sup>. With well-characterized neurological effects, capsazepine has also been shown to mediate anticancer activity through a reactive oxygen species (ROS)-mediated JNK signaling mechanism<sup>59</sup>. TRPV1 receptors are present on tumour cells, however, the mechanism of action of vanilloids on these cells was not through the conventional calcium signaling associated with TRVP1 activation<sup>60</sup>. With potential mechanisms outlined, the mode of action of all the glutamate release inhibiting compounds discovered are currently under investigation.

## CONCLUSION:

Glutamate release is involved in several painful conditions and the cell-based HTS described in the current investigation has discovered several molecules that inhibit glutamate release. Previous studies by our lab have identified system  $x_C^-$  as a major mechanism of glutamate release from cancer cells<sup>38</sup>. Several compounds identified in the screen suggest that, in addition to system  $x_C^-$ , other pathways and receptors may be at play. Our data suggest that dopamine signaling and TRPV1 activity may modulate glutamate release in MDA-MB-231 cells. We aim to further investigate the mode of action of these compounds, as target validation may contribute to the development of novel therapeutics for the treatment of several cancer-associated pathologies including glutamate-mediated CIBP. Our study represents a unique opportunity to modulate pain by targeting the tumour rather than the CNS, thus providing new insights into the mechanisms eliciting cancer pain. To pharmacologically inhibit pain propagation and hypersensitivity without affecting systemic signaling is a unique strategy for the development of novel therapeutics that address the underlying mechanism causing the pain rather than the development of those that merely mask pain intensity.

## METHODS:

### *Cell Culture:*

MDA-MB-231 human breast adenocarcinoma cells were maintained in high glucose DMEM (Life Technologies, Carlsbad, CA) supplemented with 10% fetal bovine serum (FBS) and 1% antibiotic/antimycotic (Life Technologies). Cells undergoing screening

were maintained in DMEM supplemented with 10% dialyzed FBS (dFBS) and 1% antibiotic/antimycotic (A/A; Life Technologies). All cells were incubated at 37 °C and 5% CO<sub>2</sub>.

### *Assay Optimization for High-Throughput Screening:*

Calculation of Z' factor is used to assess the size of the screening window, which statistically outlines the region in which positive hits will be selected. The fluorescent signal produced from the Amplex Red reagent (Life Technologies) was found to be significantly above background signal. Measurements were taken over 13 time points within 83 minutes and the Z' factor was calculated using the following equation:

$$Z' \text{ factor} = 1 - \left[ \frac{(3\sigma_p + 3\sigma_n)}{|\mu_p - \mu_n|} \right]$$

$\sigma$  = standard deviation of positive (p) and negative (n) controls  
 $\mu$  = mean of positive (p) and negative (n) controls

Cell-Based High-Throughput Screening for Molecules Inhibiting Glutamate Release: MDA-MB-231 cells were grown in T-75 flasks containing normal growth media as outlined above. Cells were harvested at 70-90% confluency with 0.5% trypsin/EDTA, counted by haemocytometer, and dispensed at a density of 700 cells per well of a 384 well-plate in DMEM supplemented with 10% dFBS and 1% A/A. Immediately after seeding, compounds of the Canadian Compound Collection library were dispensed at a concentration of 10  $\mu$ M. All seeding, treatments, and subsequent assays were automated using a BIOMEK FX liquid handler (Beckman Coulter, Brea, CA). All compound plates comprising the library contained technical replicates but did not

contain positive and negative controls. Positive and negative controls were therefore prepared in parallel in one plate containing 200  $\mu$ M sulfasalazine (positive control) and 1% DMSO (negative control) in screening media. Furthermore, in order to establish basal glutamate levels in the growth medium, a plate containing only media was dispensed and subjected to the same protocol for compound testing. All plates were then incubated for 48 hours at 37 °C and 5% CO<sub>2</sub>.

### *Screening Library:*

The Canadian Compound Collection HTS library consists of 29,586 compounds including synthetic small molecules, off-patent small molecules that are FDA approved, natural products, pharmacologically active small molecules and bioactives. Compound stocks were solubilized at 1 mM in 100% DMSO and validated as greater than 95% pure.

### *Measurement of Glutamate Release:*

Extracellular glutamate levels were measured after 48 hours using the Amplex Red glutamic acid assay kit (Life Technologies). This assay is modified to increase sensitivity to low glutamate concentrations by removing the L-alanine and L-glutamate-pyruvate transaminase from the reaction<sup>24</sup>. After the 48 hour incubation, the Amplex Red reaction mixture was added to each well at a ratio of 1:2. Immediately following addition, the plate was measured fluorometrically by the EnVision 2102 multilabel reader (Perkin Elmer, Waltham, MA) in continuous assay mode. Readings were acquired every 90 seconds for a total of 15 minutes at an excitation wavelength of 530-560 nm and an

emission wavelength of 590 nm. The fold difference between the negative (DMSO) and positive (SSZ) control was greatest at a time of 15 minutes post-addition of the Amplex Red reagent. The slope of relative fluorescent units versus time in seconds is used as indicator of inhibitory potency. The smaller the value for the slope, the less glutamate is in the medium.

### *Data Analysis – Determining Hit-rate:*

The glutamate release values for each compound were plotted against their technical replicate and normalized to SSZ. The results were gated to highlight compounds that had a fold change in the inhibition of glutamate release  $\leq 1.1$  relative to SSZ. From initial screening, 320 compounds that met this criterion were considered for re-screening. Of these compounds, a significant proportion were eliminated due to observable cytotoxicity which was classified as a confounding factor contributing to false positives. These compounds were not pursued in follow-up experiments.

### *Prioritization of Compound Hits and IC50 Determination:*

Re-screened compound hits were then tested in a 96-well plate format. Cells were seeded at 5,000-10,000 cells/well and compounds were added over a range of 0-200  $\mu\text{M}$  in DMEM + 10% dFBS immediately after cell seeding. Cultures were incubated at 37 °C for 48 hours from the time of plating and compound addition. Media was collected after incubation and diluted 1:10 for glutamate determination by Amplex Red assay. The Amplex Red reaction mix consists of 1X reaction buffer (0.1 M Tris-HCl, pH 7.5),

100 U/mL horseradish peroxidase, 5 U/mL L-glutamate oxidase, and 2.6 µg/mL of the Amplex Red reagent dissolved in DMSO. Media sample dilutions were added at a 1:1 ratio with the reaction mixture (25 µL of each). Fluorometric data was measured by rate as mentioned above in order to establish the change in fluorescent units over time. IC<sub>50</sub> values were calculated from the non-linear regression of slope versus log concentration of each compound.

### *Cell Number Quantification:*

Cell number was quantified by crystal violet staining in order to assess compound cytotoxicity. After media collection, each well was aspirated, rinsed with PBS and fixed in formalin for 30 minutes. Formalin was then removed and cultures were stained with a 0.25% crystal violet in 25% methanol for 15 minutes. Plates were then submerged in water and rinsed until the stain was completely removed. Once dry, crystal violet stain was solubilized with a solution of 0.05 M NaH<sub>2</sub>PO<sub>4</sub> in 50% ethanol and read on a spectrophotometer (Biotek, Winooski, VA) at λ=570 nm. Results are compared to standard growth curves generated for the cell line and cell number was interpreted from the equation of the standard curve. Calculated values were then used to normalize relative glutamate concentrations to cell number.

### *Measurement of Assay Interference:*

To determine whether any molecules interfered with the Amplex Red reaction, standard glutamate concentrations were measured in the presence and absence of SKF38393, NNDP, capsazepine and SSZ in isolation. The standard L-glutamate concentrations

ranged from 0-25  $\mu\text{M}$  and dilutions were prepared fresh before each test. All drug dilutions were added to the glutamate standards at a ratio of 1:100 as used in follow-up testing to ensure each sample has identical volumes of DMSO. The total volume of glutamate, drug and reaction buffer was 25  $\mu\text{L}$ .

### *Production of Hydrogen Peroxide:*

Because the measurement of glutamate by Amplex Red is indirect it is the production of  $\text{H}_2\text{O}_2$  that induces HRP-catalyzed conversion of the Amplex Red reagent (10-acetyl-3,7-dihydroxyphenoxazine) to its fluorescent product resorufin. To ensure drug treatment did not induce exogenous  $\text{H}_2\text{O}_2$  production/release, media samples collected from treated cells were tested in the absence of L-glutamate oxidase to allow basal  $\text{H}_2\text{O}_2$  levels to be quantified.

## FIGURES:

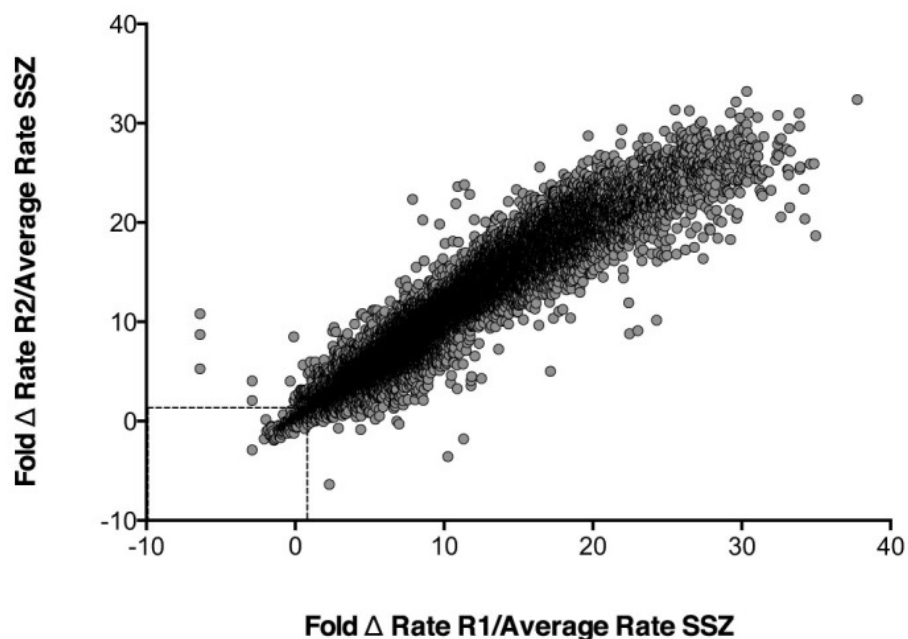


**Figure 1: High-throughput screening of 29,586 compounds for inhibitors of glutamate release by MDA-MB-231 cells.**

The level of glutamate in the cell medium was measured by Amplex Red reagent 48 hours post inoculation. Fluorescence was read every 90 seconds for 15 minutes. The rate change of fluorescent signal versus time was used as indicator of inhibitory potency. The result was expressed as the ratio of rate change between a testing compound (10  $\mu$ M) and the positive control, SSZ (200  $\mu$ M). The X and Y-axis represent the ratio of rate change of replicate 1 (R1) and replicate 2 (R2). Among 500 positive hits, 320 (enclosed in box) showed similar

to more potent glutamate release inhibition potency as SSZ and were selected for secondary screening.

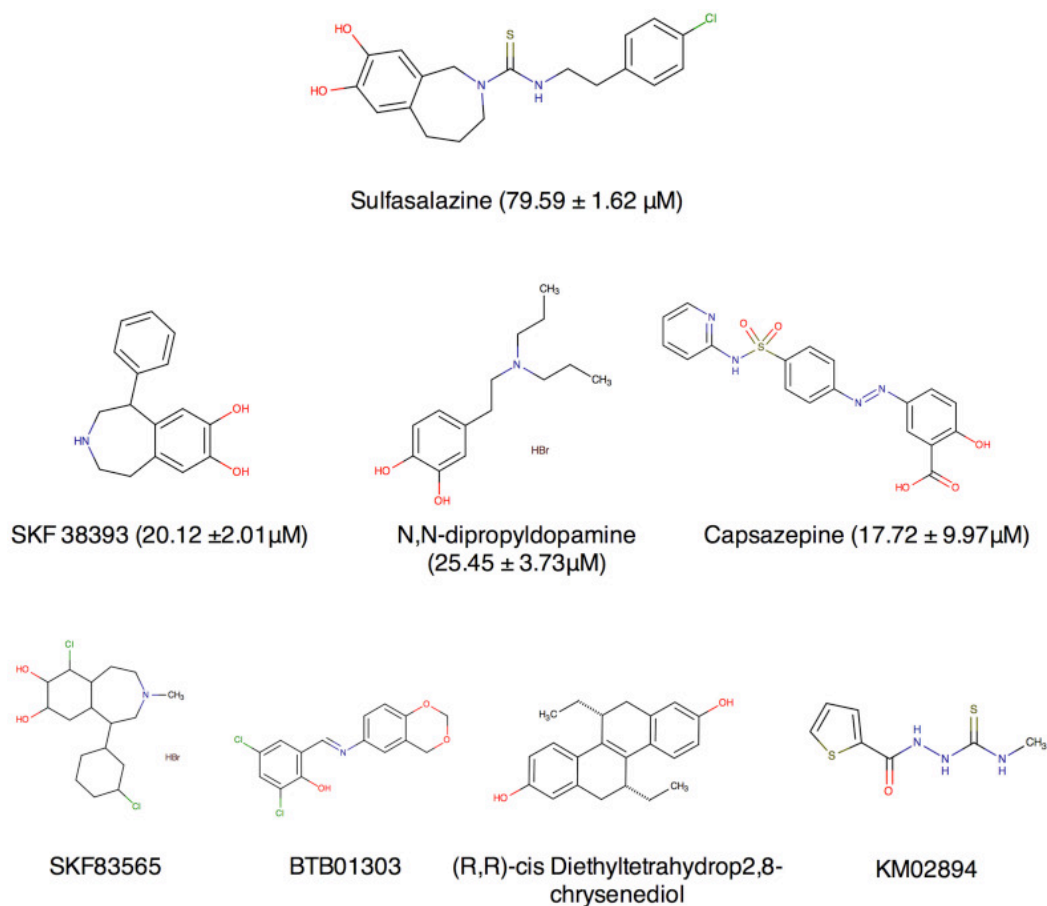


**Figure 2: Chemical structure of 8 compounds showing potent inhibition of glutamate release after secondary screening.**

Positive hits selected from HTS screening as inhibitors of glutamate release from MDA-MB-231 cells. The remaining compounds were those that were found under HTS conditions to inhibit glutamate release but were not tested in follow-up studies.

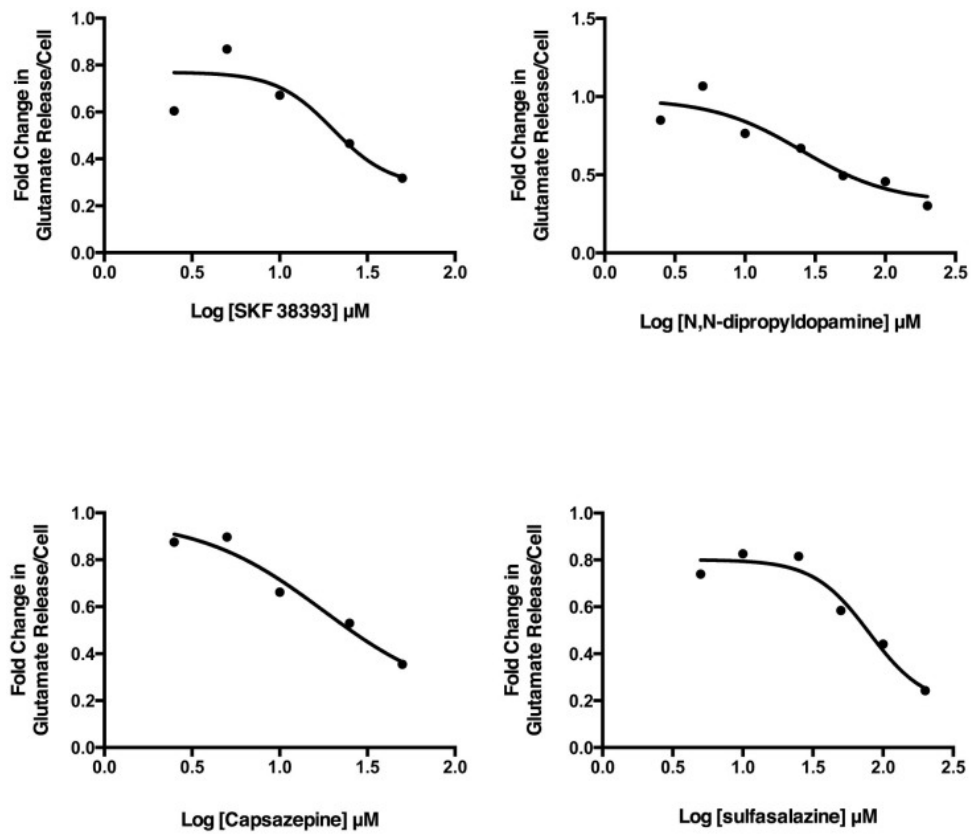


**Figure 3: IC<sub>50</sub> curves for capsazepine, NNDP, SKF38393 and sulfasalazine.**

The IC<sub>50</sub> was calculated by normalizing to the viable cell numbers. The

IC<sub>50</sub> values are as follows: capsazepine = 17.72, SKF38393 = 20.12, NNDP =

25.45 SSZ = 79.59  $\mu\text{M}$ .

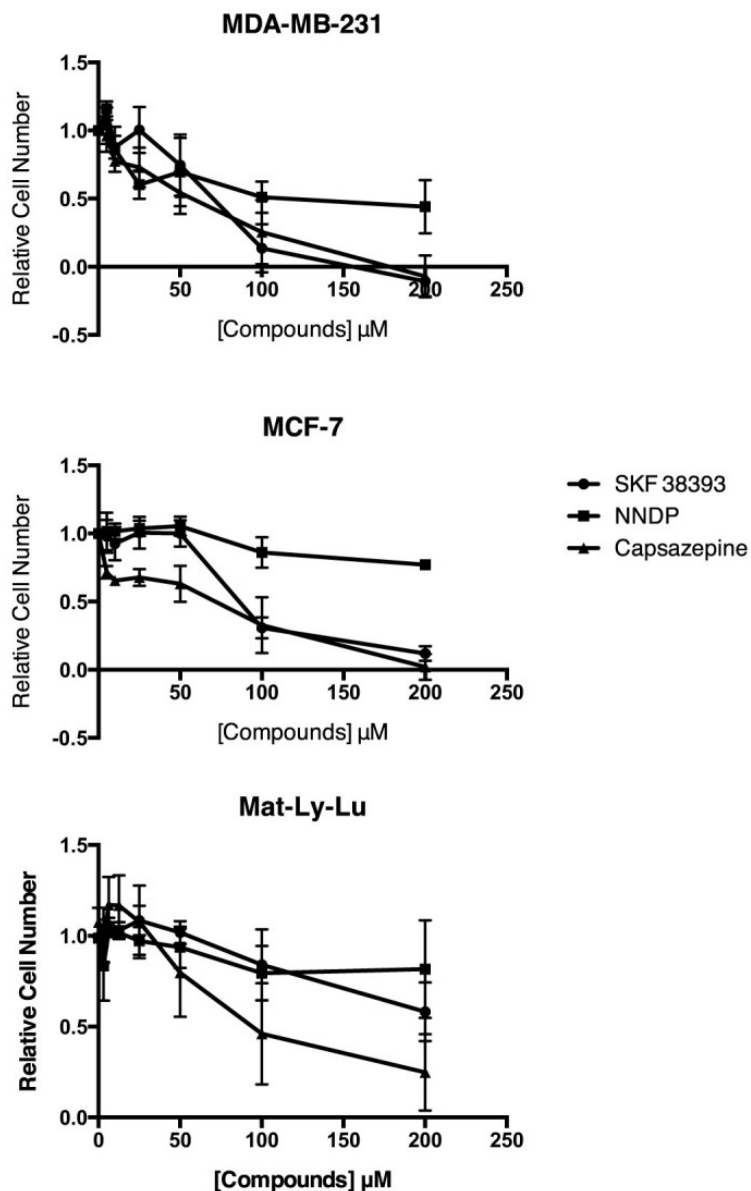


**Figure 4: Cytotoxicity of SKF38393, NNDP and capsazepine in MDA-MB-231, MCF-7 and Mat-Ly-Lu cells.**

The cell number was quantified by crystal violet staining 48 hours post-incubation. Data are represented as the mean of  $n = 3$  experiments  $\pm$  the standard error of the mean.

## REFERENCES CHAPTER 2:

1. Coleman, R. E. Skeletal complications of malignancy. *Cancer* **80**, 1588–1594 (1997).
2. Clohisy, D. R. & Mantyh, P. W. Bone cancer pain. *Clin. Orthop.* S279–288 (2003). doi:10.1097/01.blo.0000093059.96273.56
3. Vukmirovic-Popovic, S. *et al.* Morphological, histomorphometric, and microstructural alterations in human bone metastasis from breast carcinoma. *Bone* **31**, 529–535 (2002).
4. Mercadante, S. Malignant bone pain: pathophysiology and treatment. *Pain* **69**, 1–18 (1997).
5. Oldenmenger, W. H., Sillevs Smitt, P. A. E., van Dooren, S., Stoter, G. & van der Rijt, C. C. D. A systematic review on barriers hindering adequate cancer pain management and interventions to reduce them: a critical appraisal. *Eur. J. Cancer Oxf. Engl.* **1990** **45**, 1370–1380 (2009).
6. Honore, P. *et al.* Murine models of inflammatory, neuropathic and cancer pain each generates a unique set of neurochemical changes in the spinal cord and sensory neurons. *Neuroscience* **98**, 585–598 (2000).
7. Headley, P. M. & Grillner, S. Excitatory amino acids and synaptic transmission: the evidence for a physiological function. *Trends Pharmacol. Sci.* **11**, 205–211 (1990).
8. Dickenson, A. H., Chapman, V. & Green, G. M. The pharmacology of excitatory and inhibitory amino acid-mediated events in the transmission and modulation of pain in the spinal cord. *Gen. Pharmacol. Vasc. Syst.* **28**, 633–638 (1997).

9. Liu, X. J. & Salter, M. W. Glutamate receptor phosphorylation and trafficking in pain plasticity in spinal cord dorsal horn. *Eur. J. Neurosci.* **32**, 278–289 (2010).
10. Lawand, N. B., McNearney, T. & Westlund, K. N. Amino acid release into the knee joint: key role in nociception and inflammation. *Pain* **86**, 69–74 (2000).
11. Gazerani, P., Wang, K., Cairns, B. E., Svensson, P. & Arendt-Nielsen, L. Effects of subcutaneous administration of glutamate on pain, sensitization and vasomotor responses in healthy men and women. *Pain* **124**, 338–348 (2006).
12. Kreiner, F. & Galbo, H. Elevated muscle interstitial levels of pain-inducing substances in symptomatic muscles in patients with polymyalgia rheumatica. *PAIN* **152**, 1127–1132 (2011).
13. McNearney, T., Speegle, D., Lawand, N., Lisse, J. & Westlund, K. N. Excitatory amino acid profiles of synovial fluid from patients with arthritis. *J. Rheumatol.* **27**, 739–745 (2000).
14. Hinoi, E. & Yoneda, Y. Possible Involvement of Glutamatergic Signaling Machineries in Pathophysiology of Rheumatoid Arthritis. *J. Pharmacol. Sci.* **116**, 248–256 (2011).
15. Omote, K., Kawamata, T., Kawamata, M. & Namiki, A. Formalin-induced release of excitatory amino acids in the skin of the rat hindpaw. *Brain Res.* **787**, 161–164 (1998).
16. Willard, S. S. & Koochekpour, S. Glutamate signaling in benign and malignant disorders: current status, future perspectives, and therapeutic implications. *Int. J. Biol. Sci.* **9**, 728–742 (2013).

17. Carlton, S. M. Peripheral excitatory amino acids. *Curr. Opin. Pharmacol.* **1**, 52–56 (2001).
18. Brakspear, K. S. & Mason, D. J. Glutamate signaling in bone. *Front. Endocrinol.* **3**, 97 (2012).
19. Skerry, T. M. The role of glutamate in the regulation of bone mass and architecture. *J. Musculoskelet. Neuronal Interact.* **8**, 166–173 (2008).
20. Morimoto, R. *et al.* Secretion of L-glutamate from osteoclasts through transcytosis. *EMBO J.* **25**, 4175–4186 (2006).
21. Seidlitz, E. P., Sharma, M. K. & Singh, G. Extracellular glutamate alters mature osteoclast and osteoblast functions. *Can. J. Physiol. Pharmacol.* **88**, 929–936 (2010).
22. Carrascosa, J. M., Martínez, P. & Núñez de Castro, I. Nitrogen movement between host and tumor in mice inoculated with Ehrlich ascitic tumor cells. *Cancer Res.* **44**, 3831–3835 (1984).
23. Collins, C. L., Wasa, M., Souba, W. W. & Abcouwer, S. F. Determinants of glutamine dependence and utilization by normal and tumor-derived breast cell lines. *J. Cell. Physiol.* **176**, 166–178 (1998).
24. Seidlitz, E. P., Sharma, M. K., Saikali, Z., Ghert, M. & Singh, G. Cancer cell lines release glutamate into the extracellular environment. *Clin. Exp. Metastasis* **26**, 781–787 (2009).
25. Namkoong, J. *et al.* Metabotropic glutamate receptor 1 and glutamate signaling in human melanoma. *Cancer Res.* **67**, 2298–2305 (2007).
26. Takano, T. *et al.* Glutamate release promotes growth of malignant gliomas. *Nat. Med.* **7**, 1010–1015 (2001).

27. Speyer, C. L. *et al.* Metabotropic glutamate receptor-1: a potential therapeutic target for the treatment of breast cancer. *Breast Cancer Res. Treat.* **132**, 565–573 (2012).
28. Ye, Z. C. & Sontheimer, H. Glioma cells release excitotoxic concentrations of glutamate. *Cancer Res.* **59**, 4383–4391 (1999).
29. Timmerman, L. A. *et al.* Glutamine sensitivity analysis identifies the xCT antiporter as a common triple-negative breast tumor therapeutic target. *Cancer Cell* **24**, 450–465 (2013).
30. DeBerardinis, R. J., Sayed, N., Ditsworth, D. & Thompson, C. B. Brick by brick: metabolism and tumor cell growth. *Curr. Opin. Genet. Dev.* **18**, 54–61 (2008).
31. Whillier, S., Garcia, B., Chapman, B. E., Kuchel, P. W. & Raftos, J. E. Glutamine and  $\alpha$ -ketoglutarate as glutamate sources for glutathione synthesis in human erythrocytes. *FEBS J.* **278**, 3152–3163 (2011).
32. Matés, J. M. *et al.* Glutaminase isoenzymes as key regulators in metabolic and oxidative stress against cancer. *Curr. Mol. Med.* **13**, 514–534 (2013).
33. DeBerardinis, R. J. *et al.* Beyond aerobic glycolysis: transformed cells can engage in glutamine metabolism that exceeds the requirement for protein and nucleotide synthesis. *Proc. Natl. Acad. Sci. U. S. A.* **104**, 19345–19350 (2007).
34. Martino, J. J. *et al.* Metabotropic glutamate receptor 1 (Grm1) is an oncogene in epithelial cells. *Oncogene* **32**, 4366–4376 (2013).
35. Banda, M. *et al.* Metabotropic glutamate receptor-1 contributes to progression in triple negative breast cancer. *PloS One* **9**, e81126 (2014).

36. Julius, D., Livelli, T. J., Jessell, T. M. & Axel, R. Ectopic expression of the serotonin 1c receptor and the triggering of malignant transformation. *Science* **244**, 1057–1062 (1989).
37. Gutkind, J. S., Novotny, E. A., Brann, M. R. & Robbins, K. C. Muscarinic acetylcholine receptor subtypes as agonist-dependent oncogenes. *Proc. Natl. Acad. Sci. U. S. A.* **88**, 4703–4707 (1991).
38. Sharma, M. K., Seidlitz, E. P. & Singh, G. Cancer cells release glutamate via the cystine/glutamate antiporter. *Biochem. Biophys. Res. Commun.* **391**, 91–95 (2010).
39. Lee, H. J. *et al.* Glutamatergic pathway targeting in melanoma: single-agent and combinatorial therapies. *Clin. Cancer Res. Off. J. Am. Assoc. Cancer Res.* **17**, 7080–7092 (2011).
40. Doxsee, D. W. *et al.* Sulfasalazine-induced cystine starvation: potential use for prostate cancer therapy. *The Prostate* **67**, 162–171 (2007).
41. Bannai, S. & Kitamura, E. Transport interaction of L-cystine and L-glutamate in human diploid fibroblasts in culture. *J. Biol. Chem.* **255**, 2372–2376 (1980).
42. Sato, H., Tamba, M., Ishii, T. & Bannai, S. Cloning and expression of a plasma membrane cystine/glutamate exchange transporter composed of two distinct proteins. *J. Biol. Chem.* **274**, 11455–11458 (1999).
43. Verrey, F., Meier, C., Rossier, G. & Kühn, L. C. Glycoprotein-associated amino acid exchangers: broadening the range of transport specificity. *Pflüg. Arch. Eur. J. Physiol.* **440**, 503–512 (2000).
44. Bannai, S. Exchange of cystine and glutamate across plasma membrane of human fibroblasts. *J. Biol. Chem.* **261**, 2256–2263 (1986).

45. Gout, P. W., Buckley, A. R., Simms, C. R. & Bruchofsky, N. Sulfasalazine, a potent suppressor of lymphoma growth by inhibition of the x(c)- cystine transporter: a new action for an old drug. *Leukemia* **15**, 1633–1640 (2001).
46. Ungard, R. G., Seidlitz, E. P. & Singh, G. Inhibition of breast cancer-cell glutamate release with sulfasalazine limits cancer-induced bone pain. *Pain* (2013). doi:10.1016/j.pain.2013.08.030
47. Savaskan, N. E. & Eyüpoglu, I. Y. xCT modulation in gliomas: relevance to energy metabolism and tumor microenvironment normalization. *Ann. Anat. Anat. Anz. Off. Organ Anat. Ges.* **192**, 309–313 (2010).
48. Buckingham, S. C. *et al.* Glutamate release by primary brain tumors induces epileptic activity. *Nat. Med.* **17**, 1269–1274 (2011).
49. Huang, Y. & Sadée, W. Membrane transporters and channels in chemoresistance and -sensitivity of tumor cells. *Cancer Lett.* **239**, 168–182 (2006).
50. Chung, W. J. *et al.* Inhibition of cystine uptake disrupts the growth of primary brain tumors. *J. Neurosci. Off. J. Soc. Neurosci.* **25**, 7101–7110 (2005).
51. Zhen, X., Uryu, K., Wang, H.-Y. & Friedman, E. D1 Dopamine Receptor Agonists Mediate Activation of p38 Mitogen-Activated Protein Kinase and c-Jun Amino-Terminal Kinase by a Protein Kinase A-Dependent Mechanism in SK-N-MC Human Neuroblastoma Cells. *Mol. Pharmacol.* **54**, 453–458 (1998).
52. Bannai, S. & Ishii, T. A novel function of glutamine in cell culture: utilization of glutamine for the uptake of cystine in human fibroblasts. *J. Cell. Physiol.* **137**, 360–366 (1988).

53. Kebabian, J. W. & Calne, D. B. Multiple receptors for dopamine. *Nature* **277**, 93–96 (1979).
54. O’Boyle, K. M., Gaitanopoulos, D. E., Brenner, M. & Waddington, J. L. Agonist and antagonist properties of benzazepine and thienopyridine derivatives at the D1 dopamine receptor. *Neuropharmacology* **28**, 401–405 (1989).
55. Johnson, D. E., Ochieng, J. & Evans, S. L. The growth inhibitory properties of a dopamine agonist (SKF 38393) on MCF-7 cells. *Anticancer. Drugs* **6**, 471–474 (1995).
56. Sarkar, C., Chakroborty, D., Chowdhury, U. R., Dasgupta, P. S. & Basu, S. Dopamine increases the efficacy of anticancer drugs in breast and colon cancer preclinical models. *Clin. Cancer Res. Off. J. Am. Assoc. Cancer Res.* **14**, 2502–2510 (2008).
57. Shirasaki, Y., Sugimura, M. & Sato, T. Bromocriptine, an ergot alkaloid, inhibits excitatory amino acid release mediated by glutamate transporter reversal. *Eur. J. Pharmacol.* **643**, 48–57 (2010).
58. Bevan, S. *et al.* Capsazepine: a competitive antagonist of the sensory neurone excitant capsaicin. *Br. J. Pharmacol.* **107**, 544–552 (1992).
59. Sung, B., Prasad, S., Ravindran, J., Yadav, V. R. & Aggarwal, B. B. Capsazepine, a TRPV1 antagonist, sensitizes colorectal cancer cells to apoptosis by TRAIL through ROS–JNK–CHOP-mediated upregulation of death receptors. *Free Radic. Biol. Med.* **53**, 1977–1987 (2012).
60. Gonzales, C. B. *et al.* Vanilloids induce oral cancer apoptosis independent of TRPV1. *Oral Oncol.* **50**, 437–447 (2014).

**CHAPTER 3: IDENTIFICATION OF CAPSAZEPINE  
AS A NOVEL INHIBITOR OF SYSTEM  $X_C^-$  AND  
CANCER-INDUCED BONE PAIN**

## PREFACE:

In this chapter, an author-generated version of the manuscript entitled:

“Identification of capsazepine as a novel inhibitor of system  $x_c^-$  and cancer-induced bone pain” published in *The Journal of Pain Research* April 2017 is included. The paper is reproduced with permission from **Dove Press** as stated in the licence and copyright agreement:

For this paper I implemented the assay for quantifying cystine uptake as a more specific means of monitoring system  $x_c^-$  activity (Appendix I). I conducted all in vitro testing and I was responsible for writing and revising the manuscript. Animal work was conducted in conjunction with Matthew Balenko. This includes intrafemoral injection of MDA-MB-231 cells into the femur head to generate the CIBP model, drug preparation and implantation of drug pumps as well as behavioural testing and analysis. Robert Ungard assisted with tumour cell injection.

## RATIONALE:

The following chapter includes the characterization of a lead compound from the high-throughput screen from Chapter 1. Capsazepine showed robust inhibition of glutamate during follow-up testing outside of screening conditions. In addition to confirming CPZ's ability to reduce extracellular glutamate release, CPZ showed potent inhibition of cystine uptake, indicating that its ability to reduce glutamate release is

through inhibition of system  $x_c^-$  activity. For this reason, CPZ was tested in our *in vivo* model of CIBP that our lab has previously been shown to be modulated by system  $x_c^-$  inhibition. This model involves the implantation of MDA-MB-231 human, triple-negative breast cancer cells into the right femur of Balb/c nude mice and assessing pain behaviours that develop in conjunction with the proliferating tumour. These assessments include the Dynamic Weight-Bearing test of mechanical allodynia as well as the Dynamic Plantar Aesthesiometer as a measurement of mechanical hyperalgesia. Together these tests model the clinical pain characteristics of spontaneous pain and touch sensitivity respectively.

Although we showed CPZ exhibits action against system  $x_c^-$  activity, its on-target action of TRPV1 receptors cannot be ignored as a contributing factor to its anti-nociceptive mechanism. As discussed in Chapter 1, TRPV1 has an integral role in pain processing and the potential to mitigate CIBP behaviours.

## ABSTRACT:

The cystine/glutamate antiporter has been implicated in a variety of cancers as a major mediator of redox homeostasis. The excess glutamate secreted by this transporter in aggressive cancer cells has been associated with cancer-induced bone pain (CIBP) from distal breast cancer metastases. High-throughput screening of small molecule inhibitors of glutamate release from breast cancer cells identified several potential compounds. One such compound, capsazepine (CPZ), was confirmed to inhibit the functional unit of system  $x_c^-$  (xCT) through its ability to block uptake of its radiolabeled substrate, cystine. Blockade of this antiporter induced production of reactive oxygen species (ROS) within 4 hours and induced cell death within 48 hours at concentrations exceeding 25  $\mu$ M. Furthermore, cell death and ROS production were significantly reduced by co-treatment with N-acetylcysteine, suggesting that CPZ toxicity is associated with ROS-induced cell death. These data suggest that CPZ can modulate system  $x_c^-$  activity in vitro and this translates into antinociception in an in vivo model of CIBP where systemic administration of CPZ successfully delayed the onset and reversed CIBP-induced nociceptive behaviors resulting from intrafemoral MDA-MB-231 tumors.

## INTRODUCTION:

Advanced cancers of the breast are the most common source of bone metastases in women<sup>1</sup>. When in the bone, these cancers initiate a wide variety of pathological sequelae, with the primary symptom being debilitating pain<sup>2</sup>. Once tumors metastasize to the skeleton, they are associated with a dramatic change in the bone microenvironment inducing a physiologically complex pain state, which can arise from a multitude of factors including altered bone remodeling, fracturing of the bone, damage to surrounding nerves, and release of nociceptive factors from the bone tissue itself or directly from the invading tumor<sup>3-7</sup>. These skeletal-related effects correlate to a marked increase in patient morbidity and mortality<sup>2</sup> with cancer-induced bone pain (CIBP) affecting up to 75% of cancer patients making it a key indicator of patient quality of life<sup>8,9</sup>. The multiplicity of nociceptive pathways contributing to CIBP makes treatment difficult and often resistant to current analgesic therapies, with over 50% of patients having persistent, unresolved pain<sup>10</sup>. New pharmacological targets are therefore crucial to advancing therapeutic strategies that can address this clinical problem and advance patients' quality of life.

We hypothesize that cancer-specific factors are responsible for the complexity of CIBP and discovered that concentration of the nociceptive factor glutamate is greatly increased in the tumor microenvironment as a result of upregulated antioxidant machinery<sup>6,7,11</sup> namely, the cystine/glutamate antiporter, system  $x_c^-$  (xCT). System  $x_c^-$  is upregulated in many tumor types in response to the high concentrations of reactive oxygen species (ROS) produced as a consequence of their rampant cell growth and metabolism. Functional upregulation of this antiporter promotes cell survival under a

high ROS burden by promoting cystine uptake and downstream production of glutathione (GSH). This is especially seen in cancers with aggressive phenotypes that readily metastasize to bone<sup>11-13</sup>. The exchange of cystine for glutamate via system  $x_c^-$  across the plasma membrane occurs in a 1:1 stoichiometric ratio<sup>14,15</sup> driven by the intracellular concentrations of glutamate. This secreted glutamate is believed to be a major stimulus for the initiation and propagation of CIBP following metastases to the bone. Glutamate is the most common neurotransmitter in the central nervous system, and is known to play a role in pain as well as modulating cellular homeostasis in the bone<sup>16,17</sup>. With the nociceptive potential of glutamate implicated in a variety of painful disorders, targeting glutamate release via system  $x_c^-$  at the tumor site is a novel path to achieve analgesia in CIBP. Therefore, inhibition of system  $x_c^-$  in the cancer would limit the release of glutamate from the tumor, making it a pharmacologically relevant and pathology-specific target for reducing mechanical hyperalgesia associated with CIBP<sup>7</sup>. Previously, our group has published the antinociceptive effects of a known xCT inhibitor, sulfasalazine (SSZ), in an animal model of CIBP where treatment with this drug delayed the onset of nociceptive behaviors. Slosky et al. recently corroborated this in a syngeneic mouse model with complementary behavioral assessments<sup>18</sup>. Despite the success of SSZ in animal models, it has poor translational capacity for treatment of CIBP due to the limited oral bioavailability of the parent drug relative to its colonic metabolites, which have no inhibitory action toward system  $x_c^-$ <sup>19,20</sup>. In addition, common side effects of SSZ include nausea, vomiting, and anorexia, which need to be controlled not exacerbated in a cancer patient. Therefore, our aim is to identify novel inhibitors of system  $x_c^-$ . We previously ran a high throughput screen examining a chemical library of

30,000 compounds to identify lead molecules that effectively inhibit glutamate release from MDA-MB-231 cells relative to SSZ<sup>21</sup>. Capsazepine (CPZ) was one of several lead compounds found to have a high inhibition of glutamate release. Originally, CPZ was the first reported competitive antagonist of the vanilloid receptor-1 (TRPV-1)<sup>22</sup>. Although commonly used as such in pharmacological studies, it lacks potency and selectivity toward TRPV-1<sup>23,24</sup> and has several known off-target effects<sup>25,26</sup>. Therefore, it has since been replaced by newer, more selective compounds. Here, we present the first characterization of CPZ as an inhibitor of xCT in MDA-MB-231 cancer cells and corroborate this activity with antinociception in an in vivo murine model of CIBP induced by MDA-MB-231 bone colonization.

## METHODS:

### *Cell culture*

MDA-MB-231 human breast adenocarcinomas (American Type Culture Collection, Manassas, VA, USA) were maintained at sub-confluent densities with 5% CO<sub>2</sub> at 37°C in Dulbecco's Modified Eagle Medium (DMEM) supplemented with 10% fetal bovine serum (FBS) and 1X antibiotic/anti-mycotic (Life Technologies, Burlington, ON, USA). Cultures tested negative for mycoplasma contamination following testing outlined by van Kuppeveld et al.<sup>27</sup>.

### *Cell treatments*

Capsazepine (CPZ; Cayman, Madison, WI, USA) and 5-iodoresiniferatoxin (IRTX; Alomone Labs, Jerusalem, Israel) were prepared in accordance with manufacturer's recommendations using dimethyl sulfoxide (DMSO).

### *Uptake of [<sup>14</sup>C]-cystine in MDA-MB-231 cells*

The uptake of radiolabeled [<sup>14</sup>C]-cystine was measured as previously described<sup>28,29</sup>. MDA-MB-231 cells were plated in 6-well plates, 24 hours prior to testing, in complete culture medium. Prior to drug treatment, cells were washed with Hank's balanced salt solution (HBSS) and incubated with drug diluted in HBSS for 20 minutes at 37°C. [<sup>14</sup>C]-cystine (0.03 µCi/mL) was then added and incubated for an additional 20 minutes at 37°C. Cells were then washed with ice-cold HBSS and lysed in 220 µL lysis buffer (0.1% Triton X-100, 0.1 N NaOH) for 30 minutes. A 100 µL aliquot of lysate was added to 1 mL scintillation fluid (Ecoscint-H) and read in a Beckman LS6000 liquid scintillation counter. Total protein per sample was quantified using the BioRad reagent and used to normalize scintillation data.

### *Measurement of intracellular reactive oxygen species*

Intracellular ROS was quantified using a chloromethyl 2',7'-dichlorofluorescein diacetate derivative (DCFDA) after 4 and 24 hours of treatments with 12.5–50 µM CPZ. DCFDA is loaded into the cells at a concentration of 10 µM in HBSS for 30 minutes prior to drug treatment. Following incubation, cells were washed with HBSS and treated in phenol-red free DMEM supplemented with 10% FBS, sodium pyruvate (1 mM), and L-

glutamine (4 mM). Fluorescence was then read at 529 nm following the indicated time points.

### *Quantification of xCT mRNA by quantitative real-time polymerase chain reaction*

MDA-MB-231 cells treated with 25  $\mu$ M CPZ for 48 hours were harvested by trypsinization followed by mRNA extraction and purification. mRNA was then subject to reverse transcription to generate cDNA, and quantitative real-time polymerase chain reaction (RT-PCR) was carried out using the following primers for system  $x_c^-$  [SLC7A11-forward (5'-CCTCTATTCGGACCCATTTAGT) and reverse (5'-CTGGGTTTCTTGTCATATAA)]. Results were quantified using the  $2^{-[\Delta][\Delta]^{Ct}}$  method with the housekeeping gene  $\beta$ -actin and presented as fold changes relative to vehicle (DMSO)-treated control. RT-PCR was also used to confirm the presence of TRPV-1 mRNA in the MDA-MB-231 cells with the following primers: forward (5'-CAGGCTCTATGATCGCAGGAG-3') and reverse (5'-TTTGAACCTCGTTGTCTGTGAGG-3').

### *Animals*

Female athymic BALB/c nu/nu homozygous nude mice (Charles River, Montreal, QC, Canada) were used for developing MDA-MB-231 xenograft model. The mice ranged from 4–6 weeks of age and were sterile housed in groups of five. The mice were maintained at 24°C with a 12-hour light/dark cycle and were provided a sterile setting using autoclaved food and water ad libitum. All procedures were conducted according to the guidelines of the Committee for Research and Ethical Issues of the International Association for the Study of Pain and guidelines established by the Canadian Council

on Animal Care with ethical approval from the McMaster University Animal Research Ethics Board. Humane endpoints dictate euthanization if the tumor interference with the normal function of the animals causes significant pain or distress or leads to infection/risk of infection. This is monitored by frequent examination, pain behavioral testing, and body weight recordings.

### *Tumor cell xenografts*

Three days prior to cell implantation, all mice had a 0.25 mg, 21-day release  $17\beta$ -estradiol pellet (Innovative Research of America, Sarasota, FL, USA) implanted subcutaneously. At experimental day 0, mice were randomized to tumor or sham-injected groups and subject to isoflurane anesthesia followed by subcutaneous administration of buprenorphine (0.05 mg/kg) prior to cell injection. Animals in the tumor group were inoculated with  $2 \times 10^6$  cells in a 50  $\mu$ L solution of phosphate-buffered saline (PBS) (tumor mice) and sham animals received an injection of only 50  $\mu$ L of PBS into the right distal epiphysis of the femur, as previously reported<sup>7</sup>.

### *Experimental groups*

Both tumor and sham-injected mice were randomized into treatment groups on experimental day 14 following tumor cell inoculation to allow for tumor establishment (Tumor injected: n=11, 5 mg/kg CPZ; n=10, 10 mg/kg CPZ; n=13 DMSO vehicle; Sham injected: n=3, 5 mg/kg CPZ; n=5 DMSO vehicle). Drugs were delivered via Alzet model 1004 mini-osmotic pumps (0.11  $\mu$ L/hour for 28 days; Durect, Cupertino, CA, USA), which were implanted intraperitoneally to allow for stable drug delivery without constant surgical interference that may otherwise skew behavioral results. Final CPZ doses were

equal to 5 and 10 mg/kg, which have previously been shown to be safe for animal use<sup>30,31</sup>

### *Behavioral testing*

The behavioral testing period started 8 days prior to cancer cell inoculation and was performed on alternate days to acquire a total of four baseline tests. The average of these four tests represents the baseline pain score prior to tumor development and treatment. After cell implantation, behavioral testing was performed 3 days/week until endpoint was reached and involved the use of two behavioral systems; the Dynamic Plantar Aesthesiometer (DPA) (Ugo Basile, Comerio, Italy) and the Dynamic Weight Bearing (DWB) (BioSeb, Vitrolles, France) systems. All animals were randomly assigned to treatment groups during baseline behavioral testing, which also accounted for their random cage assignment. Researchers conducting behavioral tests and assessment of radiography/histology remained blinded to treatment status through each experiment. All data collected following cancer cell inoculation were normalized to these baseline scores. All animals were given a 5- and 7-minute acclimatization period in the DPA and DWB chambers, respectively.

### *Dynamic Plantar Aesthesiometer*

The DPA is an electronic Von Frey instrument measuring mechanical withdrawal thresholds as indicators of allodynia and hyperalgesia. The mice are placed individually in holding areas with grated floors and the device is manually moved under the cell-injected paw of the mouse and the actuator is triggered, raising the filament to the plantar surface of the paw. Once contact is made, the applied force increases steadily

until the paw is withdrawn. An average of five withdrawal thresholds were collected on each testing day to represent the mechanical withdrawal threshold for that day. Only mice that had visible tumors based on radiographic and histological identification were used for final data analysis. In this study, tumor implantation was successful in all animals. The final animal numbers for each group, therefore, were: vehicle: n=13; 5 mg/kg CPZ: n=11; 10 mg/kg CPZ: n=10; sham vehicle: n=5; sham 5 mg/kg CPZ: n=3.

### *Dynamic Weight Bearing system*

The DWB system records weight distribution and time spent on each limb over the course of 3 minutes using specialized weight sensors that are calibrated to the weight of the mouse and is equipped with a video camera mounted overhead to analyze the mouse's movements as the experiment progresses. The mean weight applied by each limb was measured separately, as well as the mouse as a whole, but only the rear right (tumor-bearing) limb was used to analyze changes in applied mechanical force. The daily mean weight average of the rear right paw was then compared to the baseline mean weight to calculate the difference in weight distribution placed on the affected limb. The digital recordings from the overhead camera were also used to manually validate the mouse's orientation on the sensor. The time spent on each paw was also analyzed as it provides a more specific measurement of nociceptive behavior as it highlights limb favoring and impaired ambulation of the tumor-bearing limb. Similarly to the DPA results, only mice showing confirmed radiographic tumor development in the injected limb were used, making the final group numbers as follows: vehicle: n=13; 5 mg/kg CPZ: n=11; 10 mg/kg CPZ: n=10; sham vehicle: n=5; sham 5 mg/kg CPZ: n=3.

Only results of tumor-bearing mice are reported as no differences were seen among sham-injected groups.

### *Immunohistochemistry*

Ipsilateral and contralateral tibiae, fibulae, femora, and surrounding tissues with tumor growth confirmed by radio-graphic analysis were dissected and fixed in formalin for 48 hours followed by decalcification in 10% EDTA and 4% formalin-buffered solution for 2 weeks. Fixed and decalcified samples were embedded in paraffin wax, and 4  $\mu\text{m}$  sections were prepared for hematoxylin and eosin staining to assess the extent of tumor invasion. Sections were mounted on glass slides and heated at 65°C for 25 minutes. Sections were then deparaffinized and rehydrated with multiple xylene and ethanol prior to staining and coverslipped with xylene miscible Permount (Fisher Scientific, Pittsburgh, PA, USA).

### *Statistical analysis*

All in vitro data were measured using one-way analysis of variance (ANOVA) followed by a Tukey's test to compare all groups or by unpaired *t*-test with  $P < 0.05$ . All behavioral data were measured using a one-way repeated-measures ANOVA followed by a Tukey's test comparing all data sets to one another. Behavioral data were calculated from day 25 until endpoint to limit the effects of the long lag phase from tumor implantation to onset of pain symptoms. All data presented are in terms of mean  $\pm$  standard error of mean. GraphPad Prism software version 5 for Windows (GraphPad Software, Inc., La Jolla, CA, USA) was used for all graphing and statistical analyses.

## RESULTS:

### *Radiolabeled cystine uptake identifies capsazepine as an inhibitor of xCT activity*

CPZ decreases the uptake of [ $^{14}\text{C}$ ]-cystine in MDA-MB-231 cells within 20 minutes of compound addition showing a maximal inhibitory effect at 6  $\mu\text{M}$ . This mimics the effect of the known xCT inhibitor, SSZ, indicating that CPZ does in fact show specificity for xCT (Figure 1). CPZ did not exhibit inhibition when drug was removed prior to substrate addition (data not shown).

### *Intracellular ROS levels are modulated by capsazepine in MDA-MB-231 cells*

ROS levels increased over the course of 48 hours following CPZ treatment, relative to vehicle-treated controls (Figure 2A). Within 24 hours, 25  $\mu\text{M}$  CPZ increased intracellular ROS levels by approximately three-fold ( $P < 0.005$ ). At 48 hours, this same dose increased ROS levels dramatically relative to the 24-hour time point ( $P < 0.0001$ ) and by greater than 15-fold relative to the vehicle-treated control ( $P < 0.05$ ). By contrast, treatment with IRTX, a molecule of the same TRPV-1 antagonist class as CPZ but with approximately 10 $\times$  higher affinity for TRPV-1, did not result in significant increases in ROS production over the course of 24 and 48 hours relative to the vehicle-treated control (Figure 2B). Furthermore, the observed CPZ-induced increase in ROS is abolished by the addition of 5 mM N-acetyl cysteine (NAC; Figure 2C), which is a cyst(e)ine pro-drug that supplies the cell with an exogenous source of cysteine in the absence of cystine uptake activity via system  $x_c^-$ . Furthermore, CPZ treatment induces

cell death after 48 hours, and co-treatment with 5 mM NAC significantly reduces cell death at the highest concentration of 100  $\mu$ M CPZ ( $P<0.001$ ; Figure 2D).

### *xCT transcription increases in response to CPZ treatment*

Treatment of MDA-MB-231 cells with 25  $\mu$ M CPZ results in a significant increase in xCT mRNA over the course of 24 ( $P<0.001$ ) and 48 hours ( $P<0.05$ ; Figure 3). Similarly, this increase in expression is reversed to baseline by treatment with 5 mM NAC (data not shown). This increase in xCT mRNA does not result in a functional increase in system  $x_c^-$  activity nor does it resolve the increased ROS load induced by CPZ treatment. Interestingly, it also does not induce an antioxidant response through the induction of GSH production (data not shown).

### *Behavioral analysis*

BALB/c nude mice bearing successful MDA-MB-231 grafts in the right femur as determined by histological analyses were included in the study (Figure 4). The DPA and DWB tests were consistent, showing a steady increase in nociceptive behavior with tumor development. Treatment with CPZ at both a high dose (10 mg/kg) and a low dose (5 mg/kg) exhibited pain-modulating effects with the prevention/delay in the onset of nociceptive behaviors. To confirm that CPZ treatment alone did not affect the behavioral responses, a small group ( $n=3$ ) of sham-injected animals were treated with vehicle or CPZ (5 mg/kg) with no significant differences in behavior between these two groups.

### *Dynamic Plantar Aesthesiometer*

The DPA analysis showed that both the doses of CPZ prevented the onset of pain-related behaviors as paw withdrawal thresholds did not significantly deviate from

baseline measurements over the course of the experiment (Figure 5), while vehicle-treated animals experienced a significant decrease in paw withdrawal thresholds relative to baseline at day 27 signifying the onset of pain behavior (day 27  $P<0.05$ , day 29–36  $P<0.001$ ). Both the 5 and 10 mg/kg doses of CPZ significantly increased the paw withdrawal threshold from day 25 ( $P<0.05$ ) relative to the vehicle-treated group, and the withdrawal thresholds of the 10 mg/kg-treated group did not differ significantly from the sham-injected group (results not shown), indicating that this dose was trending toward the development of a nociceptive free state. However, both the 5 and 10 mg/kg dose did not differ significantly from one another.

### *Dynamic Weight Bearing Analysis*

In this weight-based test, the mice experiencing nociception showed a dramatic decrease over time in the weight exerted on the tumor-bearing limb when compared to their baseline weight distribution obtained prior to cancer cell inoculation (Figure 6A). The onset of pain behavior in this test was marked on day 29 in which the percentage of body weight placed on the tumor-bearing limb significantly deviated from baseline (day 29  $P<0.01$ , day 32–36  $P<0.001$ ). Treatment with 5 mg/kg CPZ delayed the onset of pain behavior assessed by this method until day 36 ( $P<0.01$ ), while treatment with 10 mg/kg prevented the onset completely. When compared to the pain score of the vehicle-treated mice, both doses of CPZ were found to reverse this nociceptive behavior ( $P<0.05$ ) in tumor-bearing mice. Furthermore, the ratio of weight applied to the contralateral (rear, left) limb and the ipsilateral (rear, right) limb was also diminished with CPZ treatment relative to vehicle-treated controls (data not shown). Furthermore, measurement of the time spent on each limb was indicative of limb preference, and it

was shown that only mice experiencing severe nociception in the other behavioral tests would favor or lift their rear, right (tumor-bearing) limb (Figure 6B), consequently putting more weight on the contralateral leg. During this experiment, only the mice with the most severe pain were shown to raise their hind leg for time periods that significantly differed from that of their baseline preferences. Similarly to the other tests, both doses of CPZ were found to significantly increase the time spent on the tumor-bearing limb relative to the vehicle group ( $P < 0.05$ ), but failed to create a dose-specific response. Similarly to the DPA, the weight applied to the tumor-bearing limb of CPZ-treated mice (both 5 and 10 mg/kg treatments) did not differ significantly from that of the sham-injected mice (results not shown). For both measurements of limb use, a one-way ANOVA with repeated measures was used past day 25 when pain-related behaviors manifest.

## DISCUSSION:

From a clinical perspective, development of novel treatment strategies for CIBP is becoming more pressing as a significant proportion of oncology outpatients are reaching advanced disease stages and as a result experience greater degrees of pain coupled with inadequate pain control<sup>32</sup>. Often, achieving analgesia is at the expense of a patient's quality of life; therefore, having a peripheral and pathological target for blocking the source of a nociceptive stimuli rather than manipulating the physiological response to such stimuli offers a novel therapeutic approach that exploits pathological changes in the tumor while sparing physiological systems such as the central nervous system. In this study, a novel inhibitor of system  $x_c^-$ , CPZ, is reported and is shown to delay and, in some cases, prevent the onset of CIBP. The ability of CPZ to have similar

analgesic effects as the known xCT inhibitor, SSZ, is important due to the limited bioavailability of SSZ making it an unattractive clinical therapeutic for CIBP.

To correlate the CPZ-induced decrease in glutamate release from MDA-MB-231 cells with system  $x_c^-$  inhibition, CPZ was tested for its ability to inhibit the uptake of radiolabeled cystine, a specific system  $x_c^-$  substrate. These data show that CPZ rapidly prevents cystine uptake indicating blockade of system  $x_c^-$ . Like SSZ, CPZ must inhibit system  $x_c^-$  sterically or by another fast acting signaling mechanism, as the inhibitory action of both drugs is lost after washout (data not shown). Because system  $x_c^-$  is one of the mechanisms responsible for ROS detoxification, downstream effects of its inhibition often manifest as rising levels of intracellular ROS and decreasing levels of GSH, the major intracellular antioxidant, as a consequence of impaired cystine acquisition<sup>33,34</sup>. Cancer cells generate high titers of ROS as a byproduct of increased cellular metabolism and rapid growth, which requires upregulation of antioxidant machinery, such as system  $x_c^-$ , to survive. Therefore, blocking antioxidant synthesis through xCT inhibition results in a rise in intracellular ROS over time. This is observed following CPZ treatment in conjunction with a temporal increase in xCT mRNA likely in response to ROS production by way of antioxidant response elements in the xCT promoter. Similarly, recent data have proven that the reactive nitrogen species peroxynitrite, which is elevated in the tumor tissues, also drives system  $x_c^-$  expression and glutamate release from the tumor cell and that elimination of this species can attenuate CIBP<sup>18</sup>.

Furthermore, when cells are treated with another TRPV-1 antagonist (IRTX), a compound with greater than ten times more specificity for TRPV-1 than CPZ, this

increase in ROS is not observed (Figure 2B) corroborating an off-target action of CPZ on xCT, not on TRPV-1. Considering that CPZ is known to lose its specificity for TRPV-1 and exhibit off-target effects at doses exceeding 700 nM as used here, as well as the fact that a highly selective TRPV-1 antagonist does not mirror the effect of CPZ, suggests that CPZ modulates intracellular redox levels not via TRPV-1, but through an off-target mechanism, likely system  $x_c^-$ .

Clinically, the treatment of bone pain is often met with little success as breakthrough pain interrupts periods of analgesia even in the presence of various stages of pharmacological intervention. In order to see if CPZ's ability to modulate system  $x_c^-$  activity in vitro translates to effective analgesia in vivo, CPZ was tested in an experimental mouse model of CIBP for its ability to attenuate the nociceptive behaviors associated with an established intrafemoral tumor. There is evidence that bone cancer pain is often accompanied by skin hypersensitivity and as a result may be responsible for the manifestation of skeletal pain-related behaviors measured by common tests of nociceptive behaviors including the DWB<sup>35</sup>. Here, we include tests of both cutaneous stimulus-evoked pain and postural equilibrium/limb weight bearing using the DPA and DWB tests, respectively, thus analyzing both features associated with skeletal pain. Treatment with CPZ has a significant effect in both tests confirming that analgesia obtained by administration of this molecule is not merely associated with a decrease in skin hypersensitivity.

In vivo, the non-selective nature of CPZ has proven to be more effective in reversing the nociceptive effects of neurogenic inflammation relative to a more selective TRPV-1 antagonist SB-366791. The use of TRPV-1 inhibitors, such as CPZ, is one of the fastest

growing branches of analgesic study in the last decade, with a widely accepted rationale for the development of TRPV-1 antagonists for the treatment of various inflammatory pain conditions<sup>36</sup>. However, the role of TRPV-1 antagonists for chronic pain states, where conditions of tactile, mechanical, and spontaneous pain predominate, is less clear. TRPV-1 was identified as the primary mediator of thermal hyperalgesia following tissue injury with its expression increasing both centrally and peripherally in accordance with specific pain states including those initiated by cancers of the bone. However, absence or attenuation of this receptor does not seem to influence mechanical allodynia/hyperalgesia<sup>36–38</sup> as is measured in this study, suggesting that attenuation of mechanical-based nociception is via a novel mechanism, which we propose to be a result of diminished glutamate secretion from xCT inhibition at the tumor. Furthermore, CPZ has successfully inhibited temperature-derived behaviors relating to pain, but failed to reverse hyperalgesia induced by Complete Freund's Adjuvant, suggesting CPZ does not play a role in mitigating inflammatory-induced nociception<sup>38</sup>. CPZ also does not reverse chronic inflammatory and neuropathic pain in rats and mice, where it only blocks capsaicin-induced TRPV-1 hyperalgesia<sup>31</sup>.

The need for system  $x_c^-$  in cancer cells and its association with pain states make it a novel, peripheral, and tumor-specific target for pharmacological development.

Previously, we, and Slosky et al.<sup>18</sup>, have shown that system  $x_c^-$  inhibition, decreased the onset of nociceptive behaviors in an animal model of CIBP<sup>7</sup>. This murine model of CIBP accurately mimics human metastatic breast cancer to the bone and has the advantage of being able to isolate the affected limb. Mechanical allodynia develops in conjunction with tumor development, as evidenced by a decrease in the force required to trigger

paw withdrawal in the DPA test (Figure 5) and reduced weight bearing on the affected limb as measured by DWB testing (Figure 6A). We have shown that this behavior can be reversed toward baseline scores by systemic administration of CPZ at both 5 and 10 mg/kg. The DWB test offers advantages over the DPA testing as it reduces human interaction and produces a greater standardization of the testing procedure, limiting human error and subjectivity. This weight distribution measurement is a method of validating mechanical nociception in mice, indirectly measuring both weight bearing and spontaneous breakthrough pain, a clinically relevant assessment of CIBP.

Measurements of the time spent on each limb were also found to be a useful parameter when measuring nociception in this model. The weight-based measurements of the DWB showed that CPZ-treated mice were able to apply more weight to the tumor-bearing limb relative to vehicle treated mice. The higher dose of CPZ (10 mg/kg) prevented the development of this nociceptive behavior unlike the lower dose, which only delayed the onset of this behavior until day 36 (5 mg/kg; Figure 6). The reduction in the ratio of the weight applied to the left limb relative to the right (tumor-bearing) limb suggests that CPZ-treated mice showed normal postural equilibrium relative to vehicle-treated animals indicating the CPZ-treated mice can bear more weight on their tumor-bearing limb. This was the most sensitive behavioral test used for indirectly measuring pain behavior as its high selectivity and low sensitivity ensure that a large deviation exists between mice experiencing a high degree of pain-related behavior and those that fall into the parameters of a pain-free state (baseline; Figure 6).

Similar to CPZ's minimal selectivity for TRPV-1 in vitro at doses exceeding 700 nM, in vivo, CPZ is no longer considered selective for TRPV-1 at doses exceeding 2 mg/kg<sup>39</sup>.

Doses used in this study exceed this threshold and therefore this suggests that CPZ modulates nociceptive behavior through off-target interactions.

The ability of CPZ to modulate system  $x_c^-$  activity in vitro strongly suggests that its ability to limit progression of pain behaviors occurs at least in part through system  $x_c^-$  inhibition at the tumor. This is especially relevant considering CPZ's limited affinity for TRPV-1. Overall, targeting glutamate release in the periphery as a means of treating cancer pain suggests a novel therapeutic strategy to relieving CIBP with fewer side effects and increased effectiveness. In the future, it would be interesting to expand this study using other cancers associated with metastatic bone pain and syngeneic animal models. Further investigation into the exact mode of action of CPZ in vivo is therefore warranted and may yield promising analgesic potential in the clinic.

FIGURES:

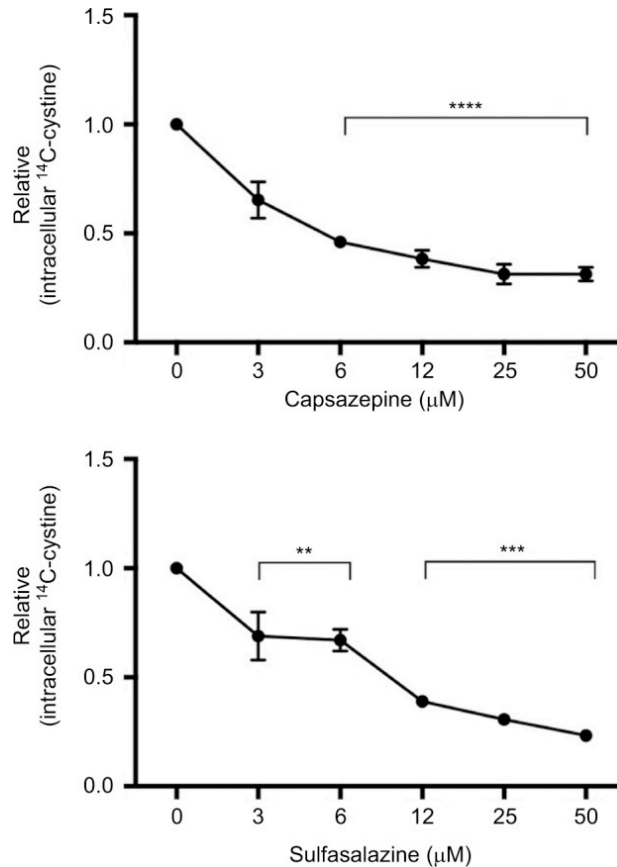


**Figure 1: Quantification of cystine acquisition in MDA-MB-231 cells in the presence of capsazepine (CPZ).**

CPZ inhibits the uptake of <sup>14</sup>C-cystine when incubated with 0–50 μM of the compound. This effect is comparable to intracellular levels of <sup>14</sup>C-cystine after incubation with sulfasalazine, a known system x<sub>c</sub><sup>-</sup> inhibitor. Data are expressed as the fold change in counts per minute/mg protein (±standard error of the mean) relative to vehicle control (dimethyl sulfoxide). \*\**P*<0.01; \*\*\**P*<0.001; \*\*\*\**P*<0.0001.

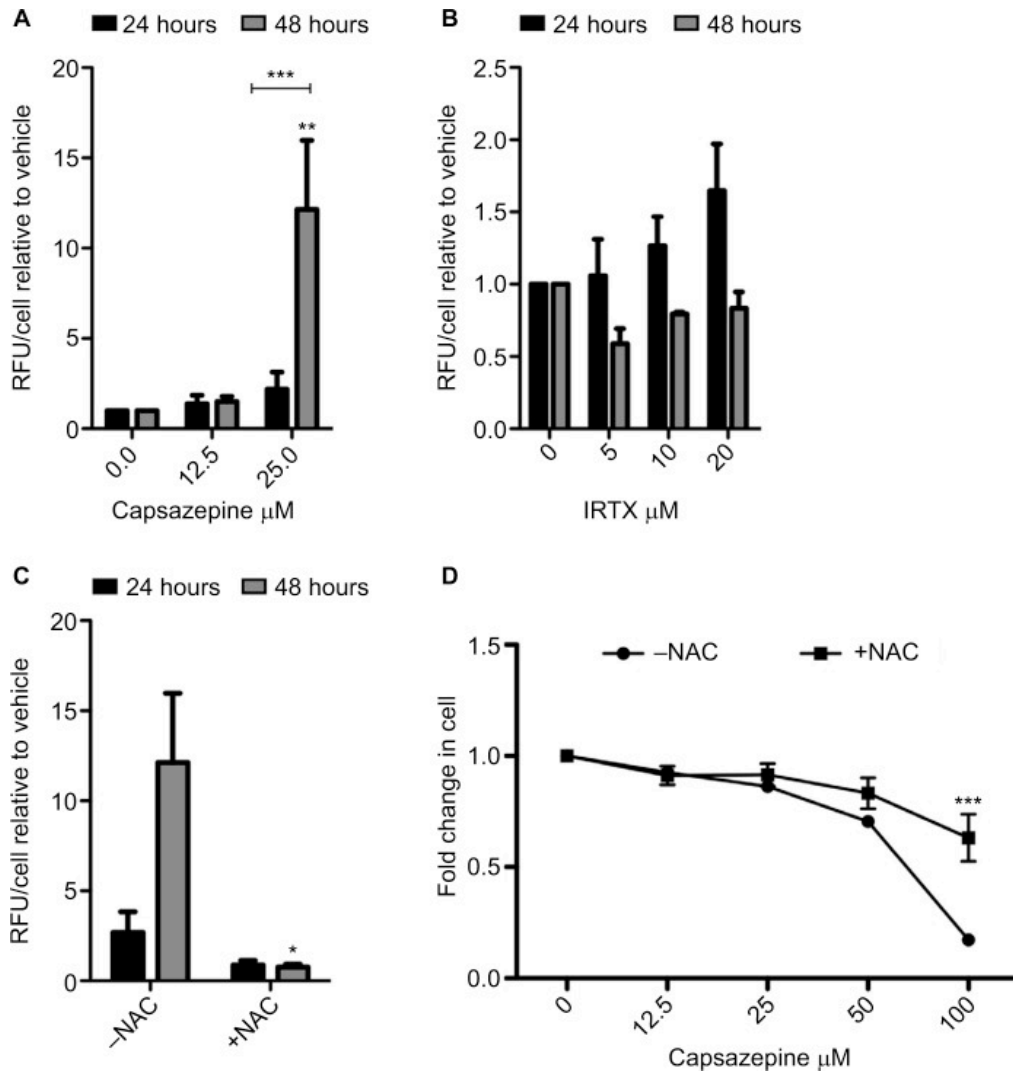


**Figure 2: Capsazepine treatment induces the production of reactive oxygen species.**

Quantification of intracellular levels of reactive oxygen species (ROS) as measured by DCFDA over 24 and 48 hours of treatment with capsazepine (CPZ) and 5'-iodoresiniferatoxin (IRTX; **A**). After 48 hours, 25  $\mu\text{M}$  of CPZ induces a significant increase in ROS relative to dimethyl sulfoxide-treated cells ( $P < 0.001$ ). Treatment with IRTX does not result in significant changes in ROS over this time

course. These data are represented as mean fold change  $\pm$  standard error of mean relative to vehicle-treated cells. One-way analysis of variance (ANOVA) was used to measure significant increases in ROS relative to vehicle-treated control. CPZ-induced ROS production is abolished by co-treatment with 5 mM N-acetyl cysteine (NAC; **B**). An unpaired *t*-test was used to assess significance of NAC addition at each time point. Cell survival decreases in a dose-dependent manner after treatment for 48 hours with CPZ. Co-treatment with 5 mM NAC increases cell survival relative to treatment with CPZ alone (**C**). Cell survival at 100  $\mu$ M CPZ is significantly higher in the presence of 5 mM NAC ( $P < 0.001$ ; one-way ANOVA comparing each concentration of CPZ without NAC to those with the addition of NAC). \* $P < 0.05$ ; \*\* $P < 0.01$ ; \*\*\* $P < 0.001$ .

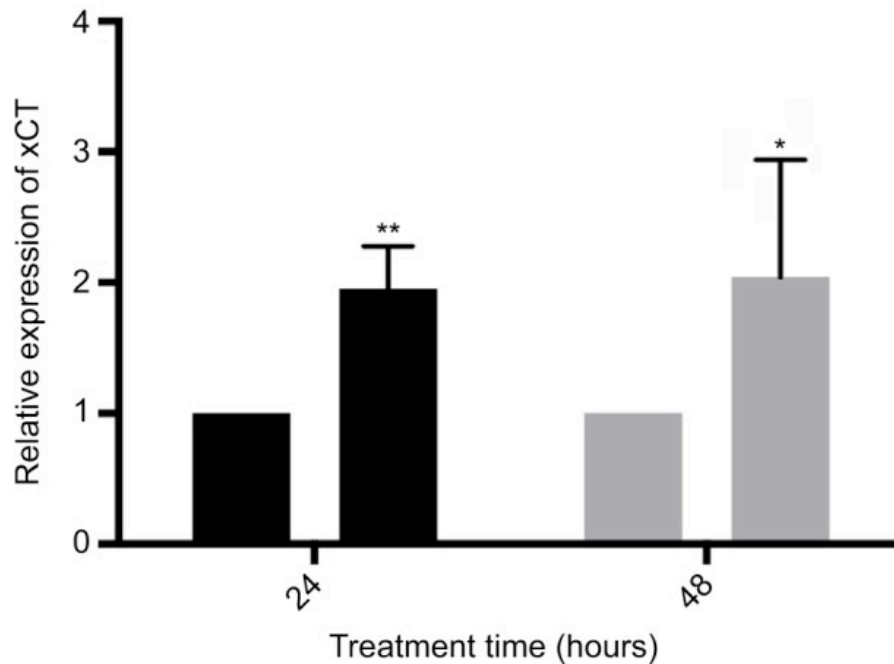


**Figure 3: Treatment with 25  $\mu$ M capsaizepine significantly induces xCT expression by 24 and 48 hours relative to dimethyl sulfoxide (DMSO) treatment.**

These data are expressed as the fold change in xCT mRNA levels relative to DMSO  $\pm$ standard error of mean and analyzed using a one-way analysis of variance (24 hours  $P<0.001$ , 48 hours  $P<0.05$ ). \* $P<0.05$ ; \*\* $P<0.01$ .

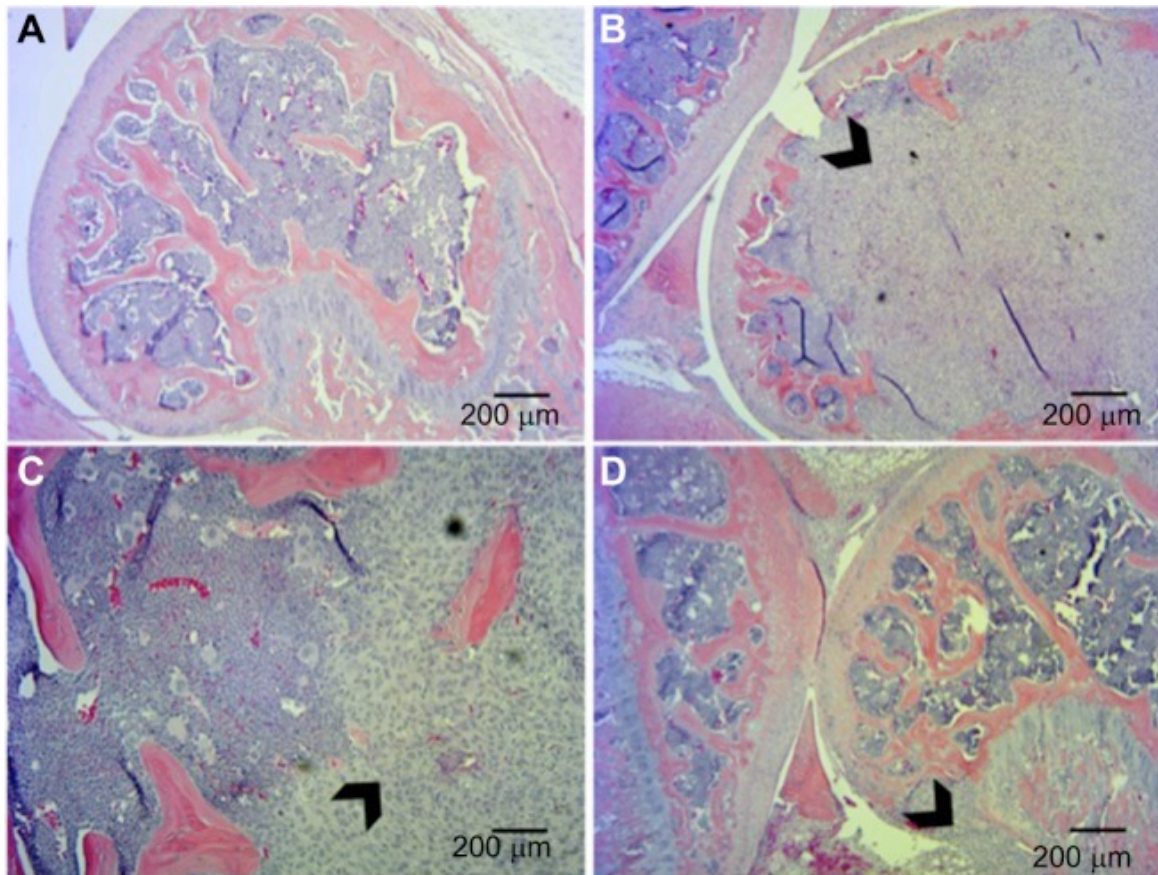


**Figure 4: Histological analysis of tumor xenografts in bone represented by hematoxylin and eosin staining.**

(A) Sham-injected mice. Tumor-injected mice show extensive invasion of xenograft into the femur with destruction of growth plate (B, D) and in some cases breaching of the periosteum (C). Arrowheads indicate tumor tissue.

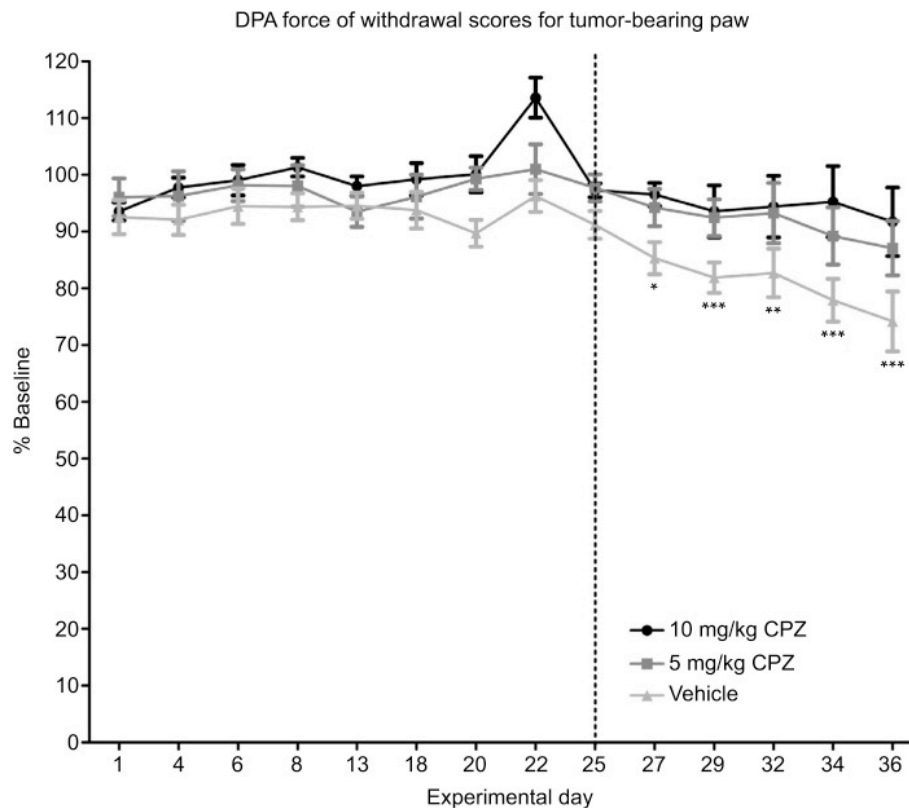


**Figure 5: DPA force-withdrawal scores of tumour-bearing paws.**

Dynamic Plantar Aesthesiometer (DPA) measurements of force required for withdrawal of the injected limb compared to the baseline results in capsazepine (CPZ)-treated and non-treated mice (100% on the y-axis is therefore equivalent to the animal's behavior pre-tumor implantation surgery). A significant decrease in the force required to induce paw withdrawal relative to baseline is only seen in the vehicle-treated group beginning on day 27 as indicated by the asterisks. Both the 5 and 10 mg/kg CPZ-treated groups do not show any significant deviation from baseline measurements. A one-way analysis of variance (ANOVA) with a Dunnett post-test was used to show significant differences between time points

relative to the baseline control. Paw withdrawal thresholds are increased in CPZ-treated mice increase in force required for paw withdrawal in the CPZ-treated mice relative to vehicle-treated mice (10 mg/kg) n=10; (5 mg/kg) n=11; (vehicle) n=13. One-way repeated measures ANOVA was used on the measurements past day 25 (marked by dotted line) showing significant differences between groups ( $P<0.0001$ ). While both doses were significantly different from vehicle mice ( $P<0.05$ ), differences between doses were not significant. Data are expressed as the mean required force as a percentage of the baseline score  $\pm$  standard error of mean. \* $P<0.05$ ; \*\* $P<0.01$ ; \*\*\* $P<0.001$ .

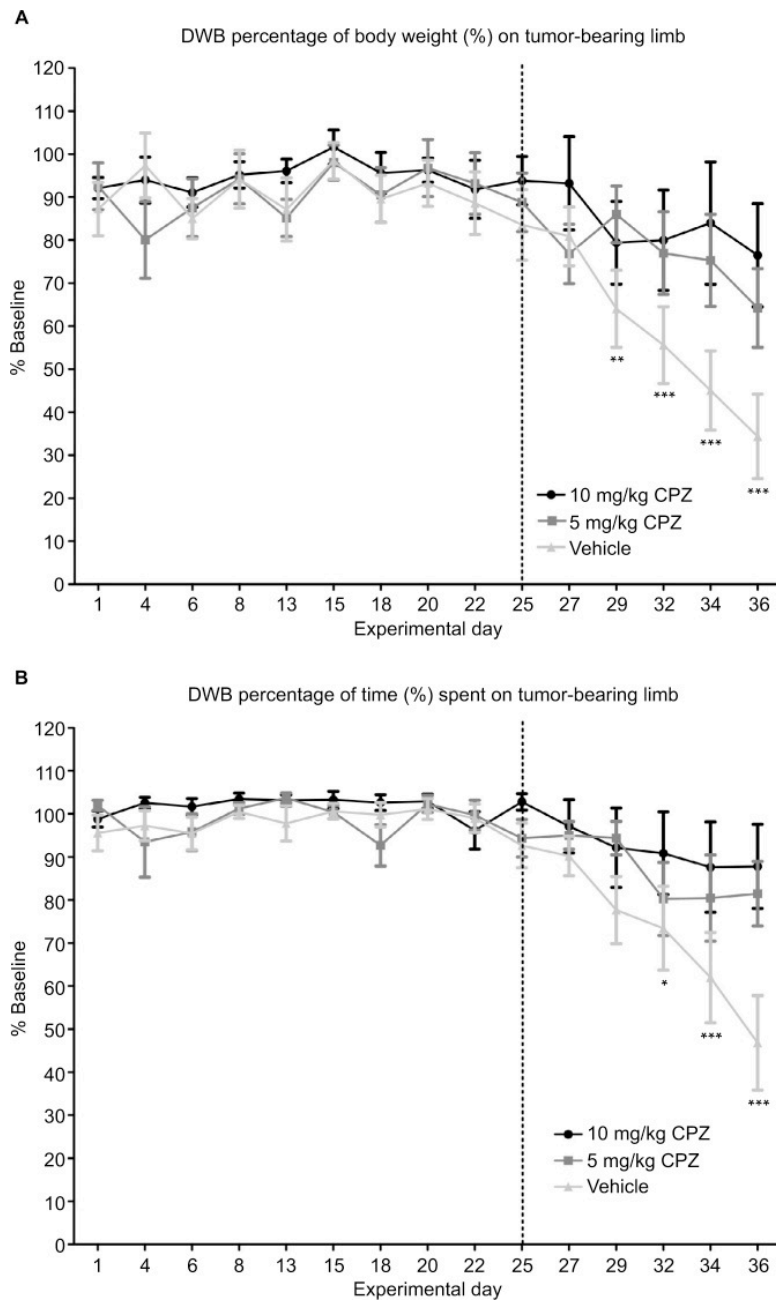


**Figure 6: Dynamic Weight Bearing (DWB) behavioural assessments.**

**(A)** Capsazepine (CPZ)-treated mice and non-treated mice. A significant decrease in weight applied to the tumor-bearing paw relative to baseline marked the onset of pain behavior in vehicle-treated mice on day 29 as indicated by the

asterisks. This is delayed until day 36 for the 5 mg/kg CPZ-treated mice, and no significant changes from baseline are seen in the 10 mg/kg CPZ-treated group. A one-way analysis of variance (ANOVA) with a Dunnett post-test was used to show significant differences between time points relative to the baseline control. This graph shows a significant increase in weight distribution in the CPZ-treated mice, relative to vehicle-treated mice (10 mg/kg) n=10; (5 mg/kg) n=11; (vehicle) n=13. A one-way repeated measures ANOVA was used on the measurements past day 25 (marked by dotted line) showing significant differences between groups ( $P=0.0008$ ). While both doses were significantly different from vehicle mice ( $P<0.05$ ), differences between doses were not significant. Data are expressed as the mean weight bearing in the injected limb as a percentage of the baseline score  $\pm$ SEM. **(B)** DWB measurements of time spent on the injected limb compared to the baseline results in CPZ-treated mice and non-treated mice. A decrease in the time spent on the tumor-bearing limb significantly deviates from baseline at day 32 with the CPZ-treated group not showing any deviation from baseline at any time point. Relative to the vehicle-treated group, an increase in time spent on injected limb is seen in the CPZ-treated mice (10 mg/kg) n=10; (5 mg/kg) n=11; (vehicle) n=13. A one-way repeated measures ANOVA was used on the measurements past day 25 (marked by dotted line) showing significant differences between groups ( $P<0.005$ ). While both doses were significantly different from vehicle mice ( $P<0.05$ ), differences between doses were not significant. Data are expressed as the mean time spent on the injected limb as a percentage of the baseline time  $\pm$ SEM. \* $P<0.05$ ; \*\* $P<0.01$ ; \*\*\* $P<0.001$ .

## REFERENCES CHAPTER 3:

1. Abdelaziz, D. M., Stone, L. S. & Komarova, S. V. Osteolysis and pain due to experimental bone metastases are improved by treatment with rapamycin. *Breast Cancer Res. Treat.* **143**, 227–237 (2014).
2. Jimenez-Andrade, J. M. *et al.* Bone cancer pain. *Ann. N. Y. Acad. Sci.* **1198**, 173–181 (2010).
3. Guise, T. A. *et al.* Molecular mechanisms of breast cancer metastases to bone. *Clin. Breast Cancer* **5 Suppl**, S46-53 (2005).
4. Lozano-Ondoua, A. N., Symons-Liguori, A. M. & Vanderah, T. W. Cancer-induced bone pain: Mechanisms and models. *Neurosci. Lett.* **557 Pt A**, 52–59 (2013).
5. Schmidt, B. L. The neurobiology of cancer pain. *Neurosci. Rev. J. Bringing Neurobiol. Neurol. Psychiatry* **20**, 546–562 (2014).
6. Seidlitz, E. P., Sharma, M. K., Saikali, Z., Ghert, M. & Singh, G. Cancer cell lines release glutamate into the extracellular environment. *Clin. Exp. Metastasis* **26**, 781–787 (2009).
7. Ungard, R. G., Seidlitz, E. P. & Singh, G. Inhibition of breast cancer-cell glutamate release with sulfasalazine limits cancer-induced bone pain. *Pain* **155**, 28–36 (2014).
8. Portenoy, R. K. Treatment of cancer pain. *Lancet Lond. Engl.* **377**, 2236–2247 (2011).
9. Sabino, M. A. C. & Mantyh, P. W. Pathophysiology of bone cancer pain. *J. Support. Oncol.* **3**, 15–24 (2005).
10. Wilson, J., Stack, C. & Hester, J. Recent advances in cancer pain management. *F1000prime Rep.* **6**, 10 (2014).
11. Sharma, M. K., Seidlitz, E. P. & Singh, G. Cancer cells release glutamate via the cystine/glutamate antiporter. *Biochem. Biophys. Res. Commun.* **391**, 91–95 (2010).
12. Banda, M. *et al.* Metabotropic glutamate receptor-1 contributes to progression in triple negative breast cancer. *PLoS One* **9**, e81126 (2014).
13. Timmerman, L. A. *et al.* Glutamine sensitivity analysis identifies the xCT antiporter as a common triple-negative breast tumor therapeutic target. *Cancer Cell* **24**, 450–465 (2013).
14. Chillarón, J., Roca, R., Valencia, A., Zorzano, A. & Palacín, M. Heteromeric amino acid transporters: biochemistry, genetics, and physiology. *Am. J. Physiol. Renal Physiol.* **281**, F995-1018 (2001).
15. Sato, H., Tamba, M., Ishii, T. & Bannai, S. Cloning and Expression of a Plasma Membrane Cystine/Glutamate Exchange Transporter Composed of Two Distinct Proteins. *J. Biol. Chem.* **274**, 11455–11458 (1999).
16. Brakspear, K. S. & Mason, D. J. Glutamate signaling in bone. *Front. Endocrinol.* **3**, 97 (2012).

17. Cowan, R. W., Seidlitz, E. P. & Singh, G. Glutamate signaling in healthy and diseased bone. *Front. Endocrinol.* **3**, 89 (2012).
18. Slosky, L. M. *et al.* The cystine/glutamate antiporter system xc<sup>-</sup> drives breast tumor cell glutamate release and cancer-induced bone pain. *Pain* **157**, 2605–2616 (2016).
19. Doxsee, D. W. *et al.* Sulfasalazine-induced cystine starvation: potential use for prostate cancer therapy. *The Prostate* **67**, 162–171 (2007).
20. Gout, P. W., Buckley, A. R., Simms, C. R. & Bruchovsky, N. Sulfasalazine, a potent suppressor of lymphoma growth by inhibition of the x(c)- cystine transporter: a new action for an old drug. *Leukemia* **15**, 1633–1640 (2001).
21. Fazzari, J., Lin, H., Murphy, C., Ungard, R. & Singh, G. Inhibitors of glutamate release from breast cancer cells; new targets for cancer-induced bone-pain. *Sci. Rep.* **5**, (2015).
22. Bevan, S. *et al.* Capsazepine: a competitive antagonist of the sensory neurone excitant capsaicin. *Br. J. Pharmacol.* **107**, 544–552 (1992).
23. Teng, H.-P. *et al.* Capsazepine elevates intracellular Ca<sup>2+</sup> in human osteosarcoma cells, questioning its selectivity as a vanilloid receptor antagonist. *Life Sci.* **75**, 2515–2526 (2004).
24. Docherty, R. J., Yeats, J. C. & Piper, A. S. Capsazepine block of voltage-activated calcium channels in adult rat dorsal root ganglion neurones in culture. *Br. J. Pharmacol.* **121**, 1461–1467 (1997).
25. Gill, C. H. *et al.* Characterization of the human HCN1 channel and its inhibition by capsazepine. *Br. J. Pharmacol.* **143**, 411–421 (2004).
26. Liu, L. & Simon, S. A. Capsazepine, a vanilloid receptor antagonist, inhibits nicotinic acetylcholine receptors in rat trigeminal ganglia. *Neurosci. Lett.* **228**, 29–32 (1997).
27. van Kuppeveld, F. J. *et al.* Detection of mycoplasma contamination in cell cultures by a mycoplasma group-specific PCR. *Appl. Environ. Microbiol.* **60**, 149–152 (1994).
28. Murphy, T. H., Miyamoto, M., Sastre, A., Schnaar, R. L. & Coyle, J. T. Glutamate toxicity in a neuronal cell line involves inhibition of cystine transport leading to oxidative stress. *Neuron* **2**, 1547–1558 (1989).
29. Shih, A. Y. *et al.* Cystine/glutamate exchange modulates glutathione supply for neuroprotection from oxidative stress and cell proliferation. *J. Neurosci. Off. J. Soc. Neurosci.* **26**, 10514–10523 (2006).
30. Menéndez, L. *et al.* Analgesic effects of capsazepine and resiniferatoxin on bone cancer pain in mice. *Neurosci. Lett.* **393**, 70–73 (2006).
31. Walker, K. M. *et al.* The VR1 antagonist capsazepine reverses mechanical hyperalgesia in models of inflammatory and neuropathic pain. *J. Pharmacol. Exp. Ther.* **304**, 56–62 (2003).

32. Fisch, M. J. *et al.* Prospective, observational study of pain and analgesic prescribing in medical oncology outpatients with breast, colorectal, lung, or prostate cancer. *J. Clin. Oncol. Off. J. Am. Soc. Clin. Oncol.* **30**, 1980–1988 (2012).
33. Bannai, S. Exchange of cystine and glutamate across plasma membrane of human fibroblasts. *J. Biol. Chem.* **261**, 2256–2263 (1986).
34. Ishii, T., Sugita, Y. & Bannai, S. Regulation of glutathione levels in mouse spleen lymphocytes by transport of cysteine. *J. Cell. Physiol.* **133**, 330–336 (1987).
35. Guedon, J.-M. G. *et al.* Dissociation between the relief of skeletal pain behaviors and skin hypersensitivity in a model of bone cancer pain. *Pain* **157**, 1239–1247 (2016).
36. Brandt, M. R., Beyer, C. E. & Stahl, S. M. TRPV1 Antagonists and Chronic Pain: Beyond Thermal Perception. *Pharmaceuticals* **5**, 114–132 (2012).
37. Caterina, M. J. *et al.* Impaired nociception and pain sensation in mice lacking the capsaicin receptor. *Science* **288**, 306–313 (2000).
38. Christoph, T. *et al.* Investigation of TRPV1 loss-of-function phenotypes in transgenic shRNA expressing and knockout mice. *Mol. Cell. Neurosci.* **37**, 579–589 (2008).
39. Rami, H. K. *et al.* Discovery of small molecule antagonists of TRPV1. *Bioorg. Med. Chem. Lett.* **14**, 3631–3634 (2004).

## **CHAPTER 4: EFFECT OF GLUTAMINASE INHIBITION ON CANCER-INDUCED BONE PAIN**

## PREFACE:

In this chapter, an author-generated version of the manuscript entitled: “Effect of Glutaminase Inhibition on Cancer-Induced Bone Pain,” prepared for submission to the *Journal of Pharmacology and Experimental Therapeutics*

For this paper I conducted all *in vitro* and *in vivo* assays including behavioural testing and validation/analysis. I assisted with HPLC protocol development (Appendix 1) which was optimized under the direction and expertise of Flavia Alves from the Centre of Microbial Chemical Biology over the course of several months. When the protocol demanded the use of another HPLC/MS system that did not permit trainee use, Flavia worked independently on optimization in this system which ultimately provided the conditions for successful separation and detection of our analytes of interest. I prepared all plasma samples for HPLC analysis which entailed liquid extraction and spiking with internal standards.

I am responsible for preparing all figures as well as writing and revising the manuscript for submission. Calithera Biosciences generously provided the test compound, CB-839.

## RATIONALE:

SKF-3839, is a known dopamine receptor 1/5 agonist that came up as a target molecule in HTS as discussed in Chapter 2 warranting further characterization for its ability to robustly prevent extracellular glutamate release in our *in vitro* HTS model.

SKF-38393 reduced extracellular glutamate release in MDA-MB-231 cells in follow-up

testing after screening but did not show any effects on cystine uptake. For this reason, this compound was not pursued for *in vivo* testing. However, upon further investigation into a rationale for this molecule's ability to inhibit glutamate release, it was discovered that SKF-38393 also appeared as an active glutaminase (GLS) inhibitor in a quantitative HTS identifying inhibitors of GLS activity from the National Centre for Advancing Translational Sciences (NCATS) Chemical Genomics Centre at the National Institute of Health (NIH) using the Library of Pharmacologically Active Compounds (LOPAC). Based on the fact that our characterization of SKF-38393 did not highlight this molecule as an inhibitor of xCT activity, these data suggested that its potential to inhibit GLS activity could account for its ability to reduce glutamate release independent of system  $x_c^-$ . Due to SKF-38393's on-target effects on dopamine receptors, it was not a viable option to test *in vivo* due to its behaviour modulating effects including diminished locomotor activity<sup>1</sup>. Therefore to investigate the role of glutaminase inhibition on CIBP behaviours, we used the selective glutaminase inhibitor CB-839 provided by Calithera Biosciences who is testing this compound in phase I clinical trials as an anti-cancer therapeutic.

Gross et al. 2014 show that expression of glutaminase 1 isoform, GAC, is increased in most triple negative breast cancer cells as is glutaminase activity. However, GLS expression does not always correlate with GLS activity as MDA-MB-231 cells have comparable activity levels to ER+ lines. However, the ability of GLS inhibition with CB-839 to reduce glutamate levels in the cell, glutamate release in culture and glutamate levels in tumour samples within 4 hrs of treatment made CB-839 an attractive

molecule to pursue for a potential CIBP modulator based on the cancer-secreted glutamate hypothesis.

They showed that CB-839 blocks glutamine utilization in TNBC cells including HCC1806 and MDA-MB-231 cells which also translated to a reduction in glutamate production in both lines. Furthermore, TCA metabolites were also reduced after treatment indicating a decreased flux through the TCA cycle which is marked by GLS-mediated conversion of glutamine to glutamate.

Furthermore, since a large fraction of glutamate derived from glutamine can be recovered in extracellular media in vitro suggests its export out of the cell. This can be correlated to a high demand for extracellular cystine for ROS detoxification by system  $x_c^{2,3}$ . Increased ROS could possibly be a result of impaired mitochondrial respiration after CB839 treatment driving cystine acquisition and GSH synthesis which directs glutamate away from TCA cycle and potentially GLS-independent glutamate production.

## ABSTRACT:

The complex nature of cancer-induced bone pain (CIBP) has led to investigation into cancer-targeted therapies. This has involved targeting glutamate release from the tumour, secreted as a byproduct of antioxidant responses and metabolic disruption. Cancer cells undergo many metabolic changes that result in increased glutamine metabolism and subsequently the production of glutamate. Glutaminase (GLS) is the enzyme that mediates the conversion of glutamine to glutamate and has been shown to be upregulated in many cancer types including malignancies of the breast. This enzyme therefore represents another potential therapeutic target for CIBP, one that lies upstream of glutamate secretion. A recently developed inhibitor of GLS, CB-839, was tested in an animal model of CIBP where it failed to modulate any of the associated nociceptive behaviours induced by intrafemoral MDA-MB-231 tumour growth. Further investigation *in vitro* revealed the sensitivity of the drug is dependent on the metabolic flexibility of the cell line being tested which can be modulated by cell culture environment. Adaptation to metabolic disturbances may explain the failure of CB-839 to exhibit any significant effects *in vivo*.

## INTRODUCTION:

Circulating glutamine is the most abundant amino acid in the plasma<sup>4</sup>. Glutamine is readily consumed by rapidly dividing cells, including cancer, for both energy synthesis and carbon/nitrogen source. Rapidly proliferating cancer cells have a modified metabolism, increasing their dependence on glutamine to sustain uncontrolled

proliferation at rates that exceed normal intracellular glutamine production, making this otherwise non-essential amino acid to become conditionally essential<sup>5,6</sup>. The nitrogen from glutamine supports the levels of many amino acids in the cell via aminotransferase activity<sup>7</sup> where at least half of the non-essential amino acids used for protein synthesis in cancer are derived from glutamine<sup>8,9</sup>.

A large proportion of intracellular glutamate is derived from glutamine<sup>10</sup> and exchanged for extracellular cystine<sup>11</sup>. This has also been observed in breast cancer cells<sup>11,3</sup>. Glutaminase (GLS) is the enzyme responsible for generating glutamate from glutamine and is transcriptionally upregulated in triple-negative breast cancer (TNBC) cells increasing their reliance on exogenous glutamine<sup>3,12</sup>. Reactive oxygen species (ROS) production increases with increased glutamine oxidation via the mitochondrial electron transport chain<sup>13</sup>, but at the same time, glutamine oxidation also suppresses ROS production through its contribution to glutathione (GSH) production<sup>14</sup>, both through the production of glutamate and the acquisition of cystine as the rate limiting step in GSH synthesis. Amino acid acquisition by cancer cells is therefore essential for both cellular metabolism and redox homeostasis<sup>15,16</sup>, making the activity of amino acid transporters, such as the cystine/glutamate antiporter, system x<sub>c</sub><sup>-</sup> (xCT), essential for cell survival<sup>17</sup>.

Previously, we have targeted this system to limit glutamate release from MDA-MB-231 cells in an effort to prevent or delay the onset of cancer-induced bone pain (CIBP) behaviour as a potential novel therapeutic strategy for this clinical issue<sup>18,19</sup>. Although effective in pre-clinical models, existing xCT inhibitors are limited for clinical use. CB-839 is a potent allosteric inhibitor of GLS in phase one clinical trials with TNBC

cells reported to show great sensitivity to this compound. CB839 exhibits antiproliferative effects, depletion of key metabolic intermediates and anti-tumour activity in TNBCs exploiting a metabolic alteration in these cells for therapeutic benefit<sup>2</sup>. Based on this work, GLS appeared to be an attractive target for CIBP based on the glutamate-induced nociception hypothesis as GLS represents a glutamate-modulating target upstream of its release through the activity of xCT.

Despite the results reported by Gross et al. 2014, we did not observe any significant delay in the development of CIBP in our MDA-MB-231 xenograft animal model after chronic CB-839 treatment. This is potentially due to the metabolic flexibility of this cell line and its ability to adapt to different nutrient conditions which may provide variable responses *in vivo* versus *in vitro*.

## MATERIALS AND METHODS:

### *Cell culture:*

MDA-MB-231 human breast adenocarcinoma (American Type Culture Collection) were maintained at sub-confluent densities with 5% CO<sub>2</sub> at 37°C in DMEM supplemented with 10% fetal bovine serum and 1X antibiotic/antimycotic (Life Technologies).

### *Quantification of extracellular glutamate:*

Media samples are collected after incubation with CB-839 for 72 hrs and the concentration of glutamate is quantified using the Amplex Red Glutamic Acid Kit (Life

Technologies). Cells are fixed with 10% formalin and stained with crystal violet to quantify cell number. Final glutamate concentrations are normalized to cell number.

*Quantification of intracellular ROS production:*

Intracellular ROS was quantified using a chloromethyl 2',7'-dichlorofluorescein diacetate derivative (CM-H<sub>2</sub>DCFDA). The production of intracellular reactive oxygen species (ROS) is quantified using DCFDA reagent loaded onto the cells prior to drug treatment. Fluorescence was quantified after either 24 or 72 hrs of CB-839 treatment. Cells were treated in phenol-red free DMEM supplemented with 10% FBS, sodium pyruvate (1mM) and L-glutamine (4 mM). Fluorescence was then read at 529 nm following the indicated time points.

*Assessing xCT activity: monitoring uptake of radiolabelled cystine:*

The uptake of radiolabelled [<sup>14</sup>C]-cystine was measured as previously described<sup>19</sup>. MDA-MB-231 cells incubated with CB-839 or DMSO for 72 hrs were washed and incubated in the uptake buffer (HBSS +0.45uCi <sup>14</sup>C-cystine) for 5 minutes and then subject to washes with ice cold HBSS and lysed in lysis buffer consisting of 0.1N NaOH and 0.1% Triton-X, for 15 minutes. One hundred microliters of lysate is then added to 1mL of scintillation fluid for quantification of radioactivity. Protein concentration for each sample is quantified using the Bradford reagent and used to normalize scintillation counts.

*Development of subcutaneous MDA-MB-231 xenograft:*

Slow release (0.25 mg, 21-day release)  $17\beta$ -estradiol pellets (Innovative Research of America, Sarasota, FL, USA) were implanted subcutaneously three days prior to tumour cell inoculation. Three million MDA-MB-231 cells were injected subcutaneously in the right flank of Balb/c nude mice. Tumours were allowed to develop until they reached on average approximately  $75\text{mm}^3$  before CB-839 administration. CB-839 was administered 2x per day at a dose of 200mg/kg by oral gavage due to the high clearance of the drug (Calithera). The treatment period extended for 24 days with daily tumour volume measurements.

*Development of intrafemoral MDA-MB-231 xenograft:*

As mentioned above, estrogen pellet implantation preceded tumour cell inoculation. Animals were subject to isoflurane anaesthesia and subcutaneous buprenorphine (0.05mg/kg) prior to intrafemoral injection. Mice were randomly assigned to CIBP or Sham groups. Animals receiving MDA-MB-231 cells were injected with 500 000 cells suspended in 25  $\mu\text{l}$  PBS into the right, distal epiphysis of the femur as previously reported<sup>18,19</sup>. For sham controls, MDA-MB-231 cells that had been subject to repeated heating and freezing were injected at the same concentration and volume as the CIBP group. The cells used for sham controls were verified to be dead by trypan blue staining. CB-839 or vehicle treatment began approximately 1 week following tumour cell inoculation.

*Behavioural testing and radiographic lesion assessment:*

Dynamic weight bearing (DWB) and dynamic plantar aesthesiometer (DPA) testing was used to assess weight distribution and mechanical withdrawal thresholds respectively as previously described<sup>16,17</sup>. Behavioural testing was done at least two times per week for continuous assessment of CIBP progression. Experimenter was blinded as to what treatment group each animal belonged. As animals had to be administered vehicle or CB-839 twice per day by oral gavage which is a potentially stressful procedure, animals were given ample time following their first gavage on testing day. For DPA testing, animals were allowed to equilibrate for 20 minutes in the testing chamber prior to testing. No equilibration time was allotted for DWB testing as exploratory behaviour (including rearing) is important to these measurements<sup>20</sup>.

Assessment of intrafemoral lesions was conducted using radiographic analysis at endpoint and blinded scoring of radiographs was conducted on a scale of 0 (no lesion)-3 (extensive osteolysis) as described previously<sup>18</sup>.

*Serum glutamate quantification by HPLC/MS:*

To quantify the concentration of glutamate in serum, a standard glutamate curve was made by spiking 10µL serum with 0.2µg/ml L-glutamate acid-2,3,3,4,4-d<sub>5</sub> as an internal standard (Sigma 616281). Injection volumes of 0.1, 0.2, 0.5 and 1µl corresponded to 0.1, 0.2, 0.5 and 1 ng/µl of the L-glutamate d<sub>5</sub> in the standard curve. Glutamine and glutamate elute in close proximity to each other and therefore, the pH of mobile phase A is essential to maximize separation and prevent overlap of peaks.

Although the concentration of glutamine itself was not quantified, the ratio of glutamine to glutamate was determined by comparing peak areas of both analytes.

Serum samples were subject to an ice cold methanol (MeOH) extraction at a ratio of 1:10 (serum:MeOH) for 1 hour on ice. Liquid chromatography was performed on an Agilent 1290 Infinity liquid chromatography system in isocratic mode equipped with a SeQuant ZIC-HILIC PEEK column (3.5 $\mu$ m, 100A; 150 x 2.1 mm; Millipore). Mobile phase consisted of (A) 10mM ammonium formate (pH 6.5) and (B) acetonitrile, Injection volume was 5  $\mu$ L with a flow rate of 0.2 mL/minute. LC/MS analysis was performed on an Agilent 6550 iFunnel Q-TOF in negative ion mode with a mass range of 100-200m/z. Additional parameters are as follows: gas temperature at 275°C, nebulizer pressure at 30 psig, sheath gas temp at 320°C, sheath gas flow at 11 L/min, capillary voltage (VCap) at 3500 V and nozzle voltage at 1500 V. Data acquisition was performed using Agilent Mass Hunter (version B.07.00).

### *Statistics:*

Data are presented as means +/- SEM. One-way ANOVA and two-way repeated measures ANOVA were used for statistical comparisons. P values <0.005 were considered statistically significant.

## RESULTS:

### *CB-839 does not prevent growth of MDA-MB-231 xenografts:*

Before testing CB-839 in the CIBP model, the effect of the drug on the growth of MDA-MB-231 xenografts was tested in a subcutaneous tumour-growth model. Differing from results observed by Gross et al. 2014 with another triple-negative breast cancer cell line (HCC1806), CB-839 treatment did not affect the growth of MDA-MB-231 cells relative to the vehicle treated control (Figure 1). Serum glutamate concentrations also did not differ significantly between groups despite the trend illustrating a decrease in serum glutamate concentrations from CB-839-treated animals (Figure 2). Furthermore, the ratio of glutamine to glutamate in the serum was significantly elevated in drug treated animals indicative of an accumulation of glutamine due to inhibition of GLS which is in agreement with Gross et al. 2014 who report elevated glutamine in plasma within 4 hours of CB-839 administration.

### *CB-839 does not prevent development of CIBP behaviours:*

CB-839-treated animals did not show any delay in the development of pain behaviours as measured by dynamic weight bearing (Figure 3A) or dynamic plantar aesthesiometer measurements (Figure 3B) relative to the vehicle treated controls. Treatment with this compound was therefore, not effective in preventing CIBP-related mechanical hyperalgesia and allodynia. The degree of osteolysis also did not differ significantly between vehicle and CB-839-treated groups (Figure 4) suggesting CB-839

did not affect tumour development consistent with our preliminary subcutaneous tumour growth analysis.

*CB-839 reduces glutamate release from MDA-MB-231 cells:*

After seeing negative results in our *in vivo* model, we wanted to confirm that CB-839 reduces extracellular glutamate release from MDA-MB-231 cells as reported. CB-839's ability to reduce extracellular glutamate is sensitive to the status of sodium pyruvate in the culture media. Extracellular glutamate concentrations decrease significantly in the absence of sodium pyruvate in the media (Figure 5a). Furthermore, only in the absence of sodium pyruvate is any significant impact on cell density observed suggesting that the presence of that metabolite in the media maintains cellular proliferation during GLS inhibition (Figure 5b).

*ROS production and uptake of radiolabelled cystine:*

In the absence of sodium pyruvate, there is an approximate 2.5 fold increase in ROS production by 72hrs relative to the DMSO control (Figure 6a). Interestingly, this is not accompanied by a significant influx of cystine uptake unless there is sodium pyruvate present in the media (Figure 6b).

## DISCUSSION:

In an effort to target glutamate release from cancer cells associated with clinical CIBP characteristics, we targeted glutamate production at a major metabolic hub that is

often associated with the reprogrammed metabolism of aggressive cancers. In such cells, GLS activity is a key mediator of anaplerosis fuelling the Tricarboxylic Acid (TCA) cycle. Glutamine-derived TCA cycle intermediates predominate as a result of a shunted glycolytic pathway where glucose metabolism is diverted to lactate production (Warburg effect). Therefore, GLS expression and activity is upregulated in many cancers including MDA-MB-231 cells. In addition to generation of TCA metabolites, glutamine-derived glutamate is essential for production of the major antioxidant tripeptide, glutathione (GSH) composed of glutamate, cystine and glycine. Glutamate has a dual role in GSH production where it not only is essential to the composition of the molecule itself, it is necessary for the cell to acquire cystine, the rate-limiting component of GSH synthesis. Glutamate/cystine exchange occurs through the xCT antiporter. Expression of xCT has been identified as a marker for glutaminase inhibitor sensitivity<sup>21</sup> as high xCT activity decreases intracellular glutamate pools increasing the cell's reliance on glutaminase to replenish this pool from glutamine. This allows the cell to maintain antioxidant production at the expense of regenerating TCA cycle intermediates from glutamine<sup>22</sup>.

It has become clear that the metabolic flexibility of the cancer must be considered when evaluating the efficacy of a potential therapeutic that targets a major metabolic pathway in the cell. To promote survival the cell must balance fueling energy production and biomass accumulation with ROS clearance, diverting potential metabolic intermediates, such as glutamate, towards antioxidant production rather than anabolism. When nutrients in the microenvironment are scarce, the cell's demand for GSH increases and a large amount of glutamate is exported in order to acquire cystine

for GSH synthesis in order to buffer intracellular reactive oxygen species. Therefore glutamine-derived glutamate can be sacrificed to promote survival over growth<sup>23</sup>.

After treatment with CB-839 ROS levels increase possibly due to impaired mitochondrial function and limited GSH production in the absence of GLS-derived glutamate. It was hypothesized that glutamate flux via xCT would be limited as well with limited intracellular glutamate available to drive antiporter activity and as a result cystine acquisition. A decrease in extracellular glutamate is not accompanied by significant changes in cystine uptake when sodium pyruvate is absent from the media which results in decreased cell proliferation. Extracellular glutamate is diminished slightly when sodium pyruvate is present in media however, cystine uptake is not halted and responds as expected to increasing ROS. ROS production is not dependent on the presence of sodium pyruvate in the media potentially due to mitochondrial dysfunction that accompanies GLS inhibition. The cell must regenerate this intracellular glutamate pool via glutamine uptake and GLS activity<sup>24</sup>. However with GLS activity inhibited, TCA cycle intermediates and GSH is depleted and growth of TNBCs is halted in the absence of sodium pyruvate<sup>2</sup>.

CB-839 sensitivity is associated with an increased basal ratio of glutamate to glutamine which is common of TNBCs including MDA-MB-231 cells<sup>2,25,26</sup>. Despite this, sensitivity of MDA-MB-231 xenografts to CB-839 treatment was limited. This has also been observed by Lampa et al. also in TNBCs<sup>27</sup>. In this investigation, the same cell lines resistant to CB-839 treatment *in vivo* exhibited increased sensitivity to GLS *in vitro*, suggesting the metabolic profile of these cells differs under *in vitro* and *in vivo* conditions. This could possibly be attributed to the nutrient availability in the tumour

microenvironment or possibly due to the drug not reaching the tumour at sufficient levels to cause adequate GLS inhibition that will result in the decreased production of downstream metabolites including glutamate. This differential response to CB-839 *in vitro* and *in vivo* has also been observed with pancreatic carcinoma and has also been attributed to compensatory metabolic networks<sup>28</sup>.

Flexibility to overcome perturbations in glutamine metabolism is important for cells conventionally labeled as glutamine addicted. Under such conditions, pyruvate carboxylase (PC) has been found to be a compensatory anaplerotic mechanism allowing the cells to use glucose-derived pyruvate for anaplerosis over glutamine<sup>29</sup>. This could be an explanation for why MDA-MB-231 cells show varied survival after CB-839 treatment in the presence or absence of sodium pyruvate. In fact, MDA-MB-231 cells have been shown to have reduced TCA cycle activity due to oncogenic kRas activity<sup>30</sup>. As a result, glycolysis is enhanced and these cells consume greater quantities of glucose relative to glutamine. Although still dependent on glutamine for anaplerosis much of the genes encoding TCA cycle enzymes are downregulated; this includes GLS. However genes involved in glutamine anabolism are increased, particularly those involved in GSH metabolism<sup>30</sup>. Although low glutamine levels do hinder proliferation of MDA-MB-231 cells it is not halted to the degree imposed by glucose limitation implying greater metabolic flexibility to overcome glutamine restriction and/or GLS inhibition.

Furthermore, in many cancer cells, glucose and glutamine are compensatory under different metabolic conditions in order to maintain the TCA cycle<sup>31</sup>. Cells deemed glutamine-addicted can therefore become glutamine independent<sup>29</sup>, using glucose to produce oxaloacetate (OAA) via pyruvate metabolism. When pyruvate is limited or not

present, there is a shift to glutamine-dependent acetyl-CoA formation, which is suppressed when pyruvate is present<sup>31</sup>. This may explain why there is an amplified impact of CB-839 on proliferation and glutamate release when pyruvate is removed from tissue culture media as under these conditions the cell is relying more heavily on glutaminolytic machinery including GLS. Pyruvate therefore aids in the cell's resistance to this metabolic stress. In glioblastoma cells, GLS suppression is accompanied by glucose-dependent anaplerosis via pyruvate carboxylase which produces OAA from pyruvate (glucose-derived<sup>29</sup>).

Despite that the majority of extracellular glutamate released from TNBC's derived from glutamine confirming activity of GLS, it is clear that this can vary between cell types in this category and under different nutrient conditions. For example, where one TNBC line, HCC1806 reported in Gross et al 2014 showed limited metabolic flexibility when it comes to GLS inhibition, we have shown that another TNBC line, MDA-MB-231 potentially has greater nutrient flexibility than HCC1806 cells and can survive perturbations in glutamine metabolism.

Furthermore, in the absence of GLS activity, glutamate can be generated from alpha-ketoglutarate ( $\alpha$ -KG) by glutamate dehydrogenase. Pyruvate feeds the TCA cycle in the absence of GLS activity generating  $\alpha$ -KG which can be diverted to make more glutamate and fuel system  $x_c^-$  exchange to balance redox homeostasis. Glutamate dehydrogenase (GDH) catalyzes the conversion of glutamate to  $\alpha$ -KG but can also convert  $\alpha$ -KG back to glutamate when there are sufficient levels of TCA cycle intermediates which may be the case when sodium pyruvate is present in the media. When pyruvate is absent in the media, the pull remains on glutamate to fuel TCA cycle

increasing reliance on GLS activity and making the cell more susceptible to GLS inhibition. However, when pyruvate is present, the TCA cycle pool can be restored in the absence of GLS activity making the cell less susceptible to GLS inhibition. Therefore under these conditions, it is possible that sufficient levels of glutamate are being produced from the  $\alpha$ -KG pool via transamination<sup>32</sup> to drive system  $x_c^-$  activity under the pressure of increasing ROS (Figure 7) as cystine uptake increases after 72hrs when ROS is also increased.

## CONCLUSION:

Sensitivity of MDA-MB-231 cells to GLS inhibition with CB-839 is variable and dependent on culture conditions. CB-839's effect on cell survival and glutamate release in these cells is dependent on the presence of sodium pyruvate in the culture media. Furthermore, the reported effect on tumour growth following CB-839 therapy was not observed with both the subcutaneous growth of MDA-MB-231 tumours and the development of intrafemoral lesions not differing significantly from vehicle-treated controls. Of most significance, CB-839 treatment also failed to modulate CIBP behaviours *in vivo*. It is possible the same metabolic adaptations observed *in vitro* are occurring *in vivo* and maintaining glutamate production in the absence of GLS activity. Balancing cellular proliferation with ROS homeostasis places different metabolic demands on the cell. When these demands can be met, cell survival persists even in the presence of metabolic perturbations.

By identifying what adaptations are taking place in MDA-MB-231 tumours following CB-839 administration will give more insight into the role of glutamine

metabolism and intratumoural glutamate production in CIBP and reveal novel combinatorial treatment approaches to overcome the metabolic plasticity of these cells.

FIGURES:

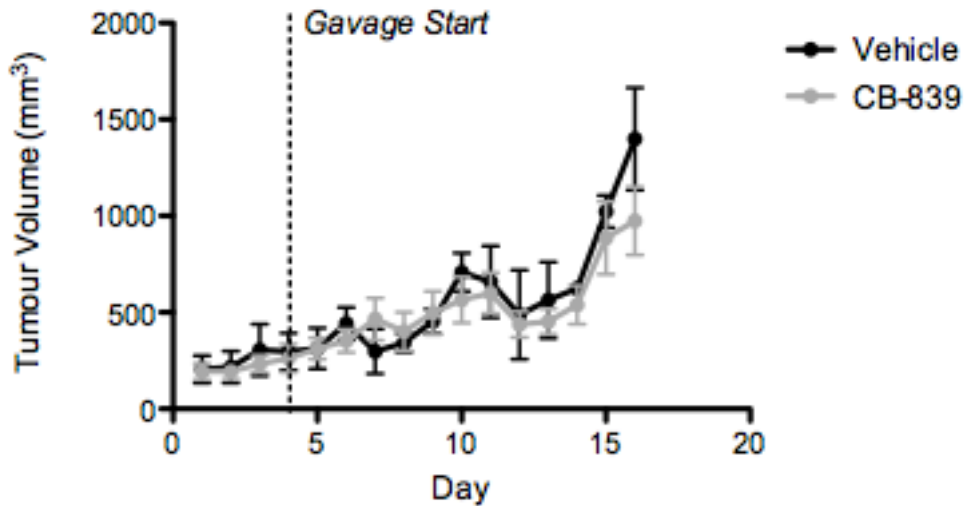


**Figure 1: Growth of subcutaneous MDA-MB-231 tumours in Balb/c nude mice treated with CB-839 or vehicle.**

Tumour volume was measured daily and CB-839 or vehicle treatment began once tumours reach approximately 100mm<sup>3</sup>. Tumour measurements continued daily until endpoint. CB-839 treatment does not affect result in a reduction in tumour volume relative vehicle-treated controls.

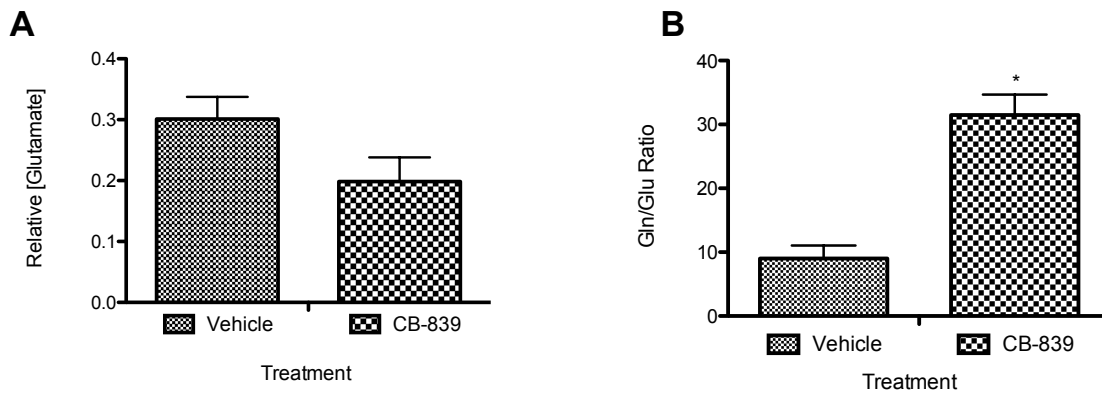


**Figure 2: Concentration of glutamate in serum from animals with subcutaneous MDA-MB-231 tumours treated with CB-839 or vehicle.**

**A)** Concentration of glutamate in serum relative to vehicle-treated animals (P=0.0781 by unpaired t-test). **B)** The ratio of glutamine to glutamate in serum indicating that glutamine levels significantly increase in the serum of mice-treated with CB-839 (P<0.001 by unpaired t-test).

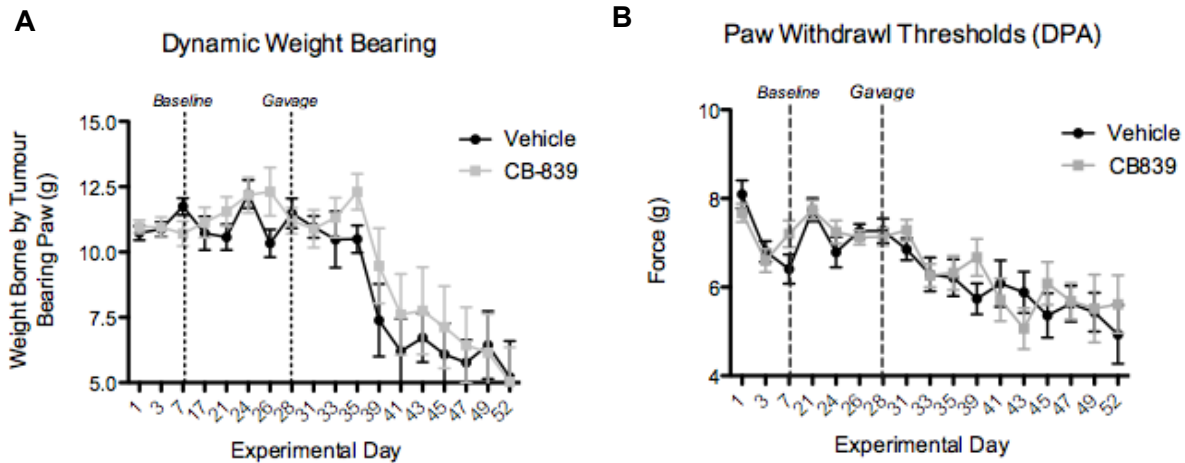


**Figure 3 : Assessment of pain behaviours- dynamic weight bearing (A), dynamic plantar aesthesiometer (B).**

Three behavioural measurements were taken prior to tumour cell inoculation to establish baseline responses to both tests. Behavioural testing resumed 10 days post tumour cell inoculation with testing conducted twice per week to monitor development of CIBP behaviours until endpoint. Treatment with CB-839 or vehicle by 2x daily oral gavage commenced two weeks following tumour initiation (experimental day 28). No significant changes in nociceptive behaviours were observed between CB-839 and vehicle treated groups were observed in both tests.

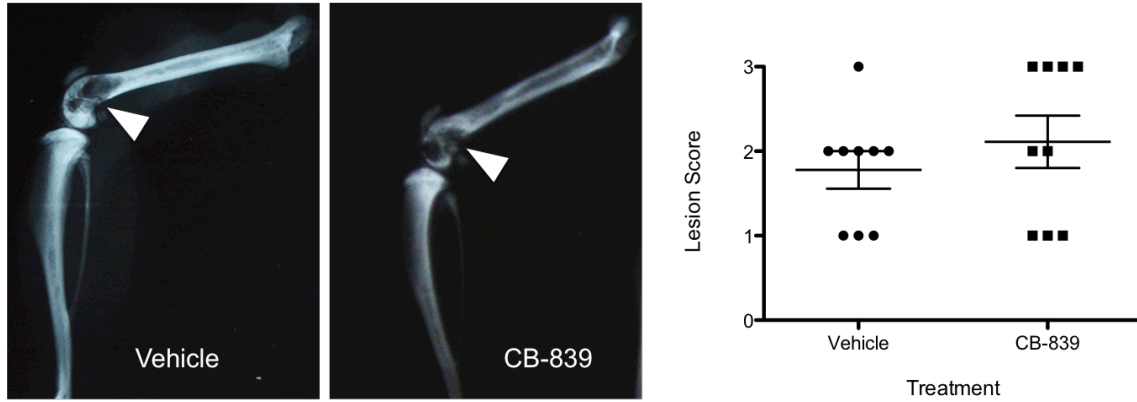


**Figure 4: Radiographic lesion scoring of MDA-MB-231 tumours at endpoint.** Representative images of vehicle and CB-839-treated groups are presented and osteolysis from tumour development is indicated by white arrows. A graphical representation of radiographic lesion scoring of all animals in each group is shown.

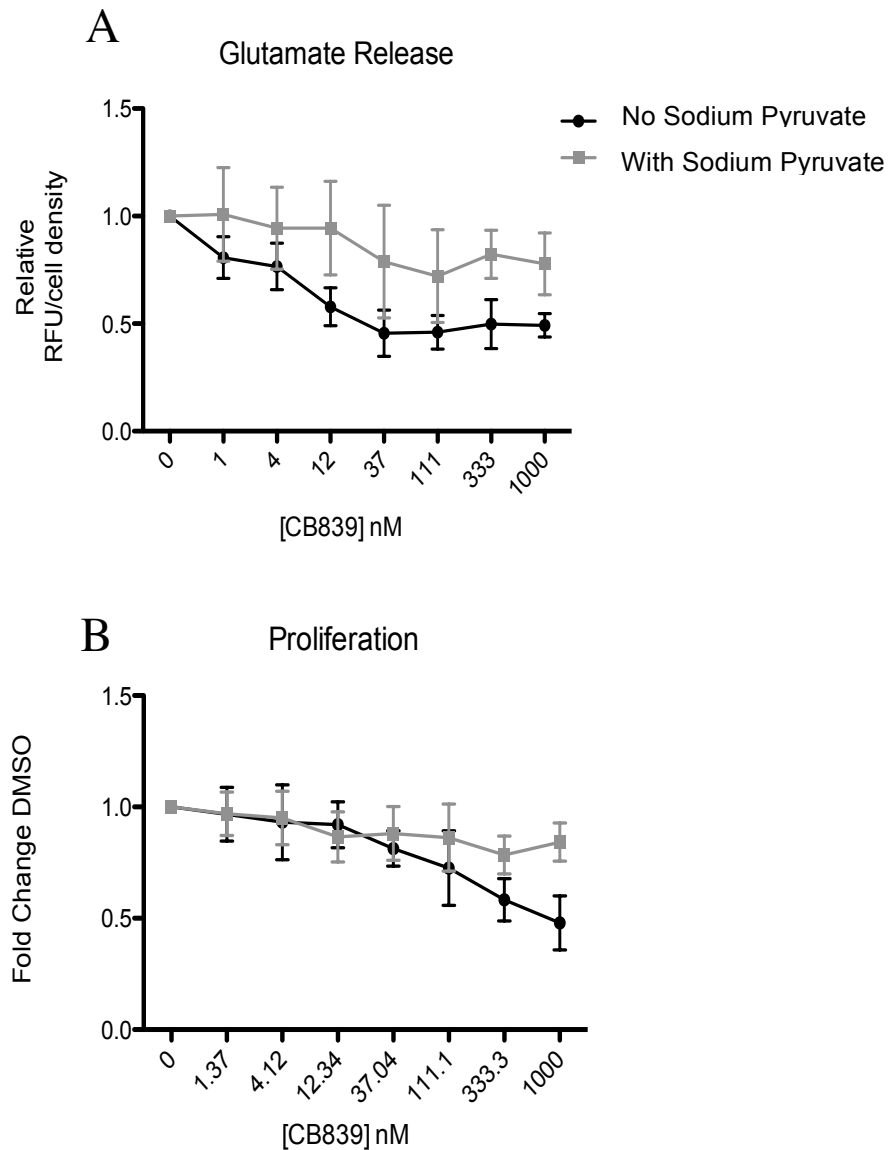


**Figure 5: Concentration of extracellular glutamate (A) and cell proliferation (B) over a dose range of CB-839 +/- sodium pyruvate in culture media.**

Non-linear regression analysis of log transformed [CB-839] vs. relative RFU/cell results in a shift in EC50 values between “no sodium pyruvate” (EC50=4997nM) and “with sodium pyruvate” (EC50=11.07). Only in the absence of sodium pyruvate is there significant reduction in glutamate relative to the vehicle (0nM) at doses of 12nM ( $P < 0.05$ ) to 1000nM ( $P < 0.005$ ) CB-839.

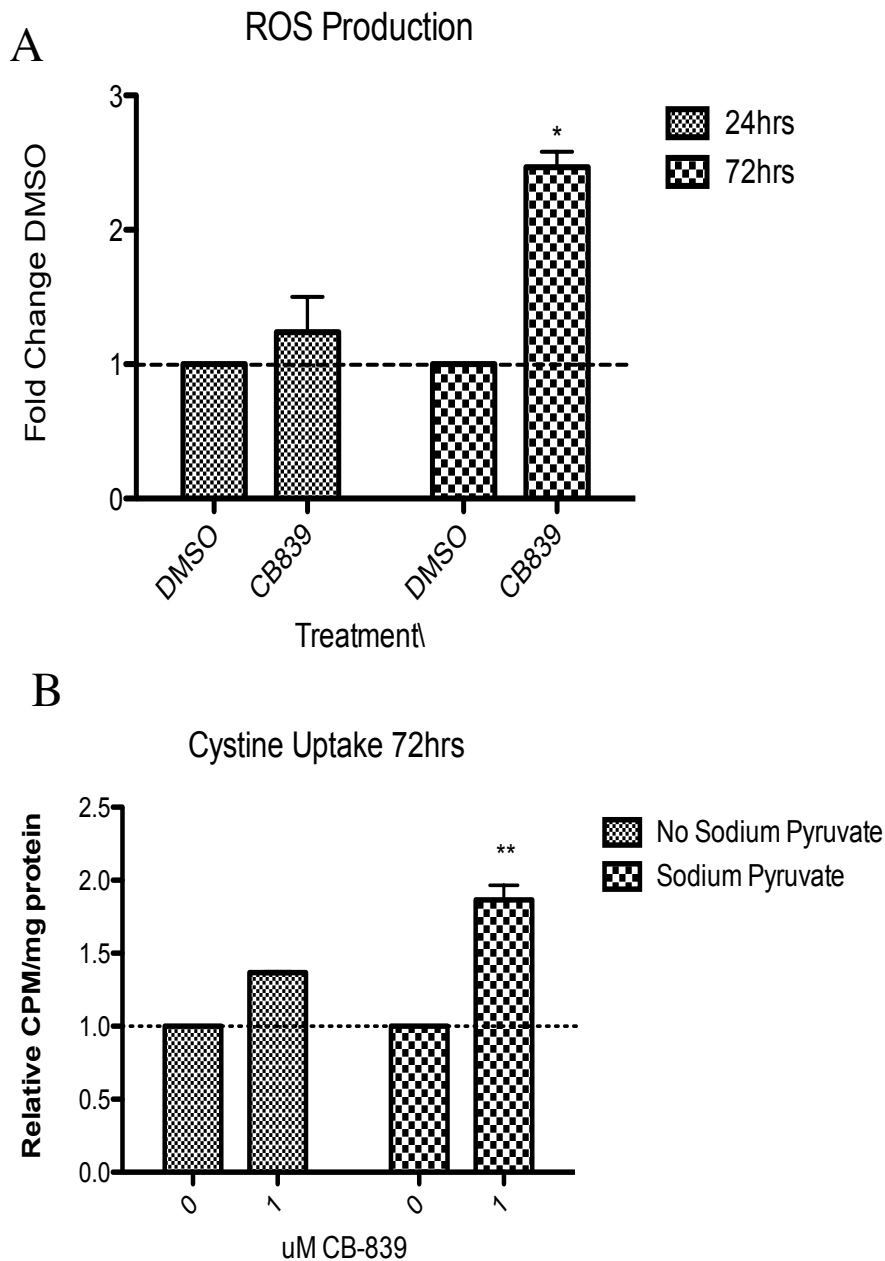


**Figure 6: Production of reactive oxygen species over the course of 24 and 72 hrs and cystine uptake after 72hr treatment with 1 $\mu$ M CB-839.**

A significant increase in ROS (A) is observed after a 72hr incubation with 1000nM CB-839 ( $P < 0.05$ ; 2-way repeated measures ANOVA). Similarly, [ $^{14}$ C]-cystine uptake (B) increases significantly by 72 hrs but only in the absence of sodium pyruvate ( $P < 0.01$ ; 2-way repeated measures ANOVA)

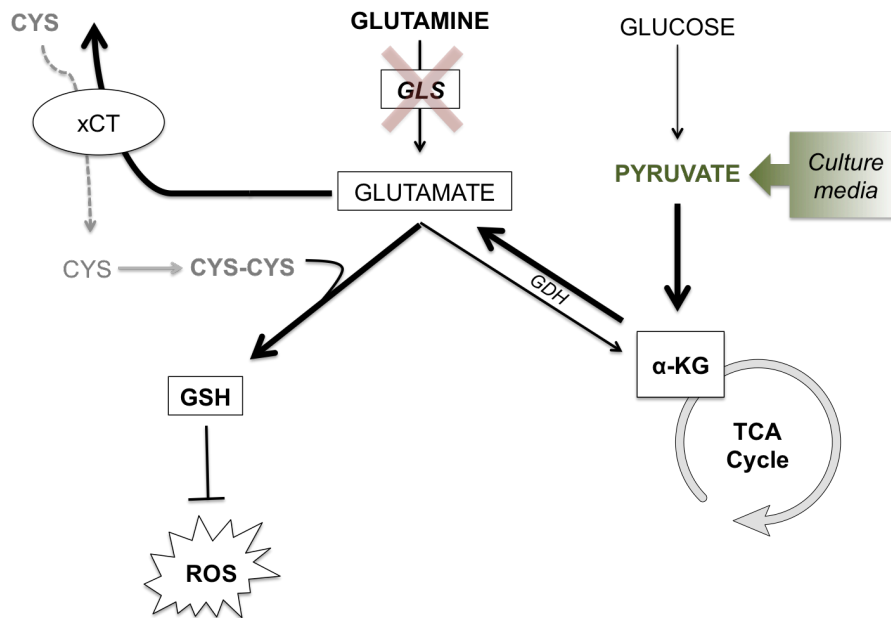


**Figure 7: Glutathione synthesis for ROS detoxification drives metabolic adaptations to maintain glutamate production and cystine acquisition in the absence of GLS activity.**

Bolded arrows represent the pathway that is hypothesized to compensate for loss of glutamine-derived glutamate under conditions of GLS inhibition or low glutamine conditions. Under *in vitro* conditions, the addition of sodium pyruvate to cell culture media drives this process.

## REFERENCES CHAPTER 4:

1. Mattingly, B. A., Rowlett, J. K. & Lovell, G. Effects of daily SKF 38393, quinpirole, and SCH 23390 treatments on locomotor activity and subsequent sensitivity to apomorphine. *Psychopharmacology (Berl.)* **110**, 320–326 (1993).
2. Gross, M. I. *et al.* Antitumor activity of the glutaminase inhibitor CB-839 in triple-negative breast cancer. *Mol. Cancer Ther.* **13**, 890–901 (2014).
3. Timmerman, L. A. *et al.* Glutamine sensitivity analysis identifies the xCT antiporter as a common triple-negative breast tumor therapeutic target. *Cancer Cell* **24**, 450–465 (2013).
4. Mayers, J. R. & Vander Heiden, M. G. Famine versus feast: understanding the metabolism of tumors in vivo. *Trends Biochem. Sci.* **40**, 130–140 (2015).
5. Hanahan, D. & Weinberg, R. A. Hallmarks of cancer: the next generation. *Cell* **144**, 646–674 (2011).
6. Vander Heiden, M. G. & DeBerardinis, R. J. Understanding the Intersections between Metabolism and Cancer Biology. *Cell* **168**, 657–669 (2017).
7. Hosios, A. M. *et al.* Amino Acids Rather than Glucose Account for the Majority of Cell Mass in Proliferating Mammalian Cells. *Dev. Cell* **36**, 540–549 (2016).
8. Wise, D. R. & Thompson, C. B. Glutamine addiction: a new therapeutic target in cancer. *Trends Biochem. Sci.* **35**, 427–433 (2010).
9. Alberghina, L. & Gaglio, D. Redox control of glutamine utilization in cancer. *Cell Death Dis.* **5**, e1561 (2014).

10. Carrascosa, J. M., Martínez, P. & Castro, I. N. de. Nitrogen Movement between Host and Tumor in Mice Inoculated with Ehrlich Ascitic Tumor Cells. *Cancer Res.* **44**, 3831–3835 (1984).
11. Collins, C. L., Wasa, M., Souba, W. W. & Abcouwer, S. F. Determinants of glutamine dependence and utilization by normal and tumor-derived breast cell lines. *J. Cell. Physiol.* **176**, 166–178 (1998).
12. Kung, H.-N., Marks, J. R. & Chi, J.-T. Glutamine synthetase is a genetic determinant of cell type-specific glutamine independence in breast epithelia. *PLoS Genet.* **7**, e1002229 (2011).
13. Weinberg, F. *et al.* Mitochondrial metabolism and ROS generation are essential for Kras-mediated tumorigenicity. *Proc. Natl. Acad. Sci. U. S. A.* **107**, 8788–8793 (2010).
14. Son, J. *et al.* Glutamine supports pancreatic cancer growth through a KRAS-regulated metabolic pathway. *Nature* **496**, 101–105 (2013).
15. Altman, B. J., Stine, Z. E. & Dang, C. V. From Krebs to clinic: glutamine metabolism to cancer therapy. *Nat. Rev. Cancer* **16**, 619–634 (2016).
16. Yang, M. & Vousden, K. H. Serine and one-carbon metabolism in cancer. *Nat. Rev. Cancer* **16**, 650–662 (2016).
17. Bhutia, Y. D., Babu, E., Ramachandran, S. & Ganapathy, V. Amino Acid transporters in cancer and their relevance to ‘glutamine addiction’: novel targets for the design of a new class of anticancer drugs. *Cancer Res.* **75**, 1782–1788 (2015).

18. Ungard, R. G., Seidlitz, E. P. & Singh, G. Inhibition of breast cancer-cell glutamate release with sulfasalazine limits cancer-induced bone pain. *Pain* **155**, 28–36 (2014).
19. Fazzari, J., Balenko, M. D., Zacal, N. & Singh, G. Identification of capsazepine as a novel inhibitor of system xc- and cancer-induced bone pain. *J. Pain Res.* **10**, 915–925 (2017).
20. Quadros, A. U. *et al.* Dynamic weight bearing is an efficient and predictable method for evaluation of arthritic nociception and its pathophysiological mechanisms in mice. *Sci. Rep.* **5**, 14648 (2015).
21. Muir, A. *et al.* Environmental cystine drives glutamine anaplerosis and sensitizes cancer cells to glutaminase inhibition. *eLife* **6**, (2017).
22. Shin, C.-S. *et al.* The glutamate/cystine xCT antiporter antagonizes glutamine metabolism and reduces nutrient flexibility. *Nat. Commun.* **8**, 15074 (2017).
23. Gu, Y. *et al.* mTORC2 Regulates Amino Acid Metabolism in Cancer by Phosphorylation of the Cystine-Glutamate Antiporter xCT. *Mol. Cell* **67**, 128-138.e7 (2017).
24. Sayin, V. I. *et al.* Activation of the NRF2 antioxidant program generates an imbalance in central carbon metabolism in cancer. *eLife* **6**, e28083 (2017).
25. Budczies, J. *et al.* Comparative metabolomics of estrogen receptor positive and estrogen receptor negative breast cancer: alterations in glutamine and beta-alanine metabolism. *J. Proteomics* **94**, 279–288 (2013).
26. Budczies, J. *et al.* Glutamate enrichment as new diagnostic opportunity in breast cancer. *Int. J. Cancer* **136**, 1619–1628 (2015).

27. Lampa, M. *et al.* Glutaminase is essential for the growth of triple-negative breast cancer cells with a deregulated glutamine metabolism pathway and its suppression synergizes with mTOR inhibition. *PLoS One* **12**, e0185092 (2017).
28. Biancur, D. E. *et al.* Compensatory metabolic networks in pancreatic cancers upon perturbation of glutamine metabolism. *Nat. Commun.* **8**, 15965 (2017).
29. Cheng, T. *et al.* Pyruvate carboxylase is required for glutamine-independent growth of tumor cells. *Proc. Natl. Acad. Sci.* **108**, 8674–8679 (2011).
30. Gaglio, D. *et al.* Oncogenic K-Ras decouples glucose and glutamine metabolism to support cancer cell growth. *Mol. Syst. Biol.* **7**, 523 (2011).
31. Yang, C. *et al.* Glutamine oxidation maintains the TCA cycle and cell survival during impaired mitochondrial pyruvate transport. *Mol. Cell* **56**, 414–424 (2014).
32. Whillier, S., Garcia, B., Chapman, B. E., Kuchel, P. W. & Raftos, J. E. Glutamine and  $\alpha$ -ketoglutarate as glutamate sources for glutathione synthesis in human erythrocytes. *FEBS J.* **278**, 3152–3163 (2011).

## **CHAPTER 5: CONCLUSION AND FUTURE DIRECTIONS**

## SUMMARY:

The work comprising this dissertation presents the early stages of developing novel therapeutics for cancer-induced bone pain in an effort to address an unmet clinical need. Cancer-related pain often increases with disease progression and becomes more difficult to manage as a result. Cancer cells are constantly adapting to and modulating their environment making CIBP a multifaceted pain state exhibiting characteristics of both inflammatory and neuropathic pain. The dynamic nature of the cancer tissue itself and the inadequacy of current therapeutics warranted a mechanistic investigation. Both increased oxidative stress and increased dependency on alternate nutrient sources involves increased production and release of glutamate into the extracellular environment. Therefore, targeting the cancer-derived nociceptive factors such as glutamate may offer a more effective peripheral treatment strategy for this complex pain state. This strategy circumvents the central targets that are the focus of most pain medications and the source of undesirable side effects.

The literature listed below outlines the works that contributed to the development of the hypothesis investigated in this dissertation.

Seidlitz E. P., Sharma M. K., Saikali Z., Ghert M. & Singh G. **Cancer cell lines release glutamate into the extracellular environment.** Clin. Exp. Metastasis 26, 781–787 (2009).

Sharma M. K., Seidlitz E. P. & Singh G. **Cancer cells release glutamate via the cystine/glutamate antiporter.** Biochem. Biophys. Res. Commun. 391, 91–95 (2010).

Ungard R. G., Seidlitz E. P. & Singh G. **Inhibition of breast cancer-cell glutamate release with sulfasalazine limits cancer-induced bone pain.** Pain (2013) 10.1016/j.pain.2013.08.030.

Slosky LM, BassiriRad NM, Symons AM, et al. **The cystine/glutamate antiporter system xc<sup>-</sup> drives breast tumor cell glutamate release and cancer-induced bone pain.** Pain. 2016;157(11):2605–2616.

Seidlitz E. P., Sharma M. K. & Singh G. **Extracellular glutamate alters mature osteoclast and osteoblast functions.** Can. J. Physiol. Pharmacol. 88, 929–936 (2010).

Walker, K.M., Urban, L., Medhurst, S.J., Patel, S., Panesar, M., Fox, A.J., and McIntyre, P. (2003). **The VR1 Antagonist Capsazepine Reverses Mechanical Hyperalgesia in Models of Inflammatory and Neuropathic Pain.** J Pharmacol Exp Ther 304, 56–62.

Collins, C.L., Wasa, M., Souba, W.W., and Abcouwer, S.F. (1998). **Determinants of glutamine dependence and utilization by normal and tumor-derived breast cell lines.** J. Cell. Physiol. 176, 166–178.

Gross, M.I., Demo, S.D., Dennison, J.B., Chen, L., Chernov-Rogan, T., Goyal, B., Janes, J.R., Laidig, G.J., Lewis, E.R., Li, J., et al. (2014). **Antitumor Activity of the Glutaminase Inhibitor CB-839 in Triple-Negative Breast Cancer.** Mol Cancer Ther 13, 890–901.

Whillier S., Garcia B., Chapman B. E., Kuchel P. W. & Raftos J. E. **Glutamine and  $\alpha$ -ketoglutarate as glutamate sources for glutathione synthesis in human erythrocytes.** FEBS J. 278, 3152–3163 (2011).

Therefore the following hypothesis was generated:

*Dysregulated cancer cell metabolism results in the production and release of glutamate into the tumour microenvironment where it acts as a pronociceptive stimulus on primary afferent nerve fibres leading to the development of CIBP.*

This hypothesis was explored through the following objectives discussed below in the context of the previous chapters and in reference to their contribution to the literature.

*Objective 1:* Establish a high-throughput screening protocol to identify novel inhibitors of glutamate release from MDA-MB-231 cells and identify lead molecules.

This work builds on the data put forth by Collins et al. 1996, Seidlitz et al. 2009 and Sharma et al. 2010 where it was shown that breast cancer cells secrete glutamate into their extracellular environment and that this release is mediated by the cystine/glutamate antiporter, system xc<sup>-</sup>. Due to the therapeutic potential of targeting glutamate release from cancer cells to treat CIBP, we screened thousands of small molecules for their ability to block this process.

*Objective 2:* Characterize antinociceptive effects of one lead molecule, Capsazepine, in a CIBP model.

This paper expands on the publications by Ungard et al. 2013 showing that systemic administration of an inhibitor of system xc<sup>-</sup>, Sulfasalazine (SSZ), significantly delayed the onset of one type of CIBP behaviour associated with clinical skeletal pain. Dynamic weight bearing analysis is designed to assess postural equilibrium and spontaneous nociceptive behaviours<sup>1</sup> which SSZ was able to modulate. However behavioral assessment using the dynamic plantar aesthesiometer measure of touch sensitivity (allodynia) was not affected in animals receiving SSZ. Poor bioavailability and off-target effects of SSZ made investigation into novel inhibitors crucial for pursuing cancer-secreted glutamate as a therapeutic target for CIBP. Slosky et al. 2016 confirmed the antinociceptive effect of SSZ through the use of flinching and guarding pain behaviours supporting the role of tumour-derived glutamate in CIBP<sup>2</sup>.

As discovered in Objective 1, Capsazepine (CPZ) was a lead candidate molecule and pursued for its ability to modulate CIBP. CPZ proved to be more effective than SSZ in preventing CIBP behaviours as well as modulating other cellular mechanisms both upstream and downstream of system xc<sup>-</sup>; xCT transcription and GSH production respectively.

Walker et al. 2003 showed that CPZ reversed mechanical hyperalgesia in inflammatory and neuropathic pain models in a species specific manner with little efficacy in the rat and mouse except for preventing capsaicin-induced nociceptive behaviours<sup>3</sup>. Their models were direct inductions of pathologies and did not represent a complex pain state that has both neuropathic and inflammatory components such as CIBP. Furthermore, effective doses used in this publication exceed 10 mg/kg whereas 5mg/kg CPZ were effective in the CIBP model from Chapter 2. Another target of CPZ was therefore identified, contributing to the possible uses of this molecule previously abandoned due to its lack of specificity for its original target TRPV1<sup>4-8</sup>. Most importantly, this is the first publication to show antihyperalgesic activity of CPZ in a mouse model of pain.

*Objective 3:* Characterize antinociceptive effects of a glutaminase inhibitor on CIBP model.

This paper presents the first investigation into cancer GLS as a target for CIBP. This builds on the glutamate hypothesis however, rather than targeting glutamate release from the cancer cell via system xc<sup>-</sup>, glutamate production is being targeted with the anticipation that reducing the intracellular glutamate pool would prevent its release.

These data reveal that targeting glutaminase activity *in vivo* can vary from *in vitro* observations highlighting the fact that each cancer line should be characterized based on its nutrient flexibility when assessing drug effectiveness. These data do not model that of Gross et al. 2014 highlighting inherent differences between cancer cell lines despite having similar clinical classification based on receptor status. This difference between *in vitro* and *in vivo* sensitivity to this drug has also been observed by other investigations in different cancer types highlighting how the metabolic demands of the same cell type can differ under *in vitro* and *in vivo* conditions.

## Future Directions:

Discovery and characterization of small molecule inhibitors of glutamate release has established a connection between cancer cell metabolism and the development of CIBP. Both processes of glutamate production by GLS and glutamate release via system xc<sup>-</sup> are driven by the cellular demand for antioxidant production. ROS detoxification is essential for cancer cell survival under conditions of rapid proliferation. Further investigation into how these metabolic changes influence the tumour microenvironment and how these changes subsequently influence peripheral and central nociception. This convergence of cancer cell metabolism with peripheral nociceptors in the tumour microenvironment a unique target for CIBP.

Peripheral afferent nerve fibres surrounding the tumour receive ongoing stimulation from tumour-derived factors which can lead to central sensitization and long-term potentiation. In addition, sprouting and reorganization of afferent fibres in the periosteum and skin in vicinity of the tumour<sup>9-11</sup>. Future investigations could reveal how

cancer secreted factors can modulate structural plasticity of the peripheral nervous system.

Targeting factors that can induce such sprouting, such as Nerve Growth Factor (NGF) has been an attractive target with NGF antagonists showing robust, pre-clinical success, clinical trials have been plagued by unwanted side-effects such as osteoarthritis, osteonecrosis<sup>12</sup> resulting in accelerated joint damage<sup>13</sup> and autonomic nervous system toxicity<sup>14</sup>. Similarly, targeting glutamate receptors themselves have not been safe due to their involvement in many physiological pathways<sup>15</sup>.

As discussed in Chapter 3, CPZ is a partial antagonist of TRPV1 which is a polymodal nociceptor and implicated in many pain disorders (See review by Holzer 2008<sup>16</sup>). TRPV1 is present on the sensory afferent fibres that innervate the femur in the mouse<sup>17</sup>, therefore, in order to fully understand the antinociceptive action of CPZ in the CIBP models described in Chapter 3, the use of a TRPV1 knockout model of CIBP would be essential to understand if the action of CPZ was indeed independent of this receptor.

Aerobic glycolysis has been the major hallmark of altered cancer cell metabolism discussed in the literature since its description by Warburg, 1956<sup>18</sup>. However, glutamine metabolism and specifically glutamine “addiction” has come to the forefront over recent years having a role as both an energy source and nitrogen source fueling biosynthetic demands of the cell (see reviews by Altman et al. 2016<sup>19</sup>; Still and Yuneva 2017<sup>20</sup>). Glutamine’s relationship to glutamate production via the glutaminase (GLS) enzyme made this enzyme another attractive target for glutamate-mediated CIBP. Having discovered that a lead molecule from Chapter 2 had been shown to have off-target

antagonist effects on GLS, highlighted the fact that this enzyme represents another way to target glutamate release and that is by preventing its production from glutamine.

With such a vast amount of literature describing the upregulation of glutaminolytic machinery<sup>21-24</sup>, GLS activity<sup>21</sup> and sensitivity of many cancer cell lines to glutamine withdrawal<sup>21,22</sup> as well as its association with oxidative stress and xCT expression<sup>22</sup> made the results discussed in Chapter 4 unexpected. The microenvironment varies greatly between *in vitro* and *in vivo* conditions with the changing conditions *in vivo* placing different demands on the cancer cell for survival. These adaptations may favour different metabolic pathways whether it be for energy production, anabolism and growth or ROS detoxification. Furthermore, metabolic pathways may also become compartmentalized and function independently of a once coordinated network limiting the metabolic flexibility of the cell and adaptation to certain nutrient conditions. Not only could these metabolic changes influence the release of potentially nociceptive factors such as glutamate they may promote resistance to drugs targeting specific metabolic networks by exploiting redundancies in the metabolic networks. Further investigation into which *in vitro* conditions best represent those *in vivo* may streamline the discovery of molecules that target major metabolic hubs in the cancer cell. A combinatorial approach to treatment to block adapting metabolic pathways may offer less variable results and more robust clinical outcomes.

## CONCLUSION:

The results of this body of work links cancer cell metabolism to CIBP behaviours. Byproducts of dysregulated cancer cell metabolism acts as a source of nociceptive

factors that can activate sensory neurons surrounding the malignancy. The preceding chapters provide evidence how novel pain therapeutics can target the peripheral pain-inducing pathologies rather than central responses to these stimuli which often leads to unwanted side effects and loss of functionality associated with common analgesics. It is the unique metabolic alterations in cancer cells that make cancer-associated comorbidities such as CIBP multifaceted and notoriously difficult to treat. However it is also these unique adaptations that offer great therapeutic potential to explore cancer-specific targets that spare disturbances in physiological systems. Exploiting pathology-specific features will be the key to developing new classes of potent analgesics with limited side effects.

## REFERENCES CHAPTER 5:

1. Robinson, I., Sargent, B. & Hatcher, J. P. Use of dynamic weight bearing as a novel end-point for the assessment of Freund's Complete Adjuvant induced hypersensitivity in mice. *Neurosci. Lett.* **524**, 107–110 (2012).
2. Slosky, L. M. *et al.* The cystine/glutamate antiporter system xc<sup>-</sup> drives breast tumor cell glutamate release and cancer-induced bone pain. *Pain* **157**, 2605–2616 (2016).
3. Walker, K. M. *et al.* The VR1 antagonist capsazepine reverses mechanical hyperalgesia in models of inflammatory and neuropathic pain. *J. Pharmacol. Exp. Ther.* **304**, 56–62 (2003).
4. Bevan, S. *et al.* Capsazepine: a competitive antagonist of the sensory neurone excitant capsaicin. *Br J Pharmacol* **107**, 544–552 (1992).
5. Teng, H.-P. *et al.* Capsazepine elevates intracellular Ca<sup>2+</sup> in human osteosarcoma cells, questioning its selectivity as a vanilloid receptor antagonist. *Life Sci.* **75**, 2515–2526 (2004).
6. Docherty, R. J., Yeats, J. C. & Piper, A. S. Capsazepine block of voltage-activated calcium channels in adult rat dorsal root ganglion neurones in culture. *Br. J. Pharmacol.* **121**, 1461–1467 (1997).
7. Gill, C. H. *et al.* Characterization of the human HCN1 channel and its inhibition by capsazepine. *Br. J. Pharmacol.* **143**, 411–421 (2004).
8. Liu, L. & Simon, S. A. Capsazepine, a vanilloid receptor antagonist, inhibits nicotinic acetylcholine receptors in rat trigeminal ganglia. *Neurosci. Lett.* **228**, 29–32 (1997).

9. Bloom, A. P. *et al.* Breast cancer-induced bone remodeling, skeletal pain, and sprouting of sensory nerve fibers. *J Pain* **12**, 698–711 (2011).
10. Jimenez-Andrade, J. M. *et al.* Pathological Sprouting of Adult Nociceptors in Chronic Prostate Cancer-Induced Bone Pain. *J. Neurosci.* **30**, 14649–14656 (2010).
11. Chapurlat, R. D. *et al.* Pathophysiology and medical treatment of pain in fibrous dysplasia of bone. *Orphanet J Rare Dis* **7**, S3 (2012).
12. Lane, N. E. *et al.* Tanezumab for the treatment of pain from osteoarthritis of the knee. *N. Engl. J. Med.* **363**, 1521–1531 (2010).
13. Miller, R. E., Block, J. A. & Malfait, A.-M. Nerve growth factor blockade for the management of osteoarthritis pain: what can we learn from clinical trials and preclinical models? *Curr Opin Rheumatol* **29**, 110–118 (2017).
14. Mullard, A. Drug developers reboot anti-NGF pain programmes. *Nature Reviews Drug Discovery* (2015). doi:10.1038/nrd4612
15. Liu, X. J. & Salter, M. W. Glutamate receptor phosphorylation and trafficking in pain plasticity in spinal cord dorsal horn. *Eur. J. Neurosci.* **32**, 278–289 (2010).
16. Holzer, P. The pharmacological challenge to tame the transient receptor potential vanilloid-1 (TRPV1) nociceptor. *Br J Pharmacol* **155**, 1145–1162 (2008).
17. Ghilardi, J. R. *et al.* Selective blockade of the capsaicin receptor TRPV1 attenuates bone cancer pain. *J. Neurosci.* **25**, 3126–3131 (2005).
18. Warburg, O. On the origin of cancer cells. *Science* **123**, 309–314 (1956).
19. Altman, B. J., Stine, Z. E. & Dang, C. V. From Krebs to clinic: glutamine metabolism to cancer therapy. *Nat. Rev. Cancer* **16**, 619–634 (2016).

20. Still, E. R. & Yuneva, M. O. Hopefully devoted to Q: targeting glutamine addiction in cancer. *British Journal of Cancer* **116**, 1375–1381 (2017).
21. Gross, M. I. *et al.* Antitumor activity of the glutaminase inhibitor CB-839 in triple-negative breast cancer. *Mol. Cancer Ther.* **13**, 890–901 (2014).
22. Timmerman, L. A. *et al.* Glutamine sensitivity analysis identifies the xCT antiporter as a common triple-negative breast tumor therapeutic target. *Cancer Cell* **24**, 450–465 (2013).
23. Cassago, A. *et al.* Mitochondrial localization and structure-based phosphate activation mechanism of Glutaminase C with implications for cancer metabolism. *PNAS* **109**, 1092–1097 (2012).
24. Redis, R. S. *et al.* Allele-Specific Reprogramming of Cancer Metabolism by the Long Non-coding RNA CCAT2. *Mol. Cell* **61**, 640 (2016).

## **APPENDIX I: ASSAY DEVELOPMENT AND OPTIMIZATION**

## Adaptation of the Amplex Red assay

### *Compound Interference:*

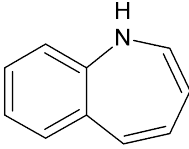
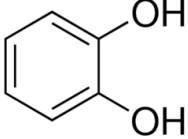
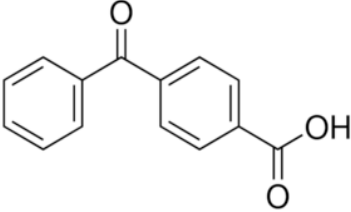
As per the established protocol, measurement of glutamate levels were obtained from a single, endpoint read (i.e. after a 30 minute incubation) and not as a time course. With some initial difficulty replicating the potency of the screening leads, it was determined that the drugs themselves, although colourless, affected the measurement possibly due to auto-fluorescence or interference with some component of the assay.

To confirm this, compounds were added over a range of 0-200  $\mu\text{M}$  to known concentrations of glutamate in the absence of cells. Reading fluorescence using the same Amplex Red detection method, it was observed that standard glutamate dose response curves were altered by the presence of some of the compounds. Due to this factor, the HTS method of reading fluorescence (i.e. as a rate) was adopted for bench-top screening and glutamate was measured in the conditioned media collected from treated cells. Measurements were taken every 90 seconds over the course of 15 minutes in order to obtain a rate of fluorescence rather than a single read as this method has the potential to under- represent the data. In contrast to screening conditions measurements were obtained from media alone whereas in the screen, cells were still present at the time of measurement. As discussed in Chapter 2 the molecule hits from the HTS share a benzazepine and/or dihydroxybenzene (**Figure 1**) functional groups. As shown in **Table 1** below, the slope of standard glutamate curves are altered in the presence of these molecules with slopes decreasing with increasing concentrations of each compound.

It has been shown that molecules containing 4-benzoylbenzoic groups (**Figure 1**) interfere with the HRP-catalyzed oxidation of Amplex Red<sup>1</sup>. In this investigation, however, the presence of these molecules enhanced Amplex Red oxidation to resorufin.

$\mu\text{M}$	DMSO	SKF-38393	N,N-DP	CPZ
0	132.94			
10		69.18	67.43	64.76
25		53.16	53.47	44.61
50		52.73	30.84	57.04

**TABLE 1: Slopes from the glutamate standard curves (0-50  $\mu\text{M}$ ) generated using the Amplex Red Glutamic Acid/Glutamate oxidase assay spiked with varying concentrations of the test molecules.**

		
Benzazepine	Dihydroxybenzene	4-benzoylbenzoic

**Figure 1: Functional groups from molecules affecting the Amplex Red glutamic acid/glutamate oxidase assay**

The Amplex Red assay assumes that fluorescence is proportional to glutamate concentration but as seen in the reaction scheme shown below in **Figure 2**, this assay is indirect. Interference with the L-glutamate oxidase and/or horseradish peroxidase reaction(s) can decouple fluorescence intensity from actual glutamate concentrations in the test media and give a false representation of these data.

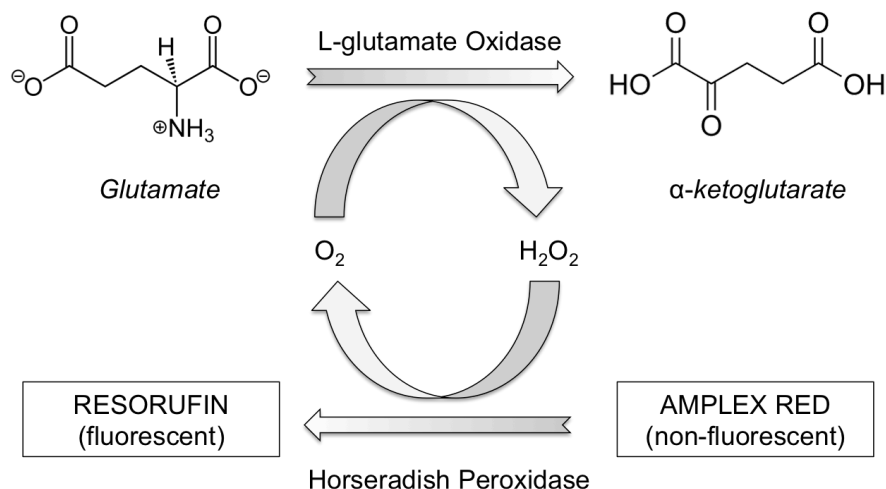


**Figure 2: Amplex Red reaction scheme.**

Quantification of the fluorescent product resorufin is proportional to the concentration of glutamate via L-glutamate oxidase.

### *Optimizing Cell Number in Follow-up Testing:*

Moving from a 384-well to a 96-well format, the increase in surface area meant that cell seeding density was a factor that may influence compound efficacy (i.e. how the cells response to the compound) as well as the concentration required to illicit same level of inhibition observed in screening. Timmerman et al. 2013 had shown that culture confluence influences cell cycle phase content of breast cancer cells as well as affecting their response to glutamine restriction<sup>2</sup>. MDA-MB-231 cells are glutamine auxotrophs and highly dependent on glutamine over other energy sources for growth. These cells have been shown to adjust growth parameters in metabolic conditions of stress by controlling expression of certain compensating factors including system xc- activity and expression<sup>2</sup>. Compounds were tested at varying cell densities (3, 000; 5, 000; 10,000

cells) which did not seem to affect the dose-response trend observed in initial tests at the seeding density of 10, 000 cells suggested in the protocol.

Follow-up screening also accounted for a major pitfall of the original high-throughput screen procedure- it did not effectively account for cytotoxicity/cell death associated with drug treatment. Although visually identified as non-toxic at 10uM, the dose-response data generated in follow-up testing was significantly affected by cell number normalization. The potency of these compounds relative to SSZ were, therefore, not as dramatic as originally observed in HTS.

#### *Impact of H<sub>2</sub>O<sub>2</sub> release on Amplex Red Fluorescence:*

Furthermore, due to the nature of the Amplex Red assay, it was necessary to rule out the production of H<sub>2</sub>O<sub>2</sub> after treatment with each molecule. H<sub>2</sub>O<sub>2</sub> could generate artificially high readings due to the indirect nature of the assay (in which H<sub>2</sub>O<sub>2</sub> is the actual product measured). It is expected that any compounds that had such an effect (i.e. induced H<sub>2</sub>O<sub>2</sub> production) would naturally be eliminated in the screening process. They would appear with low inhibitory activity (high glutamate levels after treatment) and would not be below our threshold at which positive hits were selected. However, it was important to rule out the possibility of this being a confounding factor when testing over a range of concentrations. Culture media was collected from MDA-MB-231 cells incubated with compounds as described in Chapter 2. The Amplex Red rxn scheme (**Figure 2**) was modified so that fluorescence intensity was proportional to H<sub>2</sub>O<sub>2</sub> to endogenous H<sub>2</sub>O<sub>2</sub> production. This was done by only including the Amplex Red reagent in the reaction mix. Eliminating glutamate oxidase in the reaction ensures only H<sub>2</sub>O<sub>2</sub>

generated/released from the cells will be available as the substrate for HRP to catalyze the Amplex Red to resorufin reaction.

It can be seen in Figure 3 that only at toxic doses (correlated with low cell number) is  $H_2O_2$  an issue. Due to issues associated with toxicity including a spike in glutamate release under some circumstances, these doses were eliminated from subsequent testing.

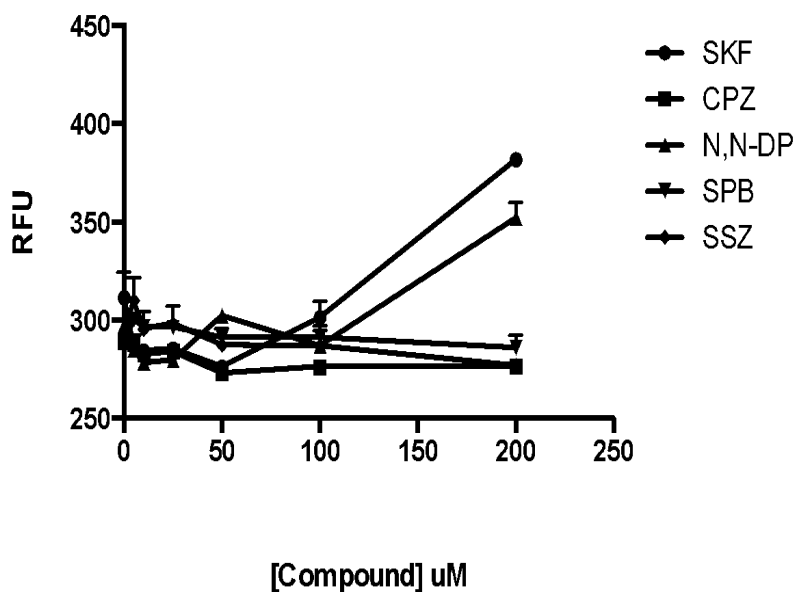


**Figure 3:  $H_2O_2$  production following treatment with compound hits from high-throughput screening for inhibitors of glutamate release from MDA-MB-231 cells.**

## Radiolabeled cystine uptake assay:

Due to the limitations of the Amplex Red assay discussed above, a more specific assay was needed to assess xCT activity. Even if the compounds did not interfere with the Amplex assay reaction, a compound's action on glutamate release does not indicate total specificity for system xc-, therefore a more direct method of quantifying xCT activity was necessary to test whether their pharmacological inhibition of glutamate release is directly related to xCT inhibition. Monitoring cystine influx into the cell is an effective way of measuring xCT activity directly. As detailed in Chapter 1, glutamate release through xCT occurs as a 1:1 exchange coupled with the uptake of cystine from the extracellular environment<sup>3</sup>. Transport activity can be quantified by monitoring the flux the uptake of cystine from the extracellular environment. [<sup>14</sup>C]L- cystine uptake to characterize xCT activity. It should be noted that even though cystine is rapidly converted to cysteine once it enters the intracellular space, with the probe often being incorporated into glutathione and cysteine-glutathione disulfides<sup>9</sup>, scintillation measurements are not biased to the presence of labeled cystine alone, therefore incorporation of labeled thiols into other molecules will still be indicative of cystine uptake. L-glutamate efflux will be quantified using the Amplex Red reagent on conditioned media samples, which is a well-established assay in our lab<sup>4,5</sup>. Although this assay represents a standard method of assessing xCT activity in the literature<sup>6-8</sup>, uptake and lysis buffers as well as concentration of radiolabeled substrate and cell seeding densities vary between protocols and optimization was therefore required for implementation in our lab. The known xCT inhibitor, SSZ, was used for assay optimization as it's ability to reduce cystine uptake is well represented in the literature<sup>8-10</sup>ograp.

Troubleshooting revealed that cell density can have a profound effect on the uptake of cystine and should be taken into consideration when planning and comparing experimental results. It was also discovered that to replicate the robust effect SSZ has on cystine uptake, the drug must be added to the uptake buffer and not removed or washed prior to lysis. It was found that washing the cells after incubation eliminates the effect of the drug on xCT activity. This implies the drug acts in a steric manner and its effects are reversible. This therefore, becomes another important consideration when testing novel compounds (modification to step 2).

The protocol was finalized as follows:

1. Cells were seeded at a density of 250 000 cells per well in a 6-well plate and left to adhere overnight before treating with experimental compound(s).
2. Cells are to be treated in cell culture media for the desired period of time (see note 1 below)
3. Prior to loading the cells with <sup>14</sup>C-cystine, aspirate culture media and wash with HBSS.
4. Add uptake buffer to cells- 300ul HBSS containing 0.009uCi
5. Incubate at 37C for 20 minutes
6. Aspirate uptake buffer and quickly wash 3X with ice-cold HBSS to stop uptake
7. Lyse cells in 220 ul of lysis buffer (0.1N NaOH containing 0.1% Triton-X) for 30 minutes
8. Add 100 ul of each cell lysate into a 5 mL scintillation vial containing 1 mL of Ecoscint-H solution. (NOTE: remaining lysate will be used to measure protein

levels using the Bradford method. This is to normalize scintillation values (provided as counts per minute;CPM) to mg protein.

9. Samples were subject to liquid scintillation using a Beckman LS500 scintillation counter

**Note 1:** *As discussed above for SSZ, if the potential action of the drug on cystine uptake in cells is lost upon its removal prior to exposure to the radiolabeled substrate, the drug should be present in the uptake buffer.*

Overall, development of this radioisotope uptake assay will allow us to directly measure xCT activity as cystine uptake is limited to the activity of this transporter. These data can then be correlated to glutamate release to provide a more robust profile of xCT activity in these cells in response to test compounds.

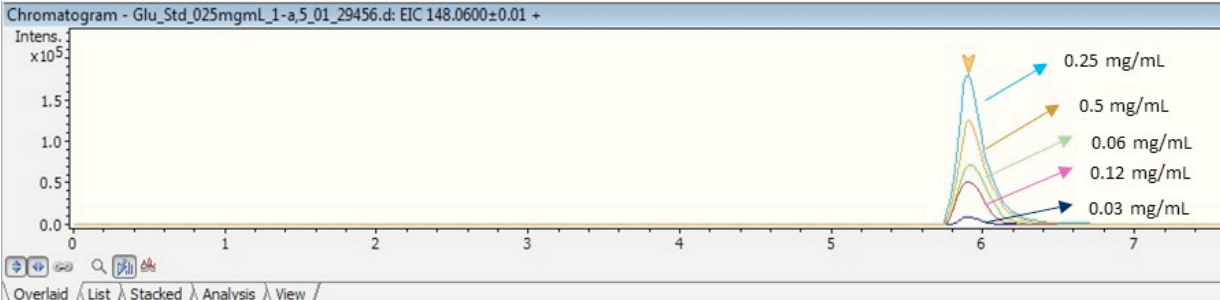
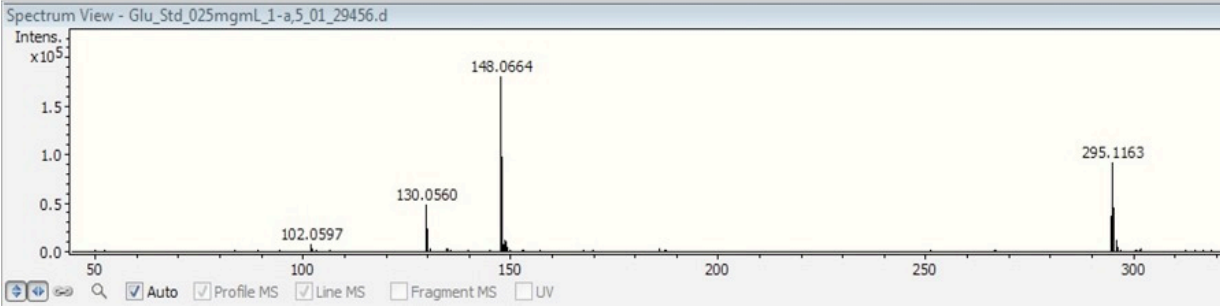
## Development of HPLC-MS Protocol for Glutamate Quantification:

Quantification of glutamate by HPLC-MS was pursued to overcome the limitations of the Amplex Red assay. This is an important tool to quantify glutamate levels from *in vivo* samples such as serum in order to see how testing of novel compounds on CIBP impacts glutamate levels. Extensive troubleshooting of methods was necessary to achieve a measurable signal, adequate separation from co-eluting analytes and appropriate detection at concentrations expected in sample..

Attempts at detection began with quantification of known concentrations of glutamate (10, 50 and 100ng) in 0.1% formic acid.

<b>Standards</b>	<b>Column</b>	<b>Mobile Phase</b>	<b>Mass Spec (mode)</b>
0.2-10ng/uL in 0.1% formic acid	C-18	A- MeOH 0.1% FA B- H2O 0.1% FA GRADIENT	Microtof (+)
Chromatogram could be extracted only at 5ng/uL concentration			
0.003-1mg/mL in H2O	HILIC	A- H2O 0.1% FA B- ACN GRADIENT	Microtof (+)
No detection			
0.003-1mg/mL in H2O	C-18	MeOH +5mM Ammonium Formate ISOCRATIC	Microtof (+)
No detection			
0.003-1mg/mL in H2O	HILIC	A- 0.1% FA +10mM ammonium formate B- 0.1% FA +ACN GRADIENT	Microtof (+)
No detection			
10ng/ul	PFP	A- ACN in 0.1% FA B- H2O in 0.1% FA	Microtof (+)
Signal but RT is 0.6min, low sensitivity, move to Orbitrap			
10ng/ul	PFP	A- ACN in 0.1% FA B- H2O in 0.1% FA	Orbitrap XL (+)
No results			
0.5mg/mL	C-8	A- ACN in 0.1% FA	Orbitrap XL (+)

		B- H2O in 0.1% FA	
Make standard curve (0.06-0.5 ng/mL) RT 3 min			
0.5mg/mL	C-8	A- ACN in 0.1% FA B- H2O in 0.1% FA	MicroTOF (+)
<p>Detection, but conc. too high Make standard curve (0.125-0.5)</p> <p>GLUTAMIC ACID STANDARD CURVE EQUATION: <math>y=8 \times 10^6 x + 236163</math> (<math>R^2=0.99666</math>)</p>			
<p>Chromatogram - Std_0125mgmL_1-c,2_01_29434.d: BPC +</p> <p>Spectrum View - Std_0125mgmL_1-c,2_01_29434.d</p>			
0.5mg/mL	C-8	A- ACN in 0.1% FA B- H2O in 0.1% FA ISOCRATIC (95% A, 5% B)	MicroTOF (+)
Make curve 0.03-0.5			

 <p>Chromatogram - Glu_Std_025mgmL_1-a_5_01_29456.d: EIC 148.0600±0.01 +</p>			
 <p>Spectrum View - Glu_Std_025mgmL_1-a_5_01_29456.d</p>			
<p>GLUTAMIC ACID STANDARD CURVE EQUATION (0.4-3.4µM): <math>y=1 \times 10^6 x + 468776</math> (<math>R^2=0.99704</math>)</p>			
0.03mg/mL	C-8 (4.6x150m m)	A- ACN in 0.1% FA B- H2O in 0.1% FA ISOCRATIC (95% A, 5% B)	Orbitrap (+)
<p>Consistently see m/z=148.06+1 but inconsistent area measurements- change column</p>			
<p>GLUTAMIC ACID STANDARD CURVE EQUATION (13-204µM): <math>y=940704x-1 \times 10^7</math> (<math>R^2=0.99908</math>)</p>			
4mg/mL	C-8 (2.1x100x3. 5 um)	A- ACN in 0.1% FA B- H2O in 0.1% FA ISOCRATIC (95% A, 5% B)	Orbitrap (+)
<p>GLUTAMIC ACID STANDARD CURVE EQUATION (1.2-25.5 µM): <math>y=164251x+83495</math> (<math>R^2=0.99784</math>)</p>			
<p>Failure to adequately separate glutamate and glutamine peaks which have similar elution times therefore cannot quantify without peak separation</p>			
	HILIC	A- 10mM Ammonium formate pH 6.5 B- ACN ISOCRATIC (30:70)	MicroTOF (-)

results have been achieved in high concentrations, using an Agilent 1200, coupled with a Bruker MicrOTOF. Therefore, to apply the conditions, described above, in plasma samples it is necessary to adapt the conditions to an Agilent Q-TOF coupled with an Agilent 1290.

	SeQuant ZIC-Hilic 3.5um, 100A, 150 x 2.1mm (PEEK)- Millipore	A- 10mM Ammonium formate pH 6.5 B- ACN ISOCRATIC (30:70)	QTOF (-)
GLUTAMIC ACID STANDARD CURVE EQUATION (145, 363, 725, 1450, 2180 and 2900 ng/mL): $y=3496.7x+397719$ ( $R^2=0.9975$ )			

Samples were spiked with a stable isotope of glutamate (L-glutamic acid-2, 3, 3, 4, 4-d<sub>5</sub>; 0.2ug/mL) as an internal standard prior to extraction in order to account for loss of analyte after sample processing (volume loss from extraction). Extraction with MeOH for 1h at -80C. Calibration curve was generated with pooled serum samples spiked with 0.1-1 ng/uL deuterated glutamate internal standard. This was to account for any matrix effects that would alter peak intensities of our analyte of interest. Therefore the standard curve must be measured in the same matrix as the sample to get accurate quantification. The equation of the final calibration curve was  **$y=3496.7x+397719$**  ( **$R^2=0.9975$** ).

## **APPENDIX II: ADDITIONAL EXPERIMENTS**

## Further characterization of SKF-38393:

### *xCT promoter activity*

In an effort to determine whether any compounds have transcriptional effects on xCT, we cloned 2.6 kilobase pairs (-2329 to +278 bp) of the human xCT promoter region from genomic DNA isolated from MDA-MB-231 breast cancer cells. Four truncations were also generated by PCR. Full length and truncated clones were transferred into a luciferase reporter gene construct (PGL3-Basic). MDA-MB-231 cells were transiently co-transfected with the dual luciferase system (PGL-3 Firefly and pRL-TK Renilla) and subsequently treated with compounds. SKF 38393 was the only compound that significantly inhibited luciferase activity (Figure 4). This result suggests that this compound could possibly be inhibiting one of the many transcription factors that we have mapped to bind the promoter of xCT.

Transfected cells were treated with 25uM of compounds for 24 hours. SKF-38393 affected the promoter activity of xCT after a 24hr treatment resulting in a 30% decrease in luciferase activity . This result suggests that SKF 38393 may be, in part, lowering glutamate release from MDA-MB-231 cells by transcriptional inhibition of xCT.

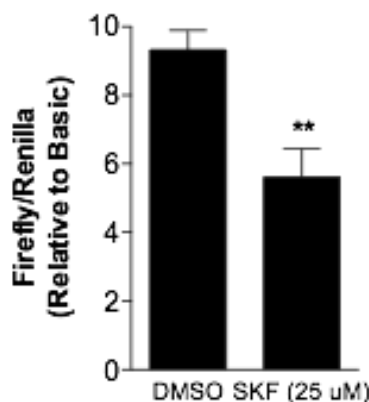


**Figure 4: SKF-38393 induces a decrease in xCT promoter activity.**

SKF-38393 affected the promoter activity of xCT after a 24hr treatment resulting in a 30% decrease in luciferase activity.

#### *Intracellular GSH*

Glutathione (GSH) levels were measured by DTNB quantification 24 hours after treatment. SKF 38393 was the only follow-up compound that showed a consistent dose-dependent decrease in total glutathione relative to cell number. Data represented as relative glutathione levels per 10<sup>6</sup> cells and normalized to vehicle levels. Correlating the decrease in GSH to a decrease in glutamate secretion suggests the target is xCT.

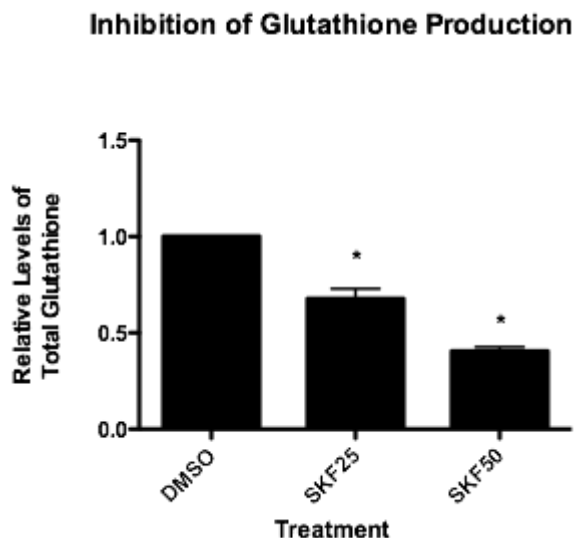


**Figure 5: SKF-38393 decreases intracellular glutathione levels in a dose-dependent manner.**

SKF 38393 was the only follow-up compound that showed a consistent dose-dependent decrease in total glutathione relative to cell number. Data represented as relative glutathione levels per 10<sup>6</sup> cells and normalized to vehicle levels. Correlating the decrease in GSH to a decrease in glutamate secretion suggests the target is xCT.

### Characterize transporter activity of HEK239T retroviral transduced xCT line:

In an effort to generate a tool to test compound specificity for xCT, Dr. Hanxin Lin and myself attempted to generate an xCT overexpression system in Human Embryonic Kidney cell line (HEK293T or 293T). In order to assess specificity, a less complicated model of xCT function is required in a cell line that has endogenously low xCT expression and glutamate secretion. HEK293T cells were chosen as a model cell line in which to overexpress the transporter. Murine system xc<sup>-</sup> has previously been overexpressed in HEK293 cells as a means of pharmacological investigation<sup>9</sup>. Adopting

the strategy used by Bridges and Zalups, 2005, the human xCT open reading frame was cloned into the pcDNA3.1 (+) vector (Life Technologies)<sup>11</sup> by Dr. Lin. Because the system xc- heavy chain, 4F2hc is ubiquitously expressed in many cell types, including HEK cells<sup>9</sup>, exogenous 4F2hc is therefore not required for proper expression/function of exogenous xCT. In fact, overexpression of 4F2hc has been shown to significantly reduce the uptake of radiolabeled substrates and was hypothesized that excess expression of this glycoprotein disrupts the stoichiometry with xCT and as a result, membrane trafficking and function<sup>9</sup>. Dual overexpression vectors may also overwhelm the transcriptional/translational machinery diverting the cell's resources away from xCT overexpression. Therefore, overexpression of system xc- light chain, xCT, was shown to retain proper localization at the membrane and was sufficient to increase activity in this cell line<sup>9</sup> consistent with activity previously described<sup>3,12,13</sup>. This includes increased uptake of radiolabelled substrates in a Na<sup>+</sup>-independent manner that can be blocked by the addition of cystine. Therefore, in a system where the background levels of xCT are very low (but measurable, as in HEK cells), an increase in glutamate secretion can be attributed to the presence of the artificial overexpression of the xCT transporter and as a result any compound showing inhibitory effects on glutamate releases in these cells can be attributed to blockade of xCT activity. This tool was also intended for potential use as a cell line for future screening of novel compounds and also for *in vivo* testing.

Although overexpression of xCT was achieved at the transcriptional and translational level, it was not accompanied by changes in glutamate output which was expected to increase based on the results described in the literature. This system failed to yield a functional upregulation in xCT and was therefore not pursued further.

## Testing CB-839 in Mouse Mammary Carcinoma Cell Line:

4T1 cells are derived from spontaneous mammary tumour from Balb/c mice (Dexter et al. 1978) and closely models late stage metastatic human breast cancer. Characterization of CB-839 in this line was conducted in order to test a syngeneic line for use in our CIBP animal model.

### *Dose Response*

4T1 cells were sensitive to CB-839 treatment as seen by a decrease in cell number in a dose-dependent manner after 72 hrs. Glutamate release also decreased with CB-839 treatment, however, the results were not as dramatic as changes in cell number possibly due to the fact that dying cells release intracellular glutamate pools confounding the quantification of physiological release of glutamate. Experiments conducted as outlined in Chapter 4 (final paper manuscript) for MDA-MB-231 testing.

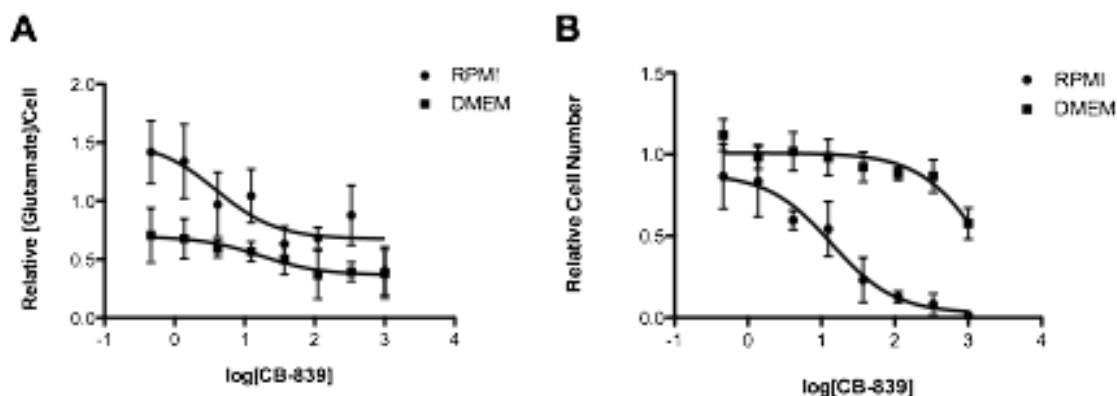


**Figure 6: Treatment of 4T1 Mammary Carcinoma Cells with CB-839**

Non-linear regression of log[CB-839] vs. relative [glutamate]/cell (A) or cell number (B) following a 72hr incubation with CB-839 in RPMI (circles) or DMEM (squares). For

RPMI the EC50 is 3.926 $\mu$ M and in DMEM the EC50 is 16.88nM (A) where the effect is CB-839 action on extracellular concentration of glutamate in culture media. Where the effect is CB-839's effect on cell number the EC50 in RPMI is 13.69nM and in DMEM is 1663nM (B).

### *Subcutaneous tumour growth*

Subcutaneous implantation of 4T1 cells was done as stated in Chapter 4 (final paper manuscript) for MDA-MB-231 cell implantation. However, only 15000 4T1 cells were injected to initiate tumour as they are syngeneic and grow rapidly in this host. CB-839 treatment and daily tumour measurements were also conducted as in chapter 4. CB-839 treatment did not show significant differences in tumour volume between vehicle and drug-treated animals.

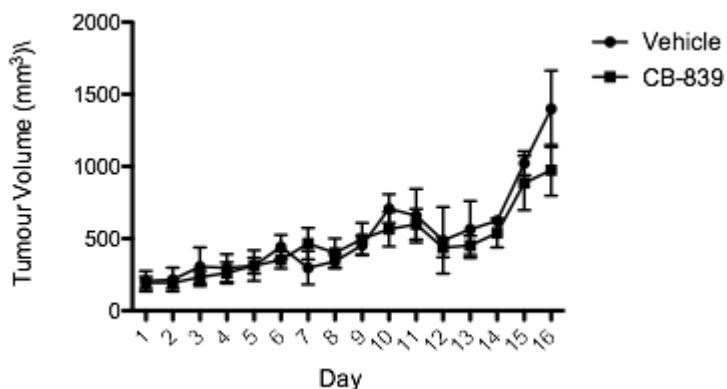


**Figure 7: Tumour volume measurements of subcutaneous 4T1 tumours in Balb/c mice treated with CB-839 or vehicle.**

## Knockdown of GLS through transient siRNA transfection:

Having been working with pharmacological inhibition of GLS with CB-839, a genetic GLS knockdown was pursued to have as a tool to investigate other changes specifically associated with GLS inhibition that may reveal the differences in sensitivity to CB-839 observed between HCC1806 and MDA-MB-231 cells. We decided to look for a link between GLS inhibition and xCT expression. Two siRNA's targeting GLS1 were successful in producing a transient decrease in GLS1 expression in HCC1806 MDA-MB-231 cells (Figure 8A and B). Transient knockdown of GLS1 (72hrs) had a differential response in its effect on xCT expression in both cell lines (Figure 8C and D). Furthermore, the effect of targeting GLS1 on glutamate release showed variation amongst constructs but successful reduction in extracellular glutamate after transfection was observed (Figure 9).

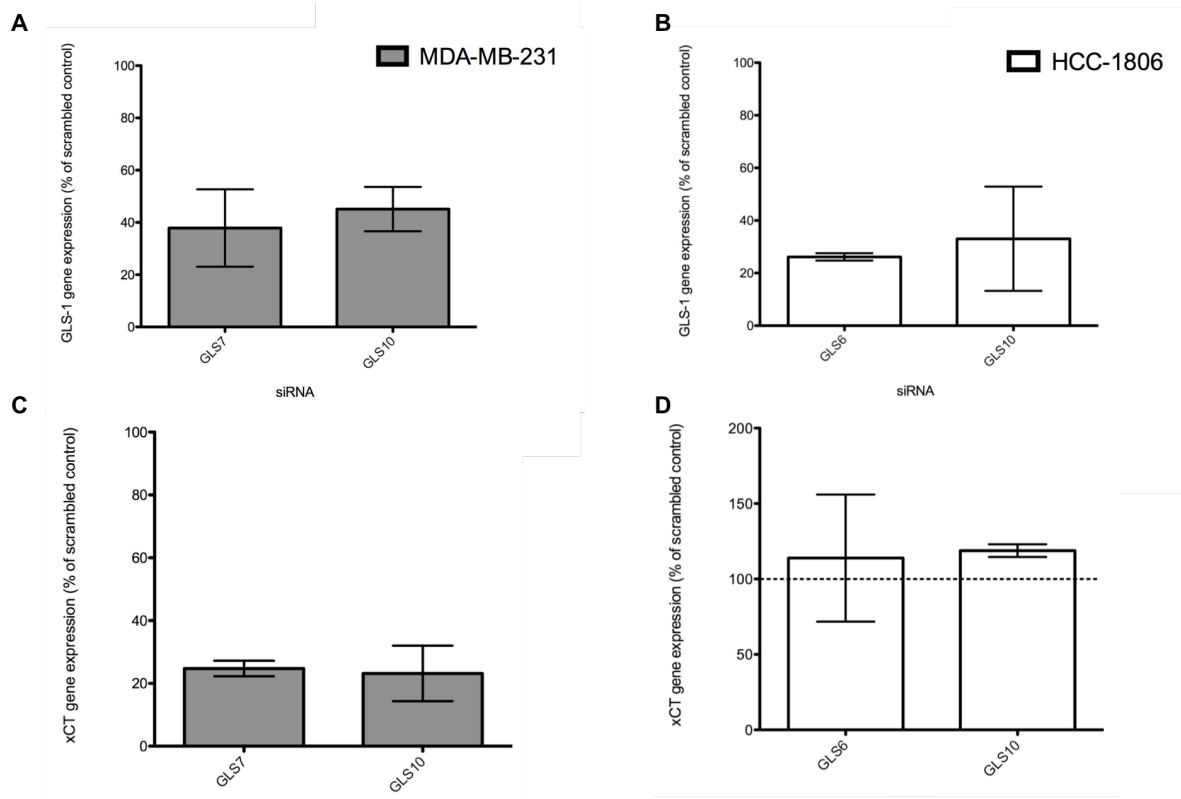


**Figure 8: Transient siRNA-mediated knockdown of GLS in HCC1806 and MDA-MB-231 triple-negative breast cancer cell lines after 72 hrs.**

GLS was successfully knocked down at the mRNA level using siRNA GLS 7 and 10 in MDA-MB-231 cells (A). In HCC1806, GLS 6 and 10 siRNA molecules were most effective (B). A differential response was observed between xCT mRNA expression after GLS transfection in these cell lines. xCT mRNA levels were decreased after transfection with the corresponding siRNA relative to a scrambled control in MDA-MB-231 cells (C) but was not observed in HCC1806 cells (D).

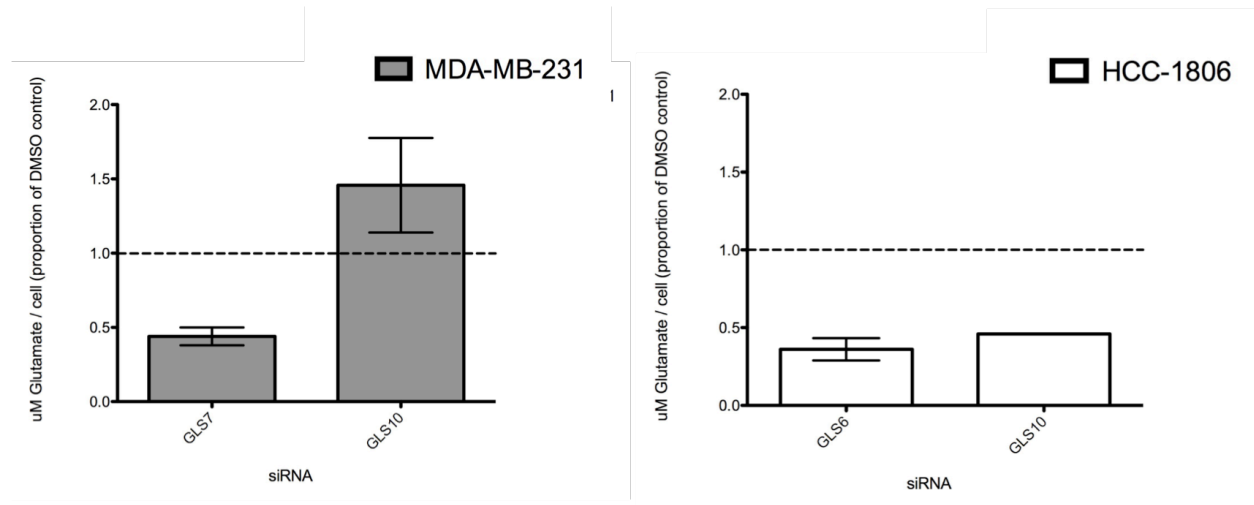


**Figure 9: Extracellular glutamate levels following transient GLS siRNA transfection.**

Only GLS7 siRNA transfection resulted in a reduction in glutamate release relative to scramble control in MDA-MB-231 cells (A). Both siRNA transfections resulted in a decreased in glutamate release from HCC1806 cells (B). Samples collected 72 hrs following transfection.

## REFERENCES FOR APPENDICES:

1. León, D. *et al.* P2X agonist BzATP interferes with amplex-red-coupled fluorescence assays. *Anal. Biochem.* **367**, 140–142 (2007).
2. Timmerman, L. A. *et al.* Glutamine sensitivity analysis identifies the xCT antiporter as a common triple-negative breast tumor therapeutic target. *Cancer Cell* **24**, 450–465 (2013).
3. Bannai, S. Exchange of cystine and glutamate across plasma membrane of human fibroblasts. *J. Biol. Chem.* **261**, 2256–2263 (1986).
4. Seidlitz, E. P., Sharma, M. K., Saikali, Z., Ghert, M. & Singh, G. Cancer cell lines release glutamate into the extracellular environment. *Clin. Exp. Metastasis* **26**, 781–787 (2009).
5. Seidlitz, E. P., Sharma, M. K. & Singh, G. Extracellular glutamate alters mature osteoclast and osteoblast functions. *Can. J. Physiol. Pharmacol.* **88**, 929–936 (2010).
6. Lutgen, V. *et al.* Reduction in phencyclidine induced sensorimotor gating deficits in the rat following increased system xc<sup>-</sup> activity in the medial prefrontal cortex. *Psychopharmacology (Berl.)* **226**, 531–540 (2013).
7. Shih, A. Y. *et al.* Cystine/Glutamate Exchange Modulates Glutathione Supply for Neuroprotection from Oxidative Stress and Cell Proliferation. *J. Neurosci.* **26**, 10514–10523 (2006).
8. Mysona, B., Dun, Y., Duplantier, J., Ganapathy, V. & Smith, S. B. Effects of hyperglycemia and oxidative stress on the glutamate transporters GLAST and system xc<sup>-</sup> in mouse retinal Müller glial cells. *Cell Tissue Res.* **335**, 477–488 (2009).

9. Shih, A. Y. & Murphy, T. H. xCt cystine transporter expression in HEK293 cells: pharmacology and localization. *Biochem. Biophys. Res. Commun.* **282**, 1132–1137 (2001).
10. Albano, R., Raddatz, N. J., Hjelmhaug, J., Baker, D. A. & Lobner, D. Regulation of System xc(-) by Pharmacological Manipulation of Cellular Thiols. *Oxid. Med. Cell. Longev.* **2015**, 269371 (2015).
11. Bridges, C. C. & Zalups, R. K. Cystine and glutamate transport in renal epithelial cells transfected with human system x<sub>c</sub><sup>-</sup>. *Kidney Int.* **68**, 653–664 (2005).
12. Sato, H., Tamba, M., Ishii, T. & Bannai, S. Cloning and Expression of a Plasma Membrane Cystine/Glutamate Exchange Transporter Composed of Two Distinct Proteins. *J. Biol. Chem.* **274**, 11455–11458 (1999).
13. Murphy, T. H., Schnaar, R. L. & Coyle, J. T. Immature cortical neurons are uniquely sensitive to glutamate toxicity by inhibition of cystine uptake. *FASEB J. Off. Publ. Fed. Am. Soc. Exp. Biol.* **4**, 1624–1633 (1990).